Swansea University
Prifysgol Abertawe

Methodological considerations and reliability of visually detecting muscle activity onset during an isometric midthigh pull.

Sayyam Kathuria

Submitted to Swansea University in fulfilment of the requirements for the Degree of *Masters in Sport Science by Research*

Swansea University

2024

Abstract

The isometric midthigh pull (IMTP) is the most commonly employed multi-joint isometric test of neuromuscular function. Performance in the IMTP is associated with several dynamic tests of neuromuscular function among weightlifters, cyclists, wrestlers, powerlifters, rugby league players, NCAA D1 track and field athletes and several other disciplines at the collegiate level. The test is commonly performed on a force platform (FP), for typically quantifying maximal force producing capacity or peak force (PF) and rate of force development (RFD). In an IMTP, PF has been reported as a valid and reliable output variable. However, there is lack of agreement and evidence regarding the reliability of RFD. In contrast to PF, quantification of RFD is dependent on the identification of a start-time. The start-time refers to an instant between the quiescent phase and the start of the athlete pulling, manifested by a sudden change in the expression of the vertical component of the ground reaction force (VGRF). The lack of agreement in the calculation procedures employed to quantify RFD has contributed to a lack of clarity regarding the level of reliability reported in previous studies. More importantly, the method of identifying the start-time varies across studies, contributing to the conflicting results that exist within the scientific literature. The method of identifying a start time in an IMTP remains to be validated and standardised for subsequent calculation of RFD and any other variable dependent on a start-time, e.g., time to peak force. The expression of mechanical force, often recorded using instruments such as the FP, is preceded by a physiological phenomenon of neural and muscular excitation that can be recorded using surface electromyography (sEMG). Considering the possibility of investigating the onset time of muscle excitation and subsequent mechanical force production, it was proposed that temporal sEMG analysis could be used to validate a method of determining the start-time of an IMTP performed on a FP. The onset of muscular activity in single-joint isometric tests of neuromuscular function has been investigated using sEMG, but this method has not been applied to multi-joint activities such as the IMTP. Consequently, the aim of this study was to develop a reliable and valid novel method for detecting the time of muscle onset in an IMTP, which could then be used in future studies to validate a start-time based interrogation of a recorded force-time history. The study consisted of two experimental sections which, when combined, satisfied the aim of the study. Study 1 investigated the methodological considerations in the identification of the time of muscle onset (T_{mo}) during an isometric midthigh pull (IMTP) using visual detection, i.e., manual visual inspection of sEMG amplitude-time history. Firstly, seven pairs of muscles were

identified that are activated during the performance of an IMTP. The study then established a 2-step visual detection method, which allowed the visual inspection of these muscle's activity during the quiescent and active phases of an IMTP. The method was thereafter used for determining the T_{mo} corresponding to the initiation of muscular activity during a maximal voluntary contraction (MVC) in an IMTP. Study 2 investigated the reliability of the methodology developed in Study 1. This was achieved by measuring the inter and intra-rater reliabilities of onset times, detected by two raters in the seven pairs of selected muscles across three experimental conditions; 'ON', 'OFF' and 'WL'. The study included nine male participants with experience (> 3 years) in weightlifting exercises, especially power cleans. One participant was recruited for both the ON and OFF experimental conditions while the remaining 8 participants proficient in weightlifting were categorised under WL. ON, denotes the test condition where sensors remained on the muscles of the participant throughout all test-retest trials. This condition was designed for the visual assessment of muscle activation patterns during IMTP test-retest trials for the same individual and its effect on reliability. In contrast OFF denotes the test condition where sensors were removed and reattached to the muscles prior to each subsequent trial. The OFF test-retest condition was designed to visually assess whether sensor placement performed by a trained individual had an effect on muscle activation patterns, in terms of the reliability. WL (weightlifters) denotes the test condition that was used to categorise the resistance and weightlifting trained participants recruited in the study. This condition aimed to evaluate reliability across a group of participants, while also exploring similarities in muscle activity among individuals and its effect on reliability. Standard deviation (SD) of differences was employed as the statistical measure for determining the variation between two independent sets of muscle onset points. Visually detecting the T_{mo} for 14 muscles (7 pairs) was assessed using a pre-set criteria of ≤ 5 ms, variations above which measurements were deemed unreliable. SD of differences between the T_{mo} as determined by the same rater on two separate occasions identified all 7 pairs of muscles as reliable (differences ≤ 5 ms) in each condition. SD of differences between the T_{mo} determined by two raters identified 3 muscle pairs as reliable, (differences ≤ 5 ms) across the three experimental conditions. These were; gastrocnemius medialis (GS) (SD of differences; ON: 0.7 ms, OFF: 0.2 ms, WL: 0.3 ms), bicep femoris (BF) (SD of differences; ON: 2.4 ms, OFF: 3.5 ms, WL: 2.5 ms) and erector spinae longissimus (ESL) (SD of differences; ON: 2.4 ms, OFF: 2.5 ms, WL: 2.3 ms). Results of both intra and inter-rater reliability demonstrate GS as the most reliable muscle across each experimental condition, demonstrating a variation of < 1 ms. Considering the results of Study 2, GS, BF and ESL are the 3 muscle pairs

recommended for future temporal investigations in the IMTP. Inspection of muscle activity via sEMG traces over the course of Study 2, revealed that GS and BF were the only two muscle pairs with negligible baseline noise prior to $T_{mo.}$ Automated methods of detecting $T_{mo,}$ that rely on the baseline noise can therefore be applied to GS and BF, potentially accounting for limitations associated with visual detection in future studies. This thesis has reported a reliable and novel method of detecting the T_{mo} during an IMTP. Furthermore, the results of this thesis can be used to validate the start-time of an IMTP, contributing towards the standardisation of IMTP research methods and improved reliability of time-dependent variables.

Author Declaration and statements

Declarations

This work has not previously been accepted in substance for any degree and is not being concurrently submitted in candidature for any degree.

Signed..... [redacted] .....

Date..... 02/ 10 / 2023 .....

This thesis is the result of my own investigations, except where otherwise stated. Other sources are acknowledged by footnotes giving explicit references. A bibliography is appended.

Signed..... [redacted] .....

Date..... 02/ 10 /2023 .....

I hereby give consent for my thesis, if accepted, to be available for electronic sharing

Signed..... [redacted] .....

Date..... 02 /10/ 2023 .....

The University's ethical procedures have been followed and, where appropriate, that ethical approval has been granted.

Signed..... [redacted] .....

Date..... 02 /10 /2023 .....

List of Contents

Acknowledgements

Starting as an undergraduate student in 2016, this thesis marks the end of a 5-year academic journey at Swansea University. Since my very first lecture, learning the importance of the word 'unbalanced' in Newton's First Law of motion, to the date of this thesis submission, Professor Nicholas Owen's support has been invaluable. As my postgraduate supervisor I would like to thank him for his patience, understanding and guidance, without which this project would not have come into fruition. His knowledge and expertise in the field of biomechanics has been instrumental in my growth as a researcher. I count myself extremely fortunate to have had the opportunity to work with you and will always cherish the countless office hours spent discussing the project or listening to stories from your time working on the oil rigs.

I would also like to express my gratitude to my co-supervisor, Dr. Shane Heffernan, who's expert input, suggestions, and attention to detail has truly inspired and influenced the quality of the thesis. I would like to thank Lewis Davies and Gareth Beer, without whom participant recruitment and data collection would not have been possible. A special thanks to Ben Morgan whose expertise in programming was instrumental in guiding the development of methods used throughout the project.

I am also very grateful to my fellow postgraduate colleague, Joe Page. I have learnt a lot from you and consider myself fortunate to have made a friend for life that shares the same passion for learning, helping and making a difference. I wish you all the success in your future endeavours and look forward to seeing you succeed in the scientific world. Thank you for the best student house experience during my time in sunny Swansea. Hewson Street M, will always be remembered.

This thesis would not be complete without acknowledging my family, Priya Kathuria, Rajeev Kathuria, Soham Kathuria, Audrey Sharwood, Megan Head and most importantly Kevin John. I will always be grateful for your support, patience, and unconditional love towards me during this challenging yet exciting journey. You are my motivation to work hard, and I promise to continue making you proud.

List of Tables

List of Figures

Figure 2.9 Frequency filtering of Identical Complex Wave: Effects of High-Pass, Bandpass and Low-pass filters. Visual representation of filters applied to the identical complex wave (left) consisting of 3 identical harmonics (10, 110, 300 Hz). The illustration was achieved by rotating the modulation transfer function such that it acts as a visual analogue of a filter to obtain the respective frequency response on the right. The shaded area is a representation of an ideal brick wall filter used for illustration purposes. (A) High-pass filter, allowing frequencies above 150 Hz to pass through unaffected. (B) Bandpass filter, allowing frequencies between 15 and 150 Hz to pass through unaffected. (A) Low-pass filter, allowing frequencies below 15 Hz to pass through unaffected

Figure 2.10 The custom designed isometric testing rack placed over force platforms, using a combination of pins and hydraulic jacks to fix the bar at the appropriate height with respect to the participant. From, Relationship Between Strength Characteristics and Unweighted and Weighted Vertical Jump Height - Scientific Figure on ResearchGate. Available from: https://www.researchgate.net/figure/Isometric-mid-thigh-clean-pull-testing-Top-schematic-isometric-mid-thigh-clean-pulls_fig1_40759599 (Kraska et al., 2009). Similar setup as the one previously used in seminal research (Haff et al., 1997, 2005).

Figure 2.11 The motor unit is composed of the motor neuron originating in the ventral horn of the spinal cord and the muscle fibres its axon innervates. Adopted from Sherrington's concept of the 'final common pathway' (Burke, 2007; Heckman & Enoka, 2012; Liddell & Sherrington, 1925). Created with BioRender.com

Figure 2.12 (A) It is an sEMG signal obtained from the right bicep femoris of a participant during the IMTP. The trace has been band-pass filtered in both directions between 10 and 400 Hz using a 4th-order Butterworth digital filter and amplified by 1000. (B) Is the TKEO conditioned output of the trace suppressing the baseline noise in (A). (C) Full-wave rectification of the trace in (B) is the final step in signal processing before visual detection of muscular activity onset. From (A) to (C) the figure illustrates the suppression of noise, improving the SNR, thus facilitating more valid analysis

Figure 3.1 Illustration of 7 pairs of muscles assessed in the current study. The colour-coded annotations are visual approximations of accurate sensor placements described in Tables 3.1 and 3.2. The images were taken from EMG works® Acquisition software, v4.8.0, Delsys INC, Boston,

Figure 3.8 Illustrates an sEMG trace with minimal baseline noise, classed under Category 1. (A) Represents the initial window viewed with a y-axis scale of 2mV and an x-axis scale of 1000 ms used to identify the region of interest, illustrated here with two red vertical lines and a red dot marked as an estimation of T_{mo} (B) Displays the final point detected at higher resolution (red dot) with a y-axis scale of 2mV and an x-axis full scale of 50 ms.
Note: The region bordered by the two red lines, ± 25 ms of the estimated T_{mo} in (A), is displayed in (B) for the final selection of T_{mo}

Figure 3.9 Illustrates an sEMG trace with relatively higher baseline noise, classed under Category 2. (A) Represents the initial window viewed with a y-axis scale of 2mV and an x-axis scale of 1000 ms used to pick the region of interest, illustrated here with two red vertical lines and a red dot marked as an estimation of T_{mo} (B) Displays the final point detected at higher resolution (red dot) with a y-axis scale of 2mV and an x-axis full scale of 50 ms.
Note: The region bordered by the two red lines, ± 25 ms of the estimated T_{mo} in (A), is displayed in (B) for the final selection of T_{mo}

Figure 3.10 Illustrates the type of traces classed under Category 3 (A) Represents the initial window viewed with a y-axis scale of 2mV and an x-axis scale of 1000 ms used to pick the region of interest, illustrated here with two red vertical lines and a red dot marked as an estimation of T_{mo} (B) Displays the final point detected at higher resolution (red dot) with a y-axis scale of 2mV and an x-axis full scale of 50 ms.
Note: The region bordered by the two red lines, ± 25 ms of the estimated T_{mo} in (A), is displayed in (B) for the final selection of T_{mo} as per the refined definition.

Figure 3.11 Illustrates an EMG trace with relatively high baseline noise. (A) Represents the initial window viewed with a y-axis scale of 2mV and an x-axis scale of 1000 ms, displaying 2000 data samples. (B) Is the expanded scale along the x-axis such that the same window in (A) is viewed with a higher resolution, y-axis scale of 2mV and an x-axis scale of 50 ms, displaying 100 data samples

Figure 4.1 Illustrates the testing day layout. (A) Participant arrival (B) Collection of anthropometric measurements and determination of IMTP rig bar height. (C) EMG sensor location, marking and dry shaving performed as a part of skin preparation. (D) Standardised warm-up. (E) Wiping EMG sensor sites and affixing the pre-assigned EMG electrodes to the

List of Abbreviations

ADC	Analog to digital converters
AGLR	Approximated generalised likelihood ratio
AP	Action potentials
AvgRFD	Average rate of force development
BB	Barbell
BM	Body mass
BF	Bicep femoris
BR	Brachioradialis
BW	Body weight
CI	Confidence intervals
CMJ	Counter movement jump
CNS	Central nervous system
CV	Coefficient of variation
DAQ	Data acquisition system
DSP	Digital signal processing
ED	Extensor digitorum
EMD	Electromechanical delay
EMG	Electromyogram
ESL	Erector spinae longissimus
F50	Force at 50 milliseconds
F90	Force at 90 milliseconds
F100	Force at 100 milliseconds
F150	Force at 150 milliseconds
F200	Force at 200 milliseconds
F250	Force at 250 milliseconds
f	Frequency
F/T	Force-time
FEMD	Functional electromechanical dynamometers
FFT	Fast Fourier Transform
FP	Force platform
GS	Gastrocnemius medialis

GLR	Generalised likelihood ratio
GM	Gluteus maximus
GRF	Ground reaction force
Hz	Hertz
ICC	Intraclass Correlation Coefficient
IMTP	Isometric midthigh pull
IP	Impulse
IP100	Impulse at 100 milliseconds
IP200	Impulse at 200 milliseconds
IP300	Impulse at 300 milliseconds
K^+	Potassium ions
kg	kilogram
LGS	Left gastrocnemius medialis
LBF	Left bicep femoris
LGM	Left gluteus maximus
LVL	Left vastus lateralis
LESL	Left erector spinae longissimus
LED	Left extensor digitorum
LBR	Left brachioradialis
m	meter
$m \cdot s^{-1}$	Metres per second
$m \cdot s^{-2}$	Metres per second squared
MJIT	Multi-joint isometric test
ms	milliseconds
MTJ	Myotendinous junction
MTU	Muscle-tendon unit
MUAP	Motor unit action potential
MVC	Maximal voluntary contraction
N	Newtons
Na^+	Sodium ions
$N.kg^{-1}$	newton per kilogram
$N \cdot s^{-1}$	newton per second
NCAA D1	National Collegiate Athletic Association Division 1

NMJJ	Neuromuscular junction
NR	Not reported
PF	Peak Force
PRFD	Peak rate of force development
r	Pearson's product-moment correlation coefficient
RFD	Rate of force development
RGS	Right gastrocnemius medialis
RBF	Right bicep femoris
RGM	Right gluteus maximus
RVL	Right vastus lateralis
RESL	Right erector spinae longissimus
RED	Right extensor digitorum
RBR	Right brachioradialis
RM	Repetition maximum
RDL	Romanian deadlift
SD	Standard deviation
sEMG	Surface electromyography
SE	Standard error of mean
SEM	Standard error of measurement
SENIAM	Surface electromyography for the non-invasive assessment of muscles
SNR	Signal to noise ratio
T	Time
TBM	Threshold based method
TE	Typical error
TKEO	Teager Kaiser energy operator
T_{mo}	Time of muscle onset
VL	Vastus lateralis
VGRF	Vertical component of ground reaction force
$\dot{V}O_{2max}$	Maximal oxygen uptake
W	Watts
WRT	With respect to time
Δ	Change

5 SD of BW	5 Standard Deviation of Body Weight during the quiescent phase of an IMTP

Chapter 1: General Introduction

1.1 Neuromuscular assessment of human performance

Neuromuscular assessment can be described as the assessment of the interaction between the nervous and muscular systems in the performance of a motor task (Watkins, 2014). Human movement is underpinned by the interaction between the nervous system and the muscles. The nervous system is responsible for generating the signals that determine the degree of muscle activation and the resultant force produced to execute a movement. The neuromuscular system can control human movements through the appropriate use and coordination of muscular endurance, strength and muscle recruitment pattern, as well as reflex activity and proprioceptive feedback (Faude et al., 2017). The neuromuscular assessments of these functions is of critical importance in human-movement, sports and exercise science. As such, a large variety of routine procedures to assess the functioning of the neuromuscular system have been applied with specific purposes. These include; identification of performance limiting factors and determining an athlete's level of muscular development (strength diagnosis), exploration of the intrinsic risk factors of sports injury, monitoring effects of training and rehabilitation programmes and talent identification (Abernethy et al., 1995; Jaric, 2002; Wilson & Murphy, 1996).

Neuromuscular activation is likely to vary given the differences in kinetic and kinematic patterns associated with movements performed in daily life and sporting activities. For example, heavy lifting tasks performed at slower speeds requires application of high muscle forces over a longer period of time (>300 ms), therefore relying on the maximal strength capacity. On the contrary, execution of time-constrained movements such as jumping, sprinting and change of direction rely on high levels of force produced rapidly (50-250 ms) (Duchateau & Baudry, 2011; Jaric, 2002; Suchomel, Nimphius, et al., 2016). Therefore, the force generating capacity of the neuromuscular system can be assessed in terms of the highest producible force (maximum strength/ peak force (PF)) and rate of force development (RFD) (Newton & Dugan, 2002).

1.2 The isometric midthigh pull

The most common method for concurrently quantifying neuromuscular performance in terms of maximal force producing capacity and RFD is through the use of isometric testing protocols (Blazevich et al., 2020; Rodríguez-Rosell et al., 2018; Wilson et al., 1995). The isometric midthigh pull (IMTP) is recognized as the most commonly employed multi-joint isometric test of neuromuscular function (Bartolomei et al., 2022; Brady et al., 2018; Comfort et al., 2019; Dylan et al., 2020; Haff et al., 1997, 2005; Hogarth et al., 2021; Stone et al., 2019; Thomas et al., 2017). It was first presented to the scientific and coaching community in 1997, and it has since been used extensively in neuromuscular performance research among weightlifters (Beckham et al., 2013; Haff et al., 2005; Kawamori et al., 2006; Stone et al., 2019), cyclists (Stone et al., 2004), wrestlers (McGuigan et al., 2006a), powerlifters (Beckham et al., 2012), rugby league players (West et al., 2011), track and field athletes (Nuzzo et al., 2008) and several others (Kraska et al., 2009; Stone et al., 2003; Thomas, Comfort, et al., 2015; Wang et al., 2016).

The IMTP is typically performed in a fixed frame with adjustable horizontal bar or a conventional power rack with a fixed but adjustable weightlifting barbell (Brady et al., 2020; Haff et al., 1997). The test is performed in conjunction with a force platform (FP) positioned directly under the horizontal bar on which the participant stands. Force platforms measure the magnitude and direction of ground reaction forces (GRF) at the feet during an IMTP. The vertical component of the GRF (VGRF)-time history is recorded and then analysed to determine key neuromuscular variables such as maximal strength, PF and RFD (West et al., 2011).

The variable PF, is simply the highest recorded force value during the test, measured in newtons (N) and reported as either absolute or relative terms (Brady et al., 2018). PF in an IMTP is a reliable measure validated against performance in numerous dynamic tests of neuromuscular function (Comfort et al., 2019). In contrast to PF, RFD measured in newtons per second ($N \cdot s^{-1}$) and is an outcome variable which is dependent on the reliable and valid identification of the time when the activity was initiated, commonly referred to as the start-time. It may be reported as peak (PRFD), average (AvgRFD), force at specific timepoints (e.g., F 50 ms) and RFD between specific time bands (e.g., 0-100 ms). There has been considerable variation across studies regarding the method of calculating RFD since the

IMTP was first introduced (Comfort et al., 2019). The lack of agreement between studies in the calculation procedures employed to quantify RFD has affected the reliability of the variable (Section 2.7.3; 2.7.4). More importantly, the method of identifying the point of initiation varies across studies, contributing to the conflicting results that exist within the scientific literature (Table 2.1; Section 2.7.3; 2.7.4) (Baena-Raya et al., 2021; Dos'Santos, Jones, et al., 2017; Dos'Santos, Thomas, et al., 2017; James et al., 2017; Oranchuk et al., 2019; Thomas, Jones, Rothwell, et al., 2015; West et al., 2011). Therefore, the method of identifying a start time in an IMTP remains to be validated and standardised for subsequent calculation of RFD variables.

1.3 Surface electromyography

Skeletal muscle contraction results from a series of synaptic inputs originating in the central nervous system (CNS) that are transmitted to the muscle fibres. The measurement and recording of electrical signal associated with the contraction of a muscle (myoelectric signals) is called an electromyogram (EMG) (Garcia & Vieira, 2011). Surface electromyography (sEMG) is a technique used to study these EMG signals obtained from superficial muscles non-invasively with electrodes placed on the skin's surface (Garcia & Vieira, 2011). Within scientific research, sEMG as a tool provides insight into how the neuromuscular system behaves by studying the activation of skeletal muscles, through the recording of electrical potentials produced during muscle contractions (Cavalcanti Garcia & Vieira, 2011; Vigotsky et al., 2018).

The electrophysiological combination, referring to the physiology of intricate electrical processes within the neuromuscular system, is what initiates skeletal muscle contraction within the human body- (Section 2.8). This physiological process is central to the generation of mechanical force required for performance in static and dynamic motor tasks (Garcia & Vieira, 2011; Disselhorst-Klug et al., 2009). In essence, the expression of mechanical force is often recorded using biomechanical instruments such as dynamometers (Tillin et al., 2010) or force platforms (Owen et al., 2014; West et al., 2011) is preceded by a physiological phenomenon of neural and muscular excitation which can be estimated using sEMG (Vigotsky et al., 2018).

In the field of biomechanics, a primary application of sEMG, is the precise detection of temporal characteristics of muscle recruitment, such as activation onset times (Crotty et al., 2021). Determining the onset time through appropriate temporal analysis is a prerequisite for studies of motor control and performance. For instance, onset times have previously been determined in single-joint neuromuscular tests of arm raising (Allison, 2003), shoulder flexion, extension and abduction (Hodges & Bui, 1996), isometric ankle plantarflexion and dorsiflexion (Crotty et al., 2021) and isometric knee extension (Solnik et al., 2010; Tillin et al., 2010). With some of these studies determining onset times by utilising mechanical force measuring tools and sEMG concurrently with the assessment of other neuromuscular performance (Crotty et al., 2021; Solnik et al., 2010; Tillin et al., 2010).

1.4 Aims and objectives of the thesis

Considering the possibility of investigating the onset time of muscle excitation and subsequent mechanical force production concurrently, temporal sEMG analysis can be used to determine the onset of mechanical force production in a given motor task. Therefore, it was proposed that, determining the onset of excitation in several muscles using sEMG could be used to validate a start-time method of an IMTP performed on a force platform or used in other studies that need knowledge of such variables.

While onset times of muscular activity has been determined in single-joint isometric tests of neuromuscular function using sEMG, it is not the case for multi-joint isometric tests. To the author's knowledge, there are no reported studies investigating the onset of several muscles in a multi-joint isometric test using sEMG. Consequently, the reliability of determining the onset of muscle activity remains to be investigated.

Therefore, the aims and objectives of the current thesis are as follows:

Aim

To develop a reliable method of detecting the time of muscle onset corresponding to the onset of maximal voluntary force in an IMTP

Objectives

I. Select muscles, based on the literature, that are most likely to be activated during the performance of an IMTP

II. Develop a method for the identification of the instant corresponding to the time of muscle onset in the muscles identified in point I, during a maximal voluntary contraction (MVC) in an IMTP

III. Assess the reliability of detecting the time of muscle onset in the method developed in II.

IV. Based on the results of III, recommend the muscles that can be used to represent the time of muscle onset during a MVC in an IMTP.

1.5 Organization of the thesis

The organisation of this thesis consists of 5 chapters. Chapter 2 comprises a review of key biomechanical principles, explores prior research on IMTP and investigates the utility of sEMG in determining the onset of muscle activity during motor tasks. Chapter 3 (Study 1) focuses on the methodological considerations associated with the development of a novel method for identifying the time of muscle onset (T_{mo}) recorded using sEMG during a MVC in an IMTP. A prominent focus of this chapter was the development of the 2-step visual detection method for the accurate and precise detection of T_{mo} in several muscles, serving as a reference point against which the start-time of an IMTP could be validated. Chapter 4 (Study 2) investigates the reliability of the 2-step visual detection method developed in Chapter 3 (Study 1). This chapter will establish the reliability of the method across three experimental conditions. Chapter 5, will provide a summary of the key findings, identify key limitations, and inform future directions for temporal investigations, undertaken with sEMG in the IMTP. More importantly, the chapter will report recommendations inferring the results of Chapter 4 on the muscles that can be used to represent the time of muscle onset during a MVC in an IMTP.

Chapter 2: Review of Biomechanical Theory and Literature

2.1 Thesis introduction

The following literature review is presented in nine sections. Section 2.2 describes how neuromuscular human movement occurs and subsequently the types of muscle contractions. Section 2.3 reviews the key terms that underpin statistical techniques of scientific research. Signals obtained from biomechanical equipment such as force platforms and EMG electrodes, require manipulation of its properties to meet specific requirements. As such, Section 2.4 and Section 2.5 were used to review and discuss key biomechanical theories with respect to signals, signal characteristics, signal processing and application of digital filters. Section 2.6 delves into the history of isometric training and the parallel rise of isometric assessment of human performance. Section 2.7 leads into the discussions surrounding the isometric midthigh pull (IMTP). This section provides a review of the IMTP force-time variables utilized in the assessment of athletic performance. It also reviews the reliability of these variables and discusses the methodological approach employed in their calculation. The subsection 2.7.4, that reviews the IMTP methods summarises the content of Section 2.7, serving as the foundation for subsequent sections. Section 2.8 provides a concise overview of the mechanism that underpins muscle contraction. It introduces readers to surface electromyography (sEMG), a technique used to study the electrical signals associated with muscle contractions called electromyogram (EMG). Of particular interest was the use of sEMG signal analysis as an indicator for the detection of the time of muscle onset, elements of which are also covered in this section. Lastly, Section 2.9 serves to summarise Chapter 2 of the thesis, highlighting its aims and objectives while providing the necessary context for the subsequent chapters. Collectively, these eleven sections provide a critical review of the literature, discussing previous research and underpinning methodological approach within this thesis.

2.2 Human movement and types of contraction

Muscles and tendons (the connective tissue that attaches muscle to bone) make up the functional unit (i.e., muscle-tendon unit (MTU)) that produces motion at a joint (Massey, 2017). The myotendinous junction (MTJ) is the transition zone between the skeletal muscle and tendon where muscle fibres interact with the tendon. During muscle contractions, large forces are transmitted from the muscle fibres to the non-contractile tendon through the MTJ (Jakobsen & Krogsgaard, 2021). Therefore, MTUs of the human body are responsible for producing forces that dictate the movement of the joints, while the nervous system controls

the intensity and timing of these forces. Motor coordination of body segments forms the basis of human movement. It is defined as the ability of the nervous system to feed information regarding body position and body movements to the muscles, which are interpreted as instructions to produce body movement. As such, the neuromuscular system can be defined as the interaction between the nervous and muscular systems in control of joint movements, bringing about coordinated body movement (Watkins, 2014).

In the case of human locomotion and consequently sporting movements, body segments are periodically subject to external load or impact forces (running, jumping) which produce muscle tension (Komi, 1994). This causes muscular contractions, wherein the muscle may either shorten, lengthen, or stay the same length. The direction and magnitude of muscle contraction is dependent on external load. If the tension produced within the muscle is greater than the external load, the muscle will shorten (Watkins, 2014). This type of contraction is called a concentric contraction wherein the net muscle moment is in the same direction as the change in joint angle resulting in positive mechanical work (Komi, 2011). Lengthening of the muscle occurs if the external load is greater than the tension produced in the muscle; this is termed as an eccentric contraction (Watkins, 2014). In this case, the net muscle moment is in the opposite direction to the change in joint angle, and the mechanical work is negative (Komi, 2011). Isometric contractions refer to no change in muscle length due to the tension produced in the muscle equalling the external load or a static resistance (Watkins, 2014). It is most frequently used to characterise the performance of human skeletal muscles resulting from the activation of the muscle while the length of the entire MTU remains the same and the mechanical work is zero (Komi, 2011).

2.3 Validity, reliability, accuracy and precision

2.3.1 Validity

In broad terms, validity indicates the degree to which the administered test compares to the criterion or 'gold standard'. Validity in scientific testing also refers to the ability of the measurement instrument to reflect what it is intended to measure (Atkinson & Nevill, 1998; Thomas et al., 2022). It can be further classified into logical, content, criterion and construct validity. However, in the presence of a well-established 'gold standard' measure it is particularly useful to establish criterion validity, which examines the extent to which scores on a test are related to some recognised standard (Thomas et al., 2022).

Criterion validity is an objective measure of validity and can be further categorised into concurrent and predictive validity (Currell & Jeukendrup, 2008; Thomas et al., 2022). Concurrent validity involves assessing an instrument simultaneously with a recognised criterion measure. For example, the use of functional electromechanical dynamometers (FEMD) concurrently with the criterion FP method to assess performance in an IMTP test (Baena-Raya et al., 2021). Wherein, FP method is a recognised 'gold-standard' method for measuring performance in an IMTP, while dynamometers such as the FEMD are yet to be validated before its use amongst athletes.

As the term suggests, predictive validity refers to the extent to which predictor variables accurately predict criterion scores. One typical example is the use of skinfold measurements to predict fat percentage (Thomas et al., 2022). Predictive validity may also involve using a performance test or protocol to predict performance subsequently. For instance, the maximal oxygen uptake ($\dot{V}O_{2max}$) test can be administered to predict performance time in trained cyclists (Hawley & Noakes, 1992).

Within scientific research, the validity of a test is often assessed by the strength of association or correlation, statistically, established using Pearson's product-moment correlation coefficient (*r*), also called Pearson's '*r*' (Karras, 1997). These correlations can be rated as trivial (0.1), small (0.1–0.29), moderate (0.3–0.49), large (0.5– 0.69), very large (0.7–0.89), or nearly perfect (0.9–0.99) (Hopkins, 2015; Till et al., 2018). The validity of a test measure or instrument can also be determined using regression analysis and plotting the two sets of data. The results of the regression analysis are presented as 'R^2', also known as the coefficient of determination. A high R^2 value indicates strong association between the test

scores and the criterion measure, suggesting good predictive validity. Overall, high values of 'r' and 'R^2' and a low standard error of the estimate (SEE) suggest strong predictive validity.

2.3.2 Reliability

Reliability is defined as the consistency of measurements, the degree of reproducibility of values recorded in repeated trials of an individual's performance on a test. It can also be described as the repeatability of a test or the ability of a test or individual to produce similar results on different occasions (Atkinson & Nevill, 1998; Hopkins, 2000a). Statistically, reliability estimates the amount of measurement attributable to error and the amount representing an accurate reading

Previous literature identified two types of reliability. i.e. relative and absolute reliability (Atkinson & Nevill, 1998; Batterham & George, 2003; Bruton et al., 2000). Relative reliability also known as stability reliability, refers to the degree to which participants maintain their rank order or position in a sample with repeated measurements. It is often assessed using a type of correlation coefficient such as the intraclass correlation coefficient denoted by '*ICC'*, and its numerical value ranges between 0 and 1. The coefficient of correlation, *ICC* = 1, demonstrates perfect reliability; however, as error increases, the reliability diminishes, so that with maximal error correlation coefficient would read *ICC* = 0 (Bruton et al., 2000). Absolute reliability refers to the degree of consistency or agreement between repeated measurements obtained from the same participant under identical conditions. This type of reliability is expressed in actual units of measurement or as a proportion of measured values. Common metrics used to quantify absolute reliability include, standard error of measurement (SEM), coefficient of variation (CV) and limits of agreement (LOA) (Atkinson & Nevill, 1998; Batterham & George, 2003; Bruton et al., 2000).

To determine the overall reliability of a test, calculations of ICC (relative reliability), CV (absolute reliability) and 90% confidence intervals (CI) are recommended (Atkinson & Nevill, 1998; Haff et al., 2015; Hopkins, 2000). While ICC provides information about the degree of consistency and agreement between two data sets, it does not detect any systematic errors (measurement bias or miscalibration). Therefore, studies that report ICC on its own must be interpreted with caution since, ICC will purport to assess the correlation and

reliability (repeatability) but the level of reliability is not quantified. Calculation of CV allows for the estimation of measurement error, while 90% CI checks the precision of these estimates owing to a more informative depiction of the reliability measure (Bland & Altman, 1986; Hopkins, 2015).

Other indirect measures of reliability include standard deviation (SD) and standard error of the mean (SE). SD is a measure of variability in terms of the dispersion or spread of the data points around the mean (Altman & Bland, 2005). It is commonly used to describe the variability of individual measurements or the spread of differences between measurements. For instance, SD can be used to capture the within-subject variation in an experimental study consisting of random variation in an individual's test scores in repeated tests or trials (Hopkins, 2000a). SE, is a type of SD, used as a measure of precision of the sample mean. SE is most useful as a means of calculating CI and depends on both, the SD and sample size by the simple relation as per equation 2.1, where 'n' is the sample size (Altman & Bland, 2005). In simple words, SD provides information about how widely scattered some measurements are while SE is used to indicate the uncertainty around the estimate of the mean measurement.

$$SE = SD/\sqrt{n} \tag{2.1}$$

Reliability is an integral part of validity, pertaining to test measures' consistency, reproducibility, or repeatability. As such, reliability assessment is essential to track and report the precision of measurements within research and practical settings.

2.3.3 Accuracy and Precision

Accuracy refers to the closeness of agreement between a test result and a valid reference value, while precision indicates how close independent measurement results obtained by replicated measurements are to one another (Menditto et al., 2007; Prenesti & Gosmaro, 2015). Accuracy can further be interpreted as the expression of the correctness of measurement, whereas precision expresses the reproducibility of measurements (Kumar, 2012).

Accuracy and precision could be easily understood using subjective examples, such as the free throw in basketball. A player who consistently makes the basket, irrespective of where the ball hits on the rim or backboard, is deemed to have high accuracy. If, however, the player misses' baskets but consistently strikes the same portion on the rim or backboard in subsequent attempts, then the player is deemed to have a high level of precision. Accuracy and precision can also be understood from experimental measurements relevant to scientific research and equipment calibration procedures. For example, if a replicated measurement of a 70.0-gram standard sample results in values of 67.5, 67.6, 67.5 and 67.6; the scale is deemed precise but not very accurate. Therefore, accuracy relates to the quality of a result and is not equal to the precision. Precision focuses on the stability of the measuring device or its reading during the measuring process itself (Strauss et al., 2006). As for scientific experimental analysis, accuracy and precision are essential concepts to consider, given that numerous pieces of equipment used within the field require periodic calibration to ensure accurate and precise readings.

2.4 Signal Characteristics

2.4.1 Signal

A signal is any natural or artificial phenomenon carrying information that varies as a function of one or more independent variables (Pohlmann, 2011). For instance, when the independent variable is time, changes in current or voltage constitute a signal that can be recorded, transmitted, or manipulated directly or indirectly. In biomechanics, the electrical, chemical, and mechanical activities, such as force and muscle contraction, produce time-varying signals that can be measured and analysed using transducers and bioamplifiers, respectively (Escabí, 2005; Winter, 2009). Biological signals, as such, are analogous (i.e., continuous in amplitude and time, representing another quantity) and often associated with noise. Noise, with respect to biological signals, is used to describe components of the final signal that are not a result of the process itself (Winter, 2009). For instance, in the present study, the signal recorded due to movement and pre-tension in muscles prior to initiating the multi-joint IMTP was defined as noise.

2.4.2 Frequency

The frequency of a signal represents how rapidly the signal oscillates, passing through a point per second. The S.I. unit of frequency is hertz (Hz) (eq. 2.2) (Figure 2.1) (Derrick, 2014). The sampling frequency is defined as the number of samples per second, whereas its reciprocal sampling rate is the time between each sample. For example, in the current study, vertical ground reaction force was sampled at 1000 Hz for 16 seconds, corresponding to 16,000 samples (1000 samples/sec) when digitised (Section 3.3.1).

$$f\ (\mathrm{Hz}) = 1/(\mathrm{T}\ (\mathrm{s})\ ) \qquad 2.2$$

f = frequency; T = *period, time to complete one cycle*

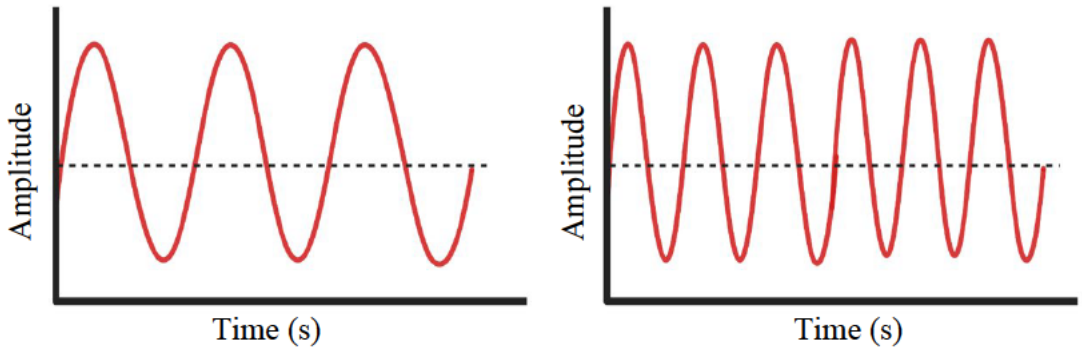

Figure 2.1 *Representation of signals with the same amplitude but different frequencies. Lower frequency (left) and higher frequency (right) for the same time. Created with BioRender.com.*

2.4.3 Amplitude

The amplitude of a signal is the maximum displacement above (peak) and below (trough) the equilibrium position (Derrick, 2014). Therefore, the amplitude of a signal quantifies the magnitude of the oscillations, in whichever units are being used to measure the displacement, for example metre (m) for a wave on water or volts (V) for an electrical signal (Figure 2.2). Gain refers to the amplification or magnification of signal amplitude, often used to make weak signals more easily detectable and measurable. It quantifies the degree to which the signal amplitude is increased by the amplification process (Derrick, 2014).

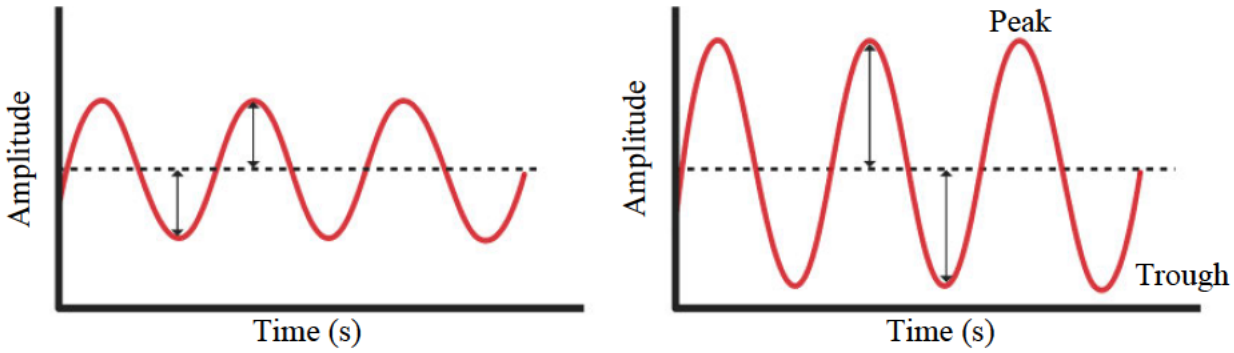

Figure 2.2 *Representation of signals with the same frequency but different amplitudes. Lower amplitude (left) and higher amplitude (right) for the same time. Created with BioRender.com.*

2.4.4 Wavelength

Wavelength refers to the distance between corresponding points of two consecutive waves. It is measured as the distance between successive crests (peaks) or troughs moving in the same direction. It is the length of one complete oscillation measured in meters (m) (Figure 2.3) (Derrick, 2014).

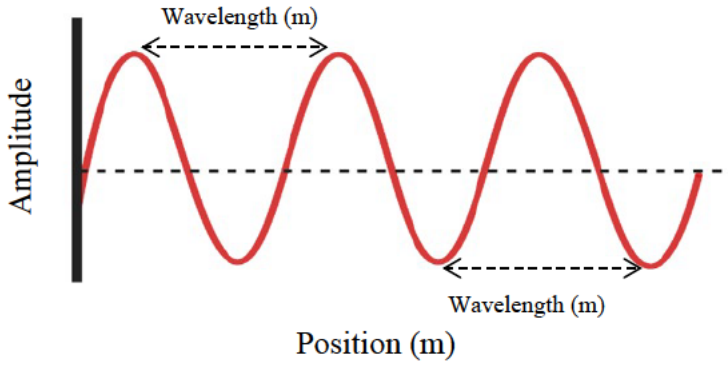

Figure 2.3 *Represents the wavelength of a signal, measured as the length between two successive crests (peak) or trough moving in the same direction. Created with BioRender.co*

2.5 Signal Processing

Signal processing refers to the manipulation of the properties of a signal, such as amplitude and frequency, to meet specific requirements. For signal processing of variables continuous with time, the analogue signal needs to be converted into a digital format, usually a sequence of numbers (Apolinário & Diniz, 2014). Analog-to-digital converters (ADC) are either built-in to the acquisition systems, or the associated software digitises the acquired analogue signal (Van Drongelen, 2018). Thus, the representation of signals in terms of sequences of digital numbers and the use of specialised software (BioWare and Delsys Data Analysis software) to process these signals to either modify or analyse the original signal is termed digital signal processing (DSP) (Apolinário & Diniz, 2014; K. Pohlmann, 2011).

2.5.1 Fourier Series

The Fourier theorem states that all composite cyclical waveforms constitute of harmonic series of sine waves (Figure 2.4; Figure 2.5) (Pohlmann, 2011). A Fourier series is the summation of harmonically related sine waves (Figure 2.4; Figure 2.5) (Pohlmann, 2011). The Fourier transform of a composite signal is the frequency-domain representation that reveals the frequency and amplitudes of the harmonic content of the complex wave (Figure 2.4) (Cook & Miller, 1992).

For example, in the current thesis, the voltage signal proportional to the applied force (obtained from FP) and muscle contraction (recorded using sEMG), as a function of time is said to be a representation in the time domain. An alternative representation of the same information is based on the Fourier theorem, wherein the signal may be represented as the sum of a set of sinusoidal waveforms, each of varying frequency and having an associated amplitude (Cook & Miller, 1992). Therefore, the voltage signal proportional to the applied force and muscle contraction as a function of frequency is said to be a representation in the frequency domain. Conversion of digitised signals from time-domain to frequency-domain is achieved via Fast Fourier Transforms (FFT), a function generally built-in to modern software (e.g., BioWare). Representation of signals in the frequency domain allows researchers to decide the sampling rate prior to the analogue-to-digital conversion of the signal. Further, the range of frequencies within the composite signal influences the frequency threshold of filters generally used to remove undesirable noise (Winter, 2009). Therefore, the representation of signals in the frequency domain and knowledge of the frequency spectrum is mandatory in making decisions about collecting and processing any given signal.

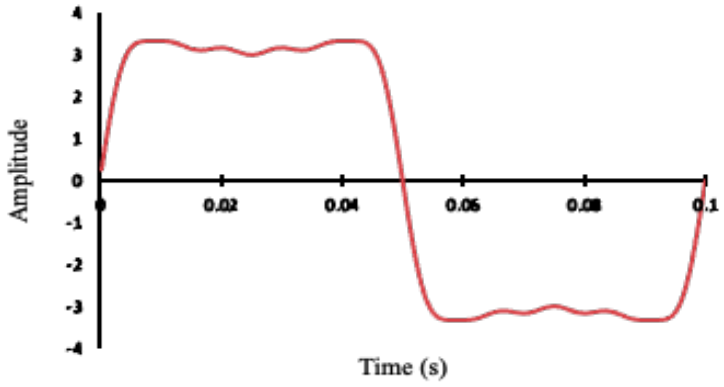

Figure 2.4 *Example of a manually simulated complex signal. It constitutes a summation of harmonically related sine waves.*

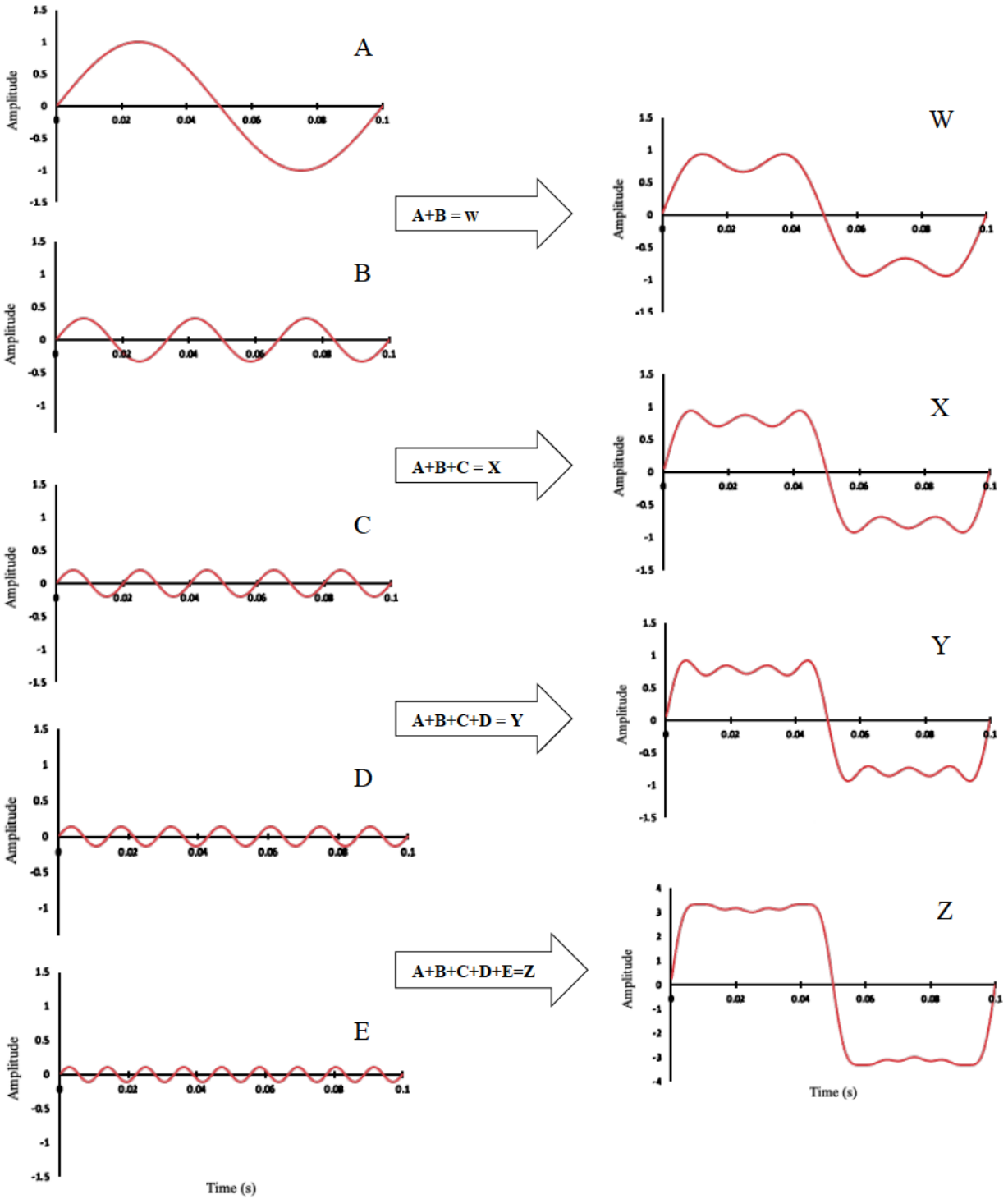

Figure 2.5 *The deconstruction of harmonically related sine waves of decreasing amplitude (A, B, C, D and E) that make up a complex signal Z. The frequencies contained in the complex signal (Z) are a summation of (A) 10 Hz, (B) 30 Hz, (C) 50 Hz, (D) 70 Hz and (E) 90 Hz. With reference to the annotations figure thus illustrates the concept of adding harmonically related series of sine waves to obtain a complex signal Z.*

2.5.2 Filters

Signals obtained from human movements (e.g., force and muscle contraction) are often confounded by unwanted signal regarded as noise, distorting the signal waveform of interest. As such, filters play an important role in analysing and processing biological signals. Filters can be used to modify the frequency spectrum contained in a complex signal in order to achieve the desired signal. There are three broad classes of filters: low-pass, high-pass and band-pass.

2.5.2.1 Low-pass filter

A low pass filter allows low frequencies of the signal to pass uninterrupted. It works by selecting a high-frequency cut-off, frequencies above which are attenuated, while lower frequencies are selectively retained (Figures 2.6 and 2.9). It is most commonly used to remove high frequencies from digitised kinetic and kinematic data (Derrick, 2014; Escabí, 2005).

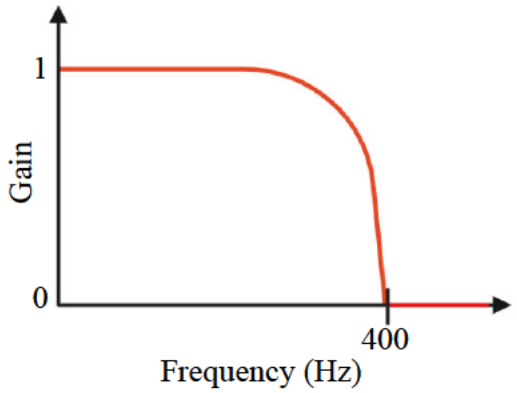

Figure 2.6 *Modulation transfer function of a low-pass filter with a high-frequency threshold of 400 Hz. Frequencies below 400 Hz contained within the signal are passed uninterrupted, while higher frequencies are attenuated. Created with BioRender.com*

2.5.2.2 High-pass filter

A high-pass filter performs the opposite function of a low-pass filter, allowing high signal frequencies to pass through uninterrupted. It works by selecting a low-frequency cut-off, frequencies below which are removed, while higher frequencies are retained (Figure 2.7; Figure 2.9). It is often used to eliminate low-frequency movement artefacts from low-voltage signals such as those obtained using sEMG (Derrick, 2014; Escabí, 2005).

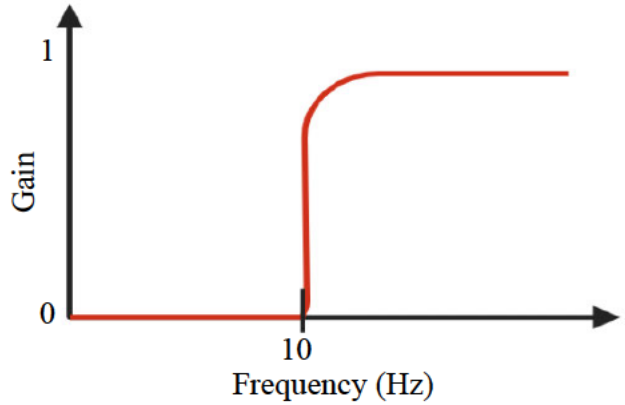

Figure 2.7 *Modulation transfer function of a high-pass filter with a low-frequency threshold of 10 Hz. Frequencies above 10 Hz contained within the signal are passed through uninterrupted, while lower frequencies are attenuated. Created with BioRender.com*

2.5.2.3 Band-pass filter

Band-pass filters are applied by selecting both a low and high-frequency cut-off, frequencies between which are passed unattenuated. Only those frequencies below the lower cut-off and above the higher cut-off are attenuated (Figure 2.8; Figure 2.9). A band-pass filter is most commonly used in sEMG signals when there is movement artefact in the low-frequency range and noise in the high-frequency range (Derrick, 2014; Escabí, 2005).

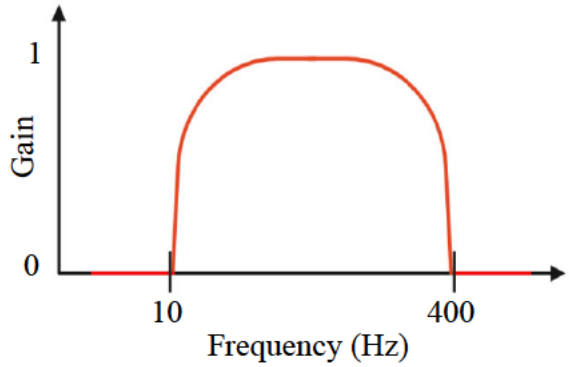

Figure 2.8 *Modulation transfer function of a band-pass filter with a low-frequency threshold of 10 Hz and high-frequency threshold of 400 Hz. Frequencies between 10 Hz and 400 Hz contained within the signal are passed through uninterrupted, while frequencies above and below the cut-off are attenuated. Created with BioRender.com.*

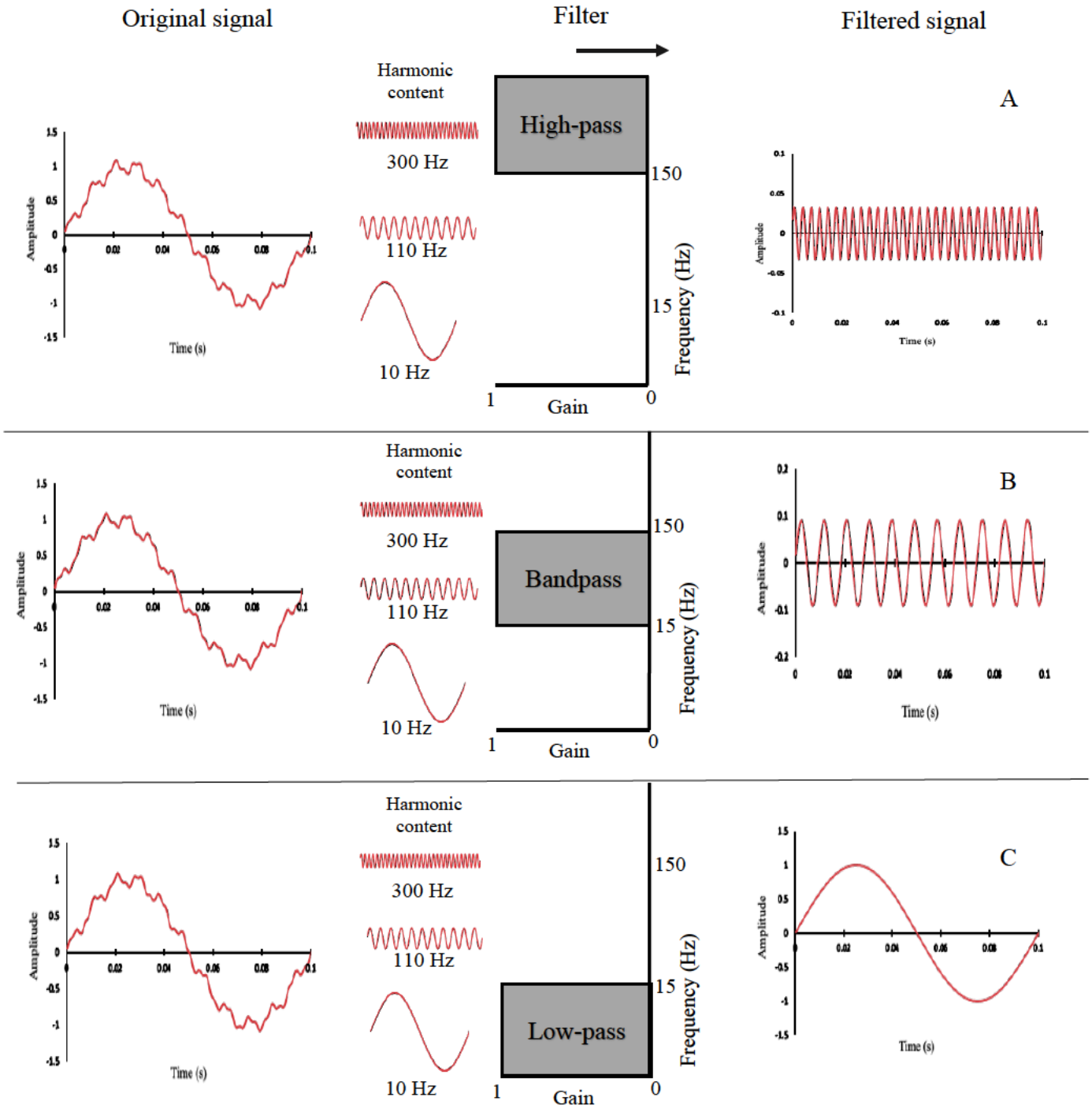

Figure 2.9 *Frequency filtering of identical complex wave: Effects of High-Pass, Bandpass and Low-Pass Filters. Visual representation of filters applied to the identical complex wave (left) consisting of 3 identical harmonics (10, 110, 300 Hz). The illustration was achieved by rotating the modulation transfer function such that it acts as a visual analogue of a filter to obtain the respective frequency response on the right. The shaded area is a representation of an ideal brick wall filter used for illustration purposes. (A) High-pass filter, allowing frequencies above 150 Hz to pass through unaffected. (B) Bandpass filter, allowing frequencies between 15 and 150 Hz to pass through unaffected. (A) Low-pass filter, allowing frequencies below 15 Hz to pass through unaffected.*

2.6 Isometric assessment of human performance

Isometric strength can be defined as the ability to develop force produced by a muscle or muscles against an immovable resistance in a sustained isometric contraction of unrestricted duration (Atha, 1981; Enoka, 1995). Further, isometric muscle activity is defined by contraction in muscles with no length change (Ryschon et al., 1997). Isometric tests involve voluntary contractions performed at specified joint angles to produce force against an immovable resistance, often aligned with a device equipped with transducers capable of measuring force (Wilson & Murphy, 1996). These tests allow for the quantification of maximal force in terms of PF, force at various time points (epochs) and the RFD (Comfort et al., 2019). The diagnostic ability of these isometric test measures maybe of critical importance when prescribing and monitoring athlete development, especially in time-constrained tasks within sports such as sprinting, jumping and change of direction (Suchomel et al., 2016)

Indications of isometric training date back to 1928, when a master's thesis researched the "short static strength of muscles" (Atha, 1981). It was not until 1953 that a study investigating muscle performance and muscle training using isometrics first surfaced in the scientific literature (Hettinger & Müller, 1953). Investigating the lowest exercise stimulus necessary to increase muscle strength, this study claimed that an isometric muscle contraction a day for six seconds at "2/3rd muscular tension" of maximum strength of the muscle group produced a maximum training response. The claims of this study gave rise to further investigations into isometric training and testing methods.

Parallel to the rise in isometric training methods in the 1900s, the isometric assessment of neuromuscular function gained popularity. One of the first detailed and standardised protocols for isometric testing was developed to measure the strength of the affected muscle groups involved in orthopaedic disabilities. Consisting of 28 tests, total body isometric strength was measured at specific joint angles about the wrist, elbow, shoulder, hip, knee, and ankle joints (Clarke, 1948). Since then, single-joint and multi-joint variations of isometric tests have been used primarily in the investigations of correlations with dynamic neuromuscular performance tests.

The isometric knee/leg extension test is the most common lower-body single-joint isometric test employed to find correlations with dynamic performance tests. Often performed

unilaterally, the isometric PF and RFD have previously been used to research correlations with performance in alpine skiing (Abe et al., 1992), one repetition maximum (RM) squat (r = 0.58) (Baker et al., 1994), variations of jumps (r = 0.22-0.81) (Anderson et al., 1991; Considine & Sullivan, 1973; Hakkinen, 1991; Jarić et al., 1989; Viitasalo et al., 1981), high jump (r = 0.31-0.53) (Viitasalo & Aura, 1984) and sprinting/maximal velocity running (r = 0.36-0.62) (Anderson et al., 1991; Considine & Sullivan, 1973; Mero et al., 1981). Much like the isometric knee extension for the lower body, the isometric bench press is a variation to test upper-body force-generating capacity. The isometric bench press test performed unilaterally (Baker et al., 1994) or bilaterally (Murphy et al., 1994) has been utilised in the past to investigate associations with performance in 1RM bench press (r = 0.57-0.78) (Baker et al., 1994; Murphy et al., 1994), bench press throw (r = 0.56-0.57) (Pryor et al., 1994) and shot-put throw (r = 0.38-0.47) (Murphy et al., 1994).

Considering the athletic population, variations of multi-joint isometric tests were developed to replicate the multi-joint nature of sporting movements or specific phases within a sport. Representative of relatively sports-specific movements, the isometric squat test has previously been employed to correlate isometric PF and RFD to performance in running (Wilson et al., 1995) and jumping (Young & Bilby, 1993). An example of an upper-body multi-joint isometric test specific to certain phases within a sport was demonstrated by Strass (1991) in sprint swimmers. To examine the "explosive strength" (which in this context appeared to mean the maximal force produced in a short period of time) of the shoulder/arm complex, Strass (1991) developed a specific testing apparatus to mimic the technical positions in swimming. The apparatus adjusted to replicate the three phases (down-sweep, in-sweep and up-sweep) of the arm stroke in water demonstrated moderate to strong correlations with 50 m swim velocity performance. Furthermore, the upper-body neuromuscular performance in the bespoke isometric apparatus could discriminate between the level of swimmers that were divided into groups based on their 50 m swim performance. Similarly, only the isometric rowing test, amongst a variety of isometric tests employed by Secher (1975), could discriminate between the level of rowers (world-class, national champions and senior rowers). Thus, highlighting the applicability of multi-joint variations while emphasising the importance of specificity in isometric testing with athletic populations.

Single-joint isometrics tests are prevalent in the scientific literature; however, research since the late 1900s has seen a shift towards multi-joint isometric tests in athletic population to

improve the specificity of isometric testing. The nature of isometric testing demands the manipulation of body segments in positioning joints at specific angles to allow for submaximal, maximal or rapid force production. While isometric tests can be performed at various joint angles, research suggests consideration of the joint angles at which peak force is developed in the dynamic performance of interest, in terms of associations (Murphy et al., 1995). The neuromuscular variables obtained from isometric testing, PF and RFD, have previously been reported to vary markedly at different joint angles. Therefore, specificity and standardisation of positioning in all isometric tests are imperative to avoid variability and ensure the reliability of resulting neuromuscular performance variables.

While research in the isometric assessment of neuromuscular function in athletes gained considerable attention in the 1900s, the reported results demonstrated weak to moderate correlations with dynamic performance (Wilson & Murphy, 1996). The continued attempt to elicit strong correlations between isometric testing modalities and dynamic performance led to the creation of a new multi-joint isometric test in the 1990s, the isometric midthigh pull (IMTP) (Haff et al., 1997; Stone et al., 2019).

2.7 The isometric midthigh pull

The IMTP is recognised as the most widely used multi-joint isometric test (MJIT) in the current literature and was developed in the early 1990s (Stone et al., 2019). After substantial pilot testing, a custom-built isometric rack (Sorinex Inc., Irmo, SC) was built and placed over a 61 x 121.9 cm AMTI forceplate (Advanced Mechanical Technologies, Newton, MA). The custom rack allowed the bar to be fixed at any desired height above the floor using a combination of pins and hydraulic jacks (Figure 2.10) (Haff et al., 1997). Presented to the scientific and coaching community in 1997, it has since been used extensively in research and across various sports (Haff et al., 2005; McGuigan et al., 2006; Stone et al., 2004; Thomas et al., 2015; Townsend et al., 2019; West et al., 2011).

Figure 2.10 *The custom designed isometric testing rack placed over force platforms, using a combination of pins and hydraulic jacks to fix the bar at the appropriate height with respect to the participant. From, Relationship Between Strength Characteristics and Unweighted and Weighted Vertical Jump Height - Scientific Figure on ResearchGate. Available from: https://www.researchgate.net/figure/Isometric-mid-thigh-clean-pull-testing-Top-schematic-isometric-mid-thigh-clean-pulls_fig1_40759599* (Kraska et al., 2009). *Similar setup as the one previously used in seminal research* (Haff et al., 1997, 2005).

2.7.1 Position in an isometric midthigh pull

The IMTP was designed to approximate the body in the power position at the beginning of the second pull during the weightlifting exercises, power cleans and snatch (Haff et al., 1997). With respect to isometric tests, results of previous research examining the relationship between isometric bench press at different joint angles and dynamic performance suggest that the selection of joint angles should not be arbitrary. This is because the relationship between isometric tests and dynamic performance of interest varies substantially as a function of joint-angle (Murphy et al., 1995). The results of this study suggest that if isometric tests are to be used to infer the functional capacity of musculature in dynamic activities, the optimal angle for conducting these tests may be the joint angle at which peak force is developed during the performance of interest. As per the recommendations of Murphy and colleagues (1995), the position and joint angles in the IMTP correspond with the phases of power clean and snatch, during which the highest bar velocities and forces are generated (Garhammer, 1993; Haff et al., 1997). Consequently, it was argued that the position in an IMTP also provides the optimal mechanical advantage to elicit the maximum vertical isometric force, observed in recent studies (Beckham et al., 2012, 2018).

2.7.2 Isometric midthigh pull force-time history variables used to assess athletic performance

Strength is defined as the ability of the neuromuscular system to generate and exert force against an external resistance or object (Abernethy et al., 1995; Duchateau & Baudry, 2011; Enoka & Duchateau, 2018; Jaric, 2002; Suchomel, Nimphius, et al., 2016; Wilson & Murphy, 1996). In line with this, Thompson et al. (2020) defined maximal strength as the ability to exert maximal force against external resistance via maximal voluntary contraction. Strength is considered a key neuromuscular variable in many sports due to its influence on sporting success, with maximal strength underpinning performance in various athletic tasks (James et al., 2017). Assessment of force production capabilities form the basis of strength diagnosis, given its influence on a range of key performance indicators such as neuromuscular mechanical power (Cormie et al., 2011), endurance (Paavolainen et al., 1999) and injury prevention (Lauersen et al., 2014). Therefore, athlete profiling through the assessment of specific strength capabilities is critical to a successful training program.

Maximal strength or maximal force-generating capabilities can be evaluated using isometric muscle contractions during isometric tests. The IMTP, much like the other isometric tests

employed in the scientific literature, are used to obtain the force-time histories, which, in turn, enables key neuromuscular variables to be quantified. The variables of particular importance are peak force (PF) and rate of force development (RFD) (Haff et al., 2005)

2.7.2.1 Peak Force

Peak force (PF), often referred to as maximal strength in the applied setting, is defined by the neuromuscular ability to generate the greatest force possible above one's own body weight (BW), in a given test under specified conditions (Komi, 1994; Stone et al., 2004). Force is a vector quantity; therefore, the expression of strength has both direction and magnitude (Stone et al., 2003). For example, the intended direction of force application in a conventional IMTP is vertically upwards, while the force platforms measure reaction force at feet, due to the force at the feet acting downwards. The measurement of PF in N can be measured through inspection of the IMTP force-time (F/T) history. The one sample with the highest numerical value of the recorded VGRF during the sampling period of the F/T history can be quantified as the PF. Assessment of PF is straightforward since it does not require the identification of a start point or any additional data processing that may be necessary for other time-dependent variables.

Maximal force generated underpins performance in sports-specific tasks such as sprinting, jumping and change of direction (Suchomel et al., 2016). In consideration of the athletic population, PF is correlated to the rate at which the force is developed, decreased injury rates (Suchomel et al., 2016), monitoring fatigue during competitions (Hoffman et al., 2002), differentiating between athlete playing level and monitoring effectiveness of training programs (Sheppard et al., 2008). Given its influence on athletic success, the quantification of PF is considered a key variable when assessing performance in isometric tests.

2.7.2.2 Rate of force development

Biomechanically, the rate of force development (RFD) can be defined as the change in force divided by the time taken for the change to occur (eq. 2.3). From a physiological perspective, it refers to the ability of the neuromuscular system to increase contractile force from a low or resting level, when muscle activation is performed as quickly as possible (Rodríguez-Rosell et al., 2018). Often incorrectly referred to as 'explosive strength', RFD may also be defined by the instantaneous change in force from a low or resting level during rapid voluntary contractions (Maffiuletti et al., 2016). RFD is a neuromuscular variable derived from the force-time history recorded during rapid voluntary contractions, the quantification of which requires the identification of a starting point. It can be reported as either peak, average or the force at specific time points during a given performance test (Aagaard et al., 2002). Peak RFD (PRFD) can be defined as the highest numerical value of the first derivative of force with respect to time. (Moir et al., 2009; West et al., 2011). Average RFD can be calculated by dividing the PF by the time taken between initiation (0) and PF values (Brady et al., 2018)

$$Rate\ of\ Force\ Development\ (RFD)(N \cdot s^{-1}) = \frac{\Delta Force\ (N)}{\Delta Time\ (s)} \qquad 2.3$$

Δ= change in quantity.

The gold standard for measuring RFD is by analysing the force-time history recorded during an isometric maximal voluntary contraction (Bellumori et al., 2011; Tillin et al., 2012). Given the time-constrained nature of athletic tasks, the ability to produce force rapidly may be more important than maximum force production. This can be understood from equation 2.4, a generalised case of Newton's 2nd law, wherein the acceleration of a massive object or one's body mass is directly proportional to the force applied or generated (Suchomel et al., 2016).

$$Force\ (N) = mass\ (kg) \times acceleration\ (m \cdot s^{-2}) \qquad 2.4$$

It therefore follows that the faster the expression of a given force, the more rapid the corresponding acceleration occurs (Stone et al., 2003). Consequently, RFD is an important factor, especially in time-constrained rapid movements where a short contraction time may not allow maximal muscle force to be reached. The assessment of RFD has been used widely in the application of strength diagnosis. It has been evidenced to be a sensitive indirect marker of acute fatigue (Farup et al., 2016; Oliveira et al., 2016; Peñailillo et al., 2015) and exercise-induced neuromuscular fatigue (Thorlund et al., 2008). Further, RFD has also been used as a supplementary outcome measure for return-to-sport decisions following severe knee joint injuries (Angelozzi et al., 2012). The evaluation of RFD is influenced by several methodological factors including mode of contraction, type of instruction, method used to define and quantify RFD and devices used (Rodríguez-Rosell et al., 2018). While these factors have been covered in the IMTP literature, a valid and reliable method to determine the initiation of the activity, commonly referred to as start-time of the IMTP, remains to be validated and standardised. This is surprising as without a temporal start point, any time-constrained variables cannot be standardised between researchers.

2.7.3 Reliability of isometric midthigh pull variables

In general, isometric tests of neuromuscular function have been reported to have high test-retest reliability. In isometric tests, reliability coefficients of the key neuromuscular variables are often measured for trials performed on multiple days (interday/ between-session) or multiple trials performed on the same day (intertrial/ within-session) (Wilson & Murphy, 1996).

Haff et al. (2015) determined the minimum acceptable reliability for the IMTP with an ICC > 0.7 and CV < 15%. With respect to IMTP literature, PF (time-independent variable) has consistently demonstrated CV values of less than 10% (Beckham et al., 2012; Beckham et al., 2014; Dos'Santos et al., 2017; Secomb et al., 2015; Thomas, Comfort, et al., 2015; Thomas, Jones, et al., 2015). Studies contemporary to and predating Haff et al. (2015) that quantified time-dependent variables, such as RFD have shown variations exceeding 10% (Beckham et al., 2014; Thomas, Comfort, et al., 2015; Thomas, Jones, et al., 2015). This explains the reliability criteria set by Haff et al. (2015) for the IMTP, accounting for a range of variation observed especially for time-dependent variables quantified in previous studies. However, these values, ICC > 0.7 represents a low level of repeatability (Baumgartner & Chung, 2001), while a CV < 15% is considered too broad (Brady et al., 2018). Therefore, the previously recommended reliability threshold of an ICC $\geq$ 0.8 and CV $\leq$ 10% continues to be prevalent in the sports medicine and science literature (Hopkins, 2000). Standardisation of methods used to identify the start-time of an IMTP and subsequent calculation of time-dependent variables such as RFD, is likely to improve its reliability (Table 2.1).

With regards to CV, it is a statistical measure indicating the relative reliability of a distribution of repeated measurements. A small CV value suggests greater reliability in the measurements. However, the cut-off value used to indicate acceptable variability in a distribution of measurements is often chosen arbitrarily, typically up to 20% (Shechtman, 2013). Among these 15% is the most commonly used threshold (Shechtman, 2013). The usual CV of biological systems has previously been reported to lie between 10% and 15% (Stokes, 1985).

The reliability criteria remains an ongoing debate since clarification is needed regarding the context in which such reliability levels are applicable, whether it pertains to different athlete

levels or group versus individual testing. It is not stated in what context such reliability level could be used i.e., level of athlete and/or group or individual testing.

The reliability of IMTP was first reported by Haff et al. (1997) for PF (r = 0.93) and PRFD (r = 0.92). The study did not report the %CV for the measured variables, however it did set the ground for future research on the assessment of neuromuscular function using the IMTP. Subsequent research among throwers, weightlifters, powerlifters, rugby league, cyclists, tennis, softball, golf, soccer, volleyball and NCAA athletes (wrestlers, track and field, American football) only reported ICC as a measure of reliability and identified PF as a highly reliable variable (ICC ≥ 0.92) (Haff et al., 2005; Kawamori et al., 2006; Khamoui et al., 2011; Kraska et al., 2009; Leary et al., 2012; McGuigan et al., 2006; McGuigan & Winchester, 2008; Nuzzo et al., 2008; Stone et al., 2003, 2004, 2005; West et al., 2011).

A study investigating the isometric strength derived from IMTP amongst powerlifters in key positions of the conventional deadlift was the first to report the CV along with the ICC of PF. The results of the intra-session test-retest reliability demonstrated PF in the mid-thigh position as a reliable variable (ICC = 0.92 and CV = 5%) (Beckham et al., 2012). Several studies since have confirmed these findings demonstrating, so called 'near-perfect' reliability of PF in the IMTP (ICC ≥ 0.96 and %CV ≤ 4.3) among collegiate and NCAA D1 athletes across different sports and junior competitive surfers (Beckham et al, 2014; Dos'Santos et al., 2017 Haff et al., 2015; Secomb et al., 2015; Thomas, Comfort, et al., 2015; Thomas, Jones, et al., 2015). Furthermore, recent studies investigating the effect of body position (hip and knee angles) on IMTP kinetics have further demonstrated high reliability of PF (ICC ≥ 0.96 and %CV ≤ 5.5) at different joint angles (Beckham et al., 2018; Dos'Santos et al., 2017; Guppy et al., 2018).

Concerning RFD measures, PRFD is the most commonly assessed variable quantified using different methods reported in the scientific literature (Table 2.1). Using ICC as the only measure of reliability, PRFD has shown to be reliable in studies using the central difference method (numerical differentiation) (Haff et al., 1997, 2005; Kawamori et al., 2006; West et al., 2011) and across specific sampling windows (5 and 10-milliseconds) (ICC ≥ 0.80) (Beckham et al., 2013; Leary et al., 2012; Stone et al., 2003). RFD quantified using the RFD equation (eq. 2.3) at specific time bands (0–30, 0–50, 0–90, 0–100, 0–150, 0–200, and 0–250 milliseconds) have also been shown to be reliable (ICC ≥ 0.81) (Beckham et al., 2013; Leary

et al., 2012). Some studies have reported RFD to be a reliable variable (ICC ≥ 0.86) but failed to report the method of quantification (Kraska et al., 2009; McGuigan et al., 2006a) (Table 2.1). The method of calculations employed to quantify RFD measures is an important factor to consider to avoid variability in reliability measures. For instance, Khamoui et al. (2011) used the method to calculate average RFD (PF ÷ Time to PF) as defined by Haff et al. (2015) to quantify PRFD, therefore reporting unreliable results (PRFD, ICC = 0.74). While the existence of varying methods to quantify some RFD measures has implications, the level of reliability amongst these studies remains questionable, having only reported ICCs, which doesn't quantify the reliability in absolute terms.

Beckham et al. (2014) were the first to report both ICC and CV for an RFD measure. The average RFD (0-200 ms) quantified in the study met the criteria only for ICC (ICC = 0.90) however, the CV did not meet the criteria (CV = 16.9%). Similar results were observed in subsequent studies using the numerical differentiation to quantify PRFD, wherein CV exceeded the minimum acceptable limit of reliability (ICC ≥ 0.81, CV > 10%) (Thomas, Comfort, et al., 2015; Thomas et al., 2015). Haff et al. (2015) analysed PRFD during five different sampling windows, average RFD and RFD at seven specific time bands to elicit differences between methods for determining RFD during IMTP. The study's results demonstrate that RFD at all time bands is the only measure that appears to meet the acceptable levels of reliability set by Hopkins. (2000) and Brady et al. (2018) (ICC ≥ 0.8 and CV ≤ 10%). PRFD quantified using a 20 ms sampling window was deemed reliable as per the criteria set by the authors (ICC > 0.7 and CV < 15%) but not by the standards set by Hopkins. (2000) and Brady et al. (2018).

RFD is a time-dependent variable, and quantifying all RFD measures (PRFD, average RFD and RFD at specific time bands) requires identification of a start time of the maximal IMTP effort. On the contrary, PF does not require the identification of a start time, which may further explain why RFD measures' reliability remains questionable compared to PF. The lack of reliability in RFD measures may be partly due to the differences in quantification methods employed and the lack of attention to identifying a valid start time, Section 2..4; Table 2.1. Therefore, without the identification of a valid temporal start point, any time-constrained variables cannot be standardised between researchers.

Amongst earlier research, the studies that identified the initiation time of the maximal isometric effort reported PRFD as a reliable variable (ICC ≥ 0.877) (Comfort et al., 2015; West et al., 2011). While these studies reported ICC as the only measure of reliability, Dos'Santos et al. (2017) demonstrated high between and within-session reliability (ICC and CV) of RFD at predetermined time bands. The minimal acceptable reliability was in accordance with that determined by Haff et al. (2015) (ICC > 0.7 and CV < 15%), and the onset of the contraction was determined when vertical ground-reaction force (GRF) deviated 5 standard deviations (SDs) of body weight (BW). The reliability of RFD measures reported, must be interpreted with caution since the method of identifying a start-time varies across all three studies (Comfort et al., 2015; Dos'Santos et al., 2017; West et al., 2011). Thus, given the lack of agreement and Standardisation of methods used to identify an IMTP start-time and quantify time-dependent variables, it remains unclear whether the reported RFD measures are reliable.

More recently, Guppy et al. (2018) reported all time-dependent variables (time to PF, PRFD, RFD time bands) as unreliable after visually detecting the onset of force application. However, the study did not report the reliability (inter-rater and intra-rater reliability) of their visual detection methods. Furthermore, repeatability of visual detection method requires one to view the signal with a constant y-axis and x-axis scale, at a resolution that allows the visual assessment of signal characteristics (Tillin et al., 2010). These factors were not considered and may explain the results reported by Guppy et al. (2018).

2.7.4 Review of isometric midthigh pull methodologies

A review of 41 articles was undertaken after searching two academic databases, PubMed and Google Scholar using key words "isometric midthigh pull", "peak force" and "rate of force development". Table 2.1 provides a chronological listing of these articles, offering a comprehensive overview of the research methods employed in each of the studies. Of particular importance were, methods used to identify the start-time (onset threshold), output variable definition and method of output variable calculation (Table 2.1). The purpose of this review was to address the discrepancy in research methods employed in the IMTP scientific literature. Studies by established authors in the field of IMTP were of particular interest. Studies cross-referencing published methods with similar participant population were excluded. A systematic review of all articles since the seminal work by Haff et al. (1997) in

the field of IMTP was beyond the scope of the present thesis. However, the articles (n = 41) listed in Table 2.1, were deemed sufficient in addressing the purpose of the review.

The absence of methodological standardisation across studies when defining the start-time of an IMTP is illustrated in Table 2.1. A study investigating the relationship between force-time characteristics of the IMTP and dynamic performance in professional rugby league players (West et al., 2011), was the first to report a method of determining the start-time. It was an objective method, robust in terms of discriminating between variation of pre-pull force-time history and the start of the pull. The authors defined the start time of an IMTP as the instant after the startling command to 'PULL', that the first derivative exceeded the mean VGRF value during the quiescent state plus 5 SDs (Table 2.1). Papers prior and contemporary to the study by West et al. (2011), whilst reporting variables which necessitated determining the start-time, did not report the methods used to determine a value for the start-time (Beckham et al., 2013; Haff et al., 1997, 2015; Stone et al., 2004) or reported determination by subjective measures or arbitrary values e.g., 40 N change in force (Comfort et al., 2015). Investigating the effect of different onset thresholds on IMTP force-time variables, Dos'Santos and colleagues (2017) reported biases of between 20 ms to 330 ms in identification of a start-time. Clearly, this is unacceptable as even at the lower end of the biases, a 20 ms error in identifying the start-time would cause a 20% (time) error in the determination of force at 100 ms (F100). Given that the force-time history is at its steepest at this time, such an error would render the data unusable.

Currently, a robust method for validating any new or existing start-time methods does not exist within the IMTP literature. This may partly explain why a standard method has not been adopted and why identification of the start-time may have been poor within the literature. Further, the lack of reporting and agreement between studies in the method of identifying a start-time, it is reasonable to question the validity and reliability of time-dependent output variables reported in previous IMTP research, section 2.7.3. This highlights the need for investigating the theoretical validity of start-time methods that currently exist in the IMTP scientific literature. With this, the thesis sought to develop a tool capable of validating an IMTP start-time.

The expression of mechanical force often recorded using biomechanical instruments such as dynamometers (Tillin et al., 2010) or force platforms (Owen et al., 2014; West et al., 2011) is preceded by a physiological phenomenon of neural and muscular excitation. Acknowledging this principle, we proposed that the time of muscle onset during an IMTP recorded using surface electromyography (sEMG) would serve as an appropriate tool for validating the onset (start-time) of mechanical force production.

Table 2.1 *Reported analytical procedures of quantified variables and associated variable definitions amongst key research in IMTP arranged chronologically.*

Author	Onset Threshold	Sampling Frequency (Hz)	Quantified Variables	Variable Definition	Variable Calculation
Haff et al. (1997)	NR	500	PF, RFD, Time to PF and Time to PRFD	NR	PRFD ($N \cdot s^{-1}$) = 2 ms window
Stone et al. (2003)	NR	600	PF and PRFD	NR	PRFD ($N \cdot s^{-1}$) = 5 ms window
Stone et al. (2004)	NR	600	PF and PRFD	NR	PRFD ($N \cdot s^{-1}$) = 1.7 ms window
Stone et al. (2005)	NR	600	PF	† PF was determined as the maximum recorded force	NA
Haff et al. (2005)	NR	500	PF and PRFD	NR	PRFD (N·s-1) = 2 ms window
McGuigan et al. (2006)	NR	500	PF and PRFD	NR	PRFD ($N \cdot s^{-1}$) = 2 ms window
Kawamori et al. (2006)	NR	500	PF, PRFD, Time to PF and Time to PRFD	NR	PRFD ($N \cdot s^{-1}$) = 2 ms window
Haff et al. (2008)	NR	600	PF and PRFD	NR	PRFD ($N \cdot s^{-1}$) = 1.7 ms window
Nuzzo et al. (2008)	NR	1000	PF, Relative PF and RFD	† PF was defined as the maximum recorded force. Relative PF was calculated to account for body mass. RFD was defined as the PF divided by the time taken to achieve PF from the point of onset (0 s)	RFD ($N \cdot s^{-1}$) = PF ÷ Time to PF; Relative PF ($N.kg^{-1}$) = PF ÷ BM
Winchester et al. (2008)	NR	NR	PF and PRFD	NR	PRFD ($N \cdot s^{-1}$) = 2 ms window
McGuigan andWinchester (2008)	NR	960	PF and PRFD	NR	PRFD ($N \cdot s^{-1}$) = 1 ms window
Kraska et al. (2009)	NR	1000	PF, RFD, F50, F90 and F250	NR	NR
Whittington et al. (2009)	NR	1000	PF and PRFD	NR	NR

Table 2.1 *Continued.*

Author	Onset Threshold	Sampling Frequency (Hz)	Quantified Variables	Variable Definition	Variable Calculation
McGuigan et al. (2010)	NR	960	PF and PRFD	NR	PRFD (N·s-1) = 2 ms window
West et al. (2011)	Mean + 5 SD of the first derivative of VGRF during the quiescent phase	1000	PF, F100 and PRFD	PF, defined as the highest force value minus BW. F100, was defined as the absolute value of the VGRF minus BW 100 ms after start time. PRFD was defined as the maximum value of the first derivative of the VGRF-time history after start time.	PF (N) = Highest force value – BW; F100 = Absolute VGRF at 100 ms – BW; PRFD ($N \cdot s^{-1}$) = 1 ms window
Beckham et al. (2012)	NR	1000	PF	† PF was defined as the highest force value obtained	NR
Beckham et al. (2013)	NR	1000	PF, F100, F150, F200, F250 and PRFD	NR	RFD = 0-100 ms, 0-150 ms, 0-200 ms and 0-250 ms; PRFD = 5 ms window
Comfort et al. (2015)	Vertical force above 40 N	600	PF, PRFD, IP100, IP200 and IP300 ms	PRFD was calculated using the difference between two adjacent force values divided by the intersample time interval. Impulse was calculated by integration of the VGRF over 100, 200 and 300 ms windows.	PRFD ($N \cdot s^{-1}$) = 1.7 ms window
Thomas, Comfort, et al. (2015)	NR	600	PF, PRFD, IP100 and IP300	† PF was defined as the maximum force recorded from the force-time curve. PRFD was calculated by dividing the difference in consecutive force readings by the time interval	PRFD ($N \cdot s^{-1}$) = 1.7 ms window
Thomas, Jones, Rothwell, et al. (2015)	NR	600	PF, Relative PF, PRFD, IP100, IP200 and IP300	† PF was defined as the maximum force recorded from the force-time curve. Relative PF was calculated to account for body mass. PRFD was calculated by dividing the difference in consecutive force readings by the time interval.	PRFD ($N \cdot s^{-1}$) = 1.7 ms window Relative PF ($N.kg^{-1}$) = PF/ BM

Table 2.1 *Continued.*

Author	Onset Threshold	Sampling Frequency (Hz)	Quantified Variables	Variable Definition	Variable Calculation
Thomas, Jones, and Comfort (2015)	NR	600	PF	† PF was determined as the maximum recorded force	NR
Haff et al. (2015)	NR	1000	PF, F30, F50, F90, F100, F150, F200, F250, RFD 0-30, RFD 0-50, RFD 0-90, RFD 0-100, RFD 0-150, RFD 0-200, RFD 0-250, PRFD, AvgRFD	† The maximum force recorded was defined as the absolute PF. Force at 30, 50, 90, 100, 150, 200 and 250 ms were defined after the initiation of the pull. RFD was defined as the change in force divided by the change in time. This was applied to predetermined time bands. PRFD was defined as the highest RFD during different sampling windows. AvgRFD was defined as the PF divided by the time taken to achieve PF from the point of onset (0 s)	PRFD (N·s-1) = 2, 5, 10, 20, 30 and 50 ms windows. RFD (N·s-1) = ΔForce ÷ ΔTime; at time bands = 0-30, 0-50, 0-90, 0-100, 0-150, 0-200, 0-250 ms. AvgRFD (N·s-1) = PF ÷ Time to PF
Secomb, Farley, et al. (2015); Secomb, Lundgren, et al. (2015); Secomb, Nimphius, et al. (2015)	NR	600	PF and Relative PF	† PF was defined as the maximum recorded force. Relative PF was defined as the PF achieved divided by the body weight.	"Relative PF (N) = PF ÷ BW"
Tran et al. (2015)	NR	600	PF and Relative PF	NR	Relative PF ($N.kg^{-1}$) = PF ÷ BM
Spiteri et al. (2015)	NR	2000	Relative PF and Relative RFD at 30, 50, 90 and 100 ms time intervals	NR	NR

Table 2.1 *Continued.*

Author	Onset Threshold	Sampling Frequency (Hz)	Quantified Variables	Variable Definition	Variable Calculation
Sjökvist et al. (2015)	NR	600	PF and Relative PF	NR	NR
Welch et al. (2015)	NR	NR	PF and Relative PF	† PF was defined as the maximum force recorded from the force-time curve. PF was normalised to body weight to determine relative PF	Relative PF ($N.kg^{-1}$) = PF ÷ BM
Mangine et al. (2016); Wang et al. (2016)	NR	1000	PF, F30, F50, F90, F100, F150, F200, F250, RFD 0-30, RFD 0-50, RFD 0-90, RFD 0-100, RFD 0-150, RFD 0-200, RFD 0-250, PRFD	PF, defined as the maximum force value minus BW. Force at 30, 50, 90, 100, 150, 200 and 250 ms were defined as the absolute value of the VGRF minus BW 30, 50, 90, 100, 150, 200 and 250 ms after the start time respectively RFD was defined as the change in force divided by the change in time. This was applied to predetermined time bands. PRFD was defined as the highest RFD determined across a 20 ms sampling window.	PF (N) = Maximum Force – BW; F30 (N) = Absolute VGRF at 30 ms – BW; F50 (N) = Absolute VGRF at 50 ms – BW; F90 (N) = Absolute VGRF at 90 ms – BW; F100 (N) = Absolute VGRF at 100 ms – BW; F150 (N) = Absolute VGRF at 150 ms – BW; F200 (N) = Absolute VGRF at 200 ms – BW; F250 (N) = Absolute VGRF at 250 ms – BW RFD (N·s-1) = ΔForce ÷ ΔTime; at time bands = 0-30, 0-50, 0-90, 0-100, 0-150, 0-200, 0-250 ms PRFD (N·s-1) = 20 ms window

Table 2.1 *Continued.*

Author	Onset Threshold	Sampling Frequency (Hz)	Quantified Variables	Variable Definition	Variable Calculation
Dos'Santos et al. (2016)	VGRF above 75 N	2000, 1500, 1000, 500	PF, F100, F150, F200 RFD 0-100, RFD 0-150, RFD 0-200	† Maximum recorded force was defined as PF. Force at 100, 150 and 200 ms were defined after VGRF exceeded the onset threshold of 75 N RFD was defined as the change in force divided by the change in time. This was applied to predetermined time bands.	RFD (N·s-1) = ΔForce ÷ ΔTime; at time bands = 0-100, 0-150, 0-200 ms
Bartolomei et al. (2017)	NR	1000	PF and PRFD	NR	PRFD ($N \cdot s^{-1}$) = 20 ms window
James et al. (2017)	Force of 20 N above rest	1000 100	PF, F30, F50, F100, F150, F200, F250, RFD 0-30, RFD 0-50, RFD 0-100, RFD 0-150, RFD 0-250, PRFD	† Greatest force value at any point during the trial was defined as the PF Force at 30, 50,100, 150, 200 and 250 ms were defined after VGRF exceeded the onset threshold of 20 N RFD was defined as the change in force divided by the change in time. This was applied to predetermined time bands PRFD was defined as the highest RFD determined across a 20 ms sampling window.	RFD (N·s-1) = ΔForce ÷ ΔTime; at time bands = 0-30, 0-50, 0-100, 0-150, 0-250 ms PRFD (N·s-1) = 20 ms window

Table 2.1 *Continued.*

Author	Onset Threshold	Sampling Frequency (Hz)	Quantified Variables	Variable Definition	Variable Calculation
de Witt et al. (2018)	NR	1000	PF, F30, F50, F90, F100, F150, F200, F250, RFD 0-30, RFD 0-50, RFD 0-90, RFD 0-100, RFD 0-150, RFD 0-200, RFD 0-250, PRFD	† The maximum force recorded was defined as the absolute PF. Force at 30, 50, 90, 100, 150, 200 and 250 ms were defined after the initiation of the pull. RFD was defined as the change in force divided by the change in time. This was applied to predetermined time bands. PRFD was defined as the highest RFD determined across a 20 ms sampling window	RFD (N·s-1) = ΔForce ÷ ΔTime; at time bands = 0-30, 0-50, 0-90, 0-100, 0-150, 0-200, 0-250 ms PRFD (N·s-1) = 20 ms window
Dos'Santos, Jones, et al. (2017)	Force above; 5 SD from BW, 2.5% from BW, 5% from BW, 10% from BW, > 75 N from BW	1000	PF, F100, F150, F200 RFD 0-100, RFD 0-150, RFD 0-200	BW was calculated as the average force during the 1 s of stationery weighing period in IMTP position immediately before initiation of pull. † Maximum recorded force was defined as PF. Force at 100, 150 and 200 ms were defined after VGRF exceeded the onset threshold of 75 N RFD was defined as the change in force divided by the change in time. This was applied to predetermined time bands.	RFD (N·s-1) = ΔForce ÷ ΔTime; at time bands = 0-100, 0-150, 0-200 ms
Dos'Santos et al. (2018)	40 N above average BW during weighing period	1000	PF, F30, F50, F90, F100, F150, F200, F250	† Maximum force generated during the trial was defined as the PF. Force at 30, 50,100, 150, 200 and 250 ms were defined after VGRF exceeded 40 N above average BW during the weighing period	NR

Table 2.1 *Continued.*

Author	Onset Threshold	Sampling Frequency (Hz)	Quantified Variables	Variable Definition	Variable Calculation
Dos'Santos, et al. (2017)	Above 5 SD of BW	1000	PF, F100, F150, F200, RFD 0-100, RFD 0-150, RFD 0-200	BW was calculated as the average force during the 1 s of stationery weighing period in IMTP position immediately before initiation of pull. † Maximum recorded force was defined as PF. Force at 100, 150 and 200 ms were defined as the absolute value of the VGRF minus BW 100, 150 and 200 ms after the start time respectively. RFD was defined as the change in force divided by the change in time. This was applied to predetermined time bands.	F100 (N) = Absolute VGRF at 100 ms – BW; F150 (N) = Absolute VGRF at 150 ms – BW; F200 (N) = Absolute VGRF at 200 ms – BW RFD (N·s-1) = ΔForce ÷ ΔTime; at time bands = 0-100, 0-150 and 0-200 ms
Beckham et al. (2018)	Visual Inspection	1000	PF F50, F90, F200, F250	Force at 50, 90, 200 and 250 ms were defined after the initiation of the pull.	NR
Oranchuk et al. (2019)	"Above 2.5% of BM"	1000	Relative PF, Relative Force at 50, 100, 150, 200 and 250 ms PRFD	PRFD was defined as the highest RFD determined across a 20 ms sampling window.	Relative PF ($N.kg^{-1}$) = PF ÷ BM PRFD (N·s-1) = 20 ms window
Townsend et al. (2019)	NR	1000	PF, F50, F100, F150, F200, F250 RFD 0-100, RFD 0-150, RFD 0-200, RFD 0-250	† Maximum recorded force was defined as PF. Force at 50, 100, 150, 200 and 250 ms were defined after the initiation of the pull RFD was defined as the change in force divided by the change in time. This was applied to predetermined time bands.	RFD (N·s-1) = ΔForce ÷ ΔTime; at time bands = 0-50, 0-100, 0-150, 0-200 and 0-250 ms

Table 2.1 *Continued.*

Author	Onset Threshold	Sampling Frequency (Hz)	Quantified Variables	Variable Definition	Variable Calculation
Brady et al. (2020)	Above 5 SD of Baseline VGRF	1000	PF, Relative PF, F100, F150, F200 RFD 0-100, RFD 0-150, RFD 0-200 IP100, IP200	† Maximum recorded force was defined as PF Force at 100, 150, 200 ms were defined after the initiation of the pull. RFD was defined as the change in force divided by the change in time. This was applied to predetermined time bands Impulse at 100 and 200 ms were defined as the average force divided by the change in time over 100 and 200 ms.	RFD (N·s-1) = ΔForce ÷ ΔTime; at time bands = 0-100, 0-150 and 0-200 ms
Baena-Raya et al. (2021)	Above 5 SD of BW	1000	PF (10 ms, 1, 2, 3 s) moving average F50, F100, F150, F200. RFD 0-50, RFD 0-100 RFD 0-150 RFD 0-200	† PF was defined as the maximum force generated using time intervals of 10ms, 1, 2 and 3 s applying moving average windows Force at 100, 150, 200 ms were defined after the initiation of the pull. RFD was defined as the change in force divided by the change in time. This was applied to predetermined time bands	RFD ($N \cdot s^{-1}$) = ΔForce ÷ ΔTime; at time bands = 0-50, 0-100, 0-150 and 0-200 ms
Comfort et al. (2022); Thomas et al. (2021)	Above 5 SD of BW	1000	PF, Relative PF, Absolute and Relative = F50, F100, F150, F200, F250	† Maximum recorded force was defined as PF Absolute Force at 50, 100, 150, 200 and 250 ms were defined after the initiation of the pull. Relative Force at 50, 100, 150, 200 and 250 ms were defined after the initiation of the pull respectively divided by BM	Relative PF ($N.kg^{-1}$) = PF ÷ BM Relative F50 ($N.kg^{-1}$) = F50 ÷ BM; Relative F100 ($N.kg^{-1}$) = F100 ÷ BM; Relative F150 ($N.kg^{-1}$) = F150 ÷ BM; Relative F200 ($N.kg^{-1}$) = F200 ÷ BM Relative F250 ($N.kg^{-1}$) = F250 ÷ BM

BW = Body weight; BM = Body mass; SD = Standard deviation; Δ = change

VGRF = Vertical component of ground reaction force; PF = Peak force; RFD = Rate of force development

PRFD = Peak rate of force development; F30, F50, F90, F100, F150, F200, F250 = Force at specific time points (ms); IP = Impulse; IP100, IP200 and IP300 = Impulse at specific time points (ms)

† = Peak force quantified without subtracting body weight

NR = Not reported

.

2.8 Surface electromyography

The electrophysiological combination that results in skeletal muscle contraction within the human body initiates mechanical force production for performance in static and dynamic motor tasks (Garcia & Vieira, 2011; Disselhorst-Klug et al., 2009). The prospect of examining the activation of skeletal muscles by recording electrical potentials produced during muscle contractions is particularly relevant in sports science and biomechanics (De Luca, 1997). The electrical signal associated with the contraction of a muscle (myoelectric signals) is called an electromyogram (EMG) (Garcia & Vieira, 2011). Surface electromyography (sEMG) is a technique used to study these EMG signals obtained from superficial muscles non-invasively with electrodes placed on the skin's surface (Garcia & Vieira, 2011).

The motor unit is the most fundamental functional unit in the neuromuscular system responsible for skeletal muscle contraction and the resulting force production (Hunter et al., 2016). Defined as the final common pathway, the motor unit transmits an activation signal originating in the brain stem or spinal cord and transforms it into contractile activity (Duchateau et al., 2006). The motor unit comprises a motor neuron, its axon and all the muscle fibres that the axonal branches innervate (Figure 2.11). A synaptic input from the brain stem or spinal cord above a threshold depolarises the cell membrane (sarcolemma, surrounding each muscle fibre) potential of a motor neuron. The depolarisation causes the influx of sodium (Na^+) and efflux of potassium (K^+) ions, thereby generating an action potential that propagates along the axon of a motor neuron towards the neuromuscular junction (NMJ) (Enoka & Duchateau, 2018). The NMJ, often anatomically located near the middle of a muscle fibre, is a synaptic connection across which the axonal action potentials are transmitted to the innervated muscle fibres (Figure 2.11). The action potentials generated in the innervated muscle fibres are conducted towards the ends of muscle fibres in both directions from the NMJ, resulting in contraction. The summation of these axonal and several hundred muscle fibre action potentials are called motor unit action potentials (MUAP) and represents the underlying mechanism of skeletal muscle contraction (Enoka & Duchateau, 2018).

The depolarisation due to ionic flow and associated action potential currents produces changes in the electric potential, recorded using surface electrodes. In other words, sEMG

records the summation of action potentials generated from the concurrently active motor units detected by electrodes attached to the skin over the muscle.

Therefore, skeletal muscle contraction results from a series of synaptic inputs originating in the central nervous system (CNS) that are transmitted to the muscle fibres (Figure 2.11). While an EMG signal is the digitised electrical manifestation of the neuromuscular activation associated with a contracting muscle, thus providing- insight into how the neuromuscular system behaves. EMG electrodes are highly sensitive voltmeters used to detect the physiological phenomenon of depolarisations and hyperpolarisations (increases and decreases in voltage, respectively) that occur on the muscle fibre membrane, the sarcolemma (Vigotsky et al., 2018).

The three primary applications of sEMG signal that dominate the field of biomechanics are: its use as an indicator for the initiation of muscle activation, its relationship to the force produced by the muscle and prediction of the onset of contractile fatigue occurring within a muscle (De Luca, 1997).

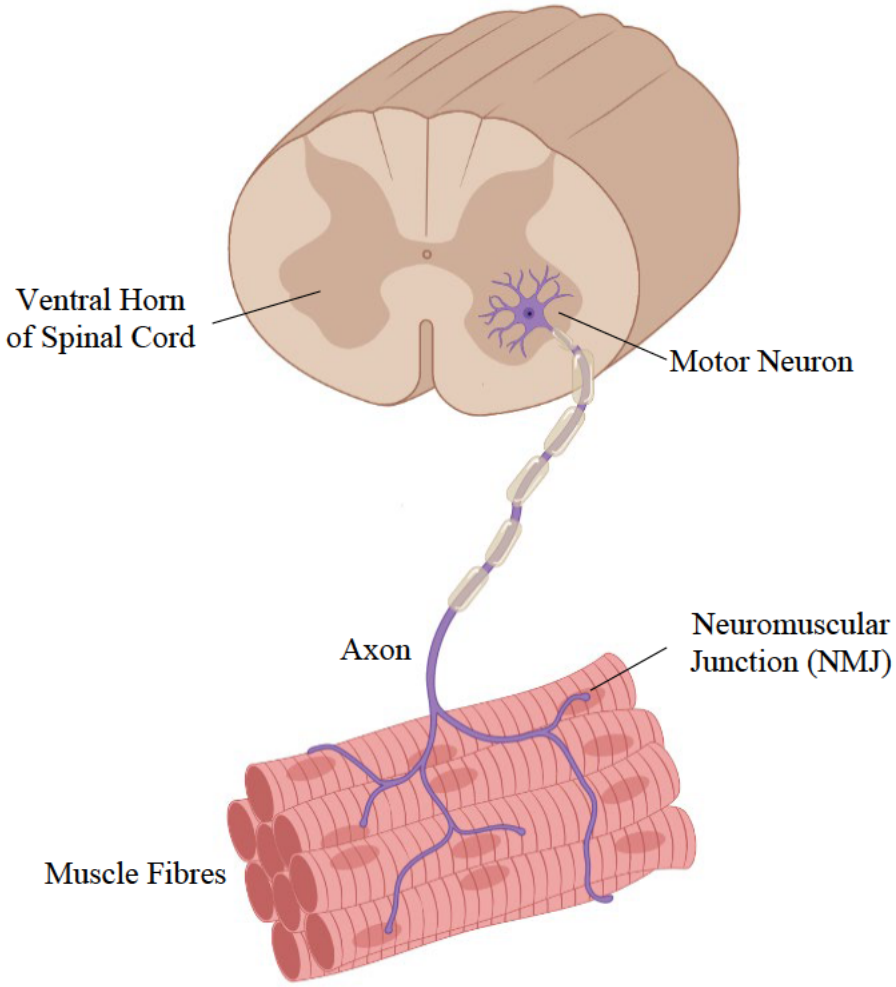

Figure 2.11 *The motor unit is composed of the motor neuron originating in the ventral horn of the spinal cord and the muscle fibres its axon innervates. Adopted from Sherrington's concept of the 'final common pathway' (Burke, 2007; Heckman & Enoka, 2012; Liddell & Sherrington, 1925). Created with BioRender.com*

2.8.1 Existing methods used to determine the time of muscle onset

One important application of EMG, amongst many, is the detection of temporal characteristics of muscle recruitment, such as onset times (Crotty et al., 2021). The precise detection of muscle onset times forms a pre-requisite in studies of biomechanics, neuromuscular performance, motor control, gait and posture analysis. For instance, temporal analysis of sEMG signals have been widely used to quantify the electromechanical delay (EMD) (Tillin et al., 2010). EMD refers to the delay between muscle activation and force production, often used as a determinant of musculoskeletal performance across a variety of tasks and muscles (Crotty et al., 2021; Tillin et al., 2010). Analysis of sEMG signals to quantify the precise onset time is one of the most commonly studied parameters, however, the methods of detection vary across the scientific literature. Further a large variability of EMG signal patterns exists across different muscles, populations and movement tasks making the onset detection a challenging task (Yang et al., 2017). Consequently, a wealth of research has focused on determining the optimal onset detection methods with high validity and reliability that would enable comparisons between muscles, participants and experimental conditions.

2.8.1.1 Visual detection

Visual detection or manual visual identification is considered the 'gold standard' method for locating the point representative of the time of muscle onset in a neuromuscular test (Allison, 2003; Buckthorpe et al., 2012; Crotty et al., 2021; Hodges & Bui, 1996; Staude, 2001; Tillin et al., 2010; Van Boxtel et al., 1993). With reference to a pre-set definition of signal onset, this method requires skilled experimenters to examine the sEMG traces and visually determine the time of muscle onset. For example, the time of muscle onset has previously been defined as the last point of the trough (base of the first peak) before the signal deflects away from baseline noise (Crotty et al., 2021; Tillin et al., 2010). Muscular activity patterns resulting from pre-tension or movement just before the onset of intended activity are generally referred to as the baseline noise. Thus, noise is any unwanted signal (Challis, 2008).

Dependent on the experience of the assessors, the method of visual detection is associated with variability due to errors within and between researchers, especially when the signal-to-noise ratio (SNR) is low. Furthermore, it is considered to be time-consuming, involving a risk of subjective bias (Crotty et al., 2021; Tenan et al., 2017).

To counter these limitations, several automated computer-based detection methods have previously been employed in the literature. These automated methods were developed to increase objectivity and reduce experimenter bias while concurrently optimising analysis time. The automated methods recently reported in the literature for the neuromuscular assessment of muscle activity onset during explosive isometric contractions include: the threshold-based method (TBM) (Allison, 2003; Crotty et al., 2021; Hodges & Bui, 1996), approximated generalised likelihood ratio (AGLR) (Crotty et al., 2021; G. Staude et al., 2000; G. Staude & Wolf, 1999) and Teager-Kaiser energy operator (TKEO) (Crotty et al., 2021; Solnik et al., 2010).

2.8.1.2 Threshold based method

The threshold-based method (TBM) involves the calculation of the mean and standard deviation (SD) of the muscle baseline amplitude characteristics to determine a threshold value. The onset of muscle activity is then defined as the first time point that exceeds the threshold value. The TBM method is dependent on the processing methods (filtering), the magnitude of deviation from baseline muscle activity required to indicate the threshold (SD) and the number of samples that must exceed the threshold value. Consider the following equation, where the threshold '*T'* is determined as;

$$T = \mu + h.\sigma \qquad 2.5$$

μ = mean; σ = Standard deviation (SD); h = numerical threshold value

With reference to equation 2.5, it is worth noting that the '±' sign is not used since the signal has been full-wave rectified, as such only positive values are displayed. Therefore, TBM involves the identification of a point where the mean of a specified number of samples exceeds the baseline noise by a specified number of SD.

Previous research evaluated the differences in TBM parametric combinations and its influence on muscle activity onset detection in a single-joint postural task of rapid shoulder extension, flexion and abduction. A total of 27 possible parameter combinations were compared which varied in EMG signal processing (low-pass filtering at 10, 50 and 500 Hz), threshold value (1,2 and 3 SD above baseline noise) and the number of samples for which the mean must exceed the calculated threshold (25, 50 and 100 ms). In comparison to the visual

detection method, of the 27, 3 parametric combinations that most accurately approximated the EMG onset times were identified. These combinations were reported as "number of samples/ threshold value/ low-pass filter frequency"; 25 ms/ 3 SD/ 50 Hz, 50 ms/ 1 SD/ 50 Hz and 10 ms/ 1 SD/ 500 Hz. Therefore, the results highlighted that multiple parametric combinations could accurately approximate onset times (Hodges & Bui, 1996)

The study showed that excessive smoothing of the data by applying a low-pass filter of 10 Hz to an already bandpass filtered (10-1000 Hz) signal resulted in errors of 56.44-144.87 ms prior to the visually determined value. Conversely, insufficient data smoothing resulted in delayed identification of muscle activity onset. The low pass filter frequency of 500 Hz in this study produced errors of 60.4-153.49 ms after the visually derived EMG onset (Hodges & Bui, 1996). The 3 parametric combinations that most accurately identified the onset of muscle activity resulted from the most appropriate combinations of the positive and negative influences of each of the parameters. The study also reported, consistently delayed onset values for EMG traces with high baseline noise when identified using TBM compared to visual detection (Hodges & Bui, 1996).

Despite the 3 parametric combinations capable of accurately approximating EMG onset, the results recommend the use of visual inspection for characterization of EMG traces prior to the application of different parameter combinations (Hodges & Bui, 1996).

2.8.1.3 Approximated generalised likelihood ratio

Another commonly applied computerised automated method used for detecting the onset of muscle activity is the approximated generalised likelihood ratio (AGLR) test. Developed by Staude et al. (2000), the test is highly complex and computationally expensive. It involves the segmental comparison of a signal to see the likelihood of them being statistically different using a pre-defined likelihood threshold.

$$g(n) = \ln\left(\prod_{n=1}^{k} \cdot \frac{(p1\ (x_n)|H_1)}{(p0\ (x_n)|H_0)}\right) \gtrless h \qquad 2.6$$

As per the equation 2.6, the AGLR is based on the generalised likelihood test (GLR) '$g(n)$' statistically testing two hypotheses. The null hypothesis 'H_0' indicates no change within the analysed segment of the EMG signal and alternate hypotheses 'H_1' indicates that change has occurred in the analysed segment. 'H_0' and 'H_1' describe the statistical properties of series of EMG samples $x_{1,}\, x_{2,}\, x_{3,}\, \ldots\ldots\, x_{k.}$ In the equation, 'ln' is the natural logarithm, 'x_n' represents a series of EMG samples '$p1$' and '$p0$' represent the probability density associated with 'H_1' and 'H_0' respectively. When '$g(n)$' becomes higher than the pre-set threshold 'h' then the alternate hypothesis 'H_1' is more probable and signal change is detected within the analysed segment of the EMG signal. The AGLR hypothesis test is performed over a predefined sliding window of size *L* (e.g., 25 ms). A log-likelihood ratio is calculated for every location of the window step, along the series of EMG data. After the signal change is detected, the estimated onset time is found by maximising the likelihood estimators for each sample from the last window position (Crotty et al., 2021; G. Staude et al., 2000).

Therefore, EMG onset detection can be considered a binary testing problem between the null hypothesis related to a relaxed state of the muscle (baseline noise) with no change in statistical properties of the sequence and the alternate hypothesis related to a contracted state with a change in statistical properties.

Previous studies have employed AGLR for detection of muscle activity onset in gait analysis (Roetenberg et al., 2003), muscle reflex responses in sudden trunk loading (Cholewicki et al., 2005; Lee et al., 2007) and maximal voluntary contractions (MVC) during isometric knee extensions (Solnik et al., 2010). The AGLR method consistently demonstrated greater accuracy in estimating activity onset compared to TBM when applied to both artificially simulated and experimental signals in these studies (Cholewicki et al., 2005; Lee et al., 2007; Roetenberg et al., 2003; Solnik et al., 2010).This was due to the results suggesting TBM to be more sensitive to random fluctuations in signal amplitude (baseline noise) immediately before muscle contractions during the intended activity. Consequently, the TBM consistently generated false onset detections in comparison to the AGLR method.

2.8.1.4 Teager-Kaiser energy operator

In a different study, the AGLR test was compared to the Teager-Kaiser energy operator (TKEO) for the detection of muscle activity onset (Li & Aruin, 2005). TKEO, has previously been used in speech signal analysis (Maragos et al., 1993) and in the detection of neural spikes and spiky waveforms in electroencephalography (EEG) signals, a neurophysiological technique that records electrical activity in the brain (Kim & Kim, 2000, 2003; Mukhopadhyay & Ray, 1998). Defined in the time domain, the discrete TKEO 'Ψ' is described by the equation;

$$\Psi[x(n)] = x^2(n) - x\,(n+1)\,x\,(n-1) \qquad 2.7$$

Here 'x' is the EMG value and 'n' is the sample number. Therefore, the output of TKEO is proportional to the product of the instantaneous amplitude and frequency of the input signal. Simultaneously considering the instantaneous frequency and amplitude information of the artificially simulated sEMG signals, TKEO was first applied to make the action potential spikes clearer. Then a threshold level in the TKEO output was determined by equation 2.5. The onset time of the muscle activity was then defined as the point where the TKEO output exceeded the determined threshold. The results of the study (Li & Aruin, 2005) were reported as the mean and SD of latency which was smaller for AGLR (SNR 10 dB; 11.28 ± 7.55 ms) at high SNR when compared to the TKEO method (SNR 10 dB; 19.06 ± 24.78 ms). Conversely, in the case of poor signal quality (SNR: 2 dB) the mean and SD of latency was lowest for TKEO (28.76 ± 30.59 ms) performing better than the AGLR method (45.77 ± 10.32 ms). Therefore, the AGLR performs best in the presence of high SNR, while TKEO is capable of dealing with low SNR signals.

The findings of Li and Aruin (2005), Li et al. (2007) and the preliminary data reported by Solnik et al. (2008) suggest the use of TKEO as a signal conditioning tool as opposed to a method for onset detection. Consequently, Solnik et al. (2010) studied whether the inclusion of TKEO in signal conditioning would increase the accuracy of visual detection, AGLR and TBM. As hypothesized signal conditioning with TKEO demonstrated marked improvements in the accuracy of all three methods compared to conditioning without TKEO. Most notable improvements of TKEO conditioning in onset detection accuracy was reported for the AGLR method on sEMG signals reconstructed from isometric knee extension MVCs. Further, the

accuracy of visual detection compared with the true (known) onset times of the reconstructed signal improved following TKEO conditioning.

More recently, Crotty et al. (2021) examined the acceptability of TKEO, AGLR and TBM as alternatives to visual sEMG onset detection across experimental isometric contractions with varying rates of amplitude increases. Based on the evidence provided by Solnik et al. (2010), the study also compared the accuracy of all four detection methods with and without TKEO as a signal conditioning step. TKEO as a detection method and AGLR with TKEO conditioning displayed the best agreement with visual detection of the onset time. AGLR with TKEO conditioning had a lower level of bias (2.0 ± 8.4 ms) compared to TKEO as a detection method (4.7 ± 5.6 ms). Despite these positive results, the automated methods did not produce acceptable agreement of detection bias in the region of 3 ms compared to visual detection (Crotty et al., 2021). The results of the study suggest that automated methods are not sensitive enough to be applied as a detection method when relating EMG onset to a motor event of short duration. Further, inclusion of TKEO as conditioning step improved both the intra-rater and inter-rater reliability for visual detection across contractions of varying rates of amplitude increases (ICC = 0.998 – 1.000). Consequently, the inclusion of TKEO in signal processing prior to visual detection of sEMG onset is recommended by the authors, to improve visual detection reliability, especially when analysing fast explosive contractions (Crotty et al., 2021).

2.8.2 Signal conditioning using Teager-Kaiser energy operator

Surface electromyography (sEMG) is a widely used method employed in the scientific literature to study biomechanical aspects and neuromuscular functions of human movement and performance. A fundamental application of the sEMG, via temporal analysis of the signal, is the precise detection of motor events, such as determining the exact onset time of muscle contraction (De Luca, 1997). However, due to the stochastic characteristics of the sEMG signal that is the random fluctuations in the signal, precise detection of temporal characteristics of muscle recruitment can be challenging. This is especially the case when the sEMG response of a muscle is weak, and the signal-to-noise ratio (SNR) is very low (Li et al., 2007). EMG signals with high baseline noise and low amplitude are prone to false detection by visual inspection, thereby increasing the magnitude of error (Solnik et al., 2010). Signal conditioning methods such as the Teager Kaiser energy operator (TKEO) have previously been used to reduce movement artefacts and minimise background noise, thereby facilitating precise onset detection (Crotty et al., 2021; Li et al., 2007; Solnik et al., 2010). The TKEO was first derived in 1990 in the discrete-time domain to compute the energy of sound and later modified to cover continuous signals (Li et al., 2007). The output of TKEO applied to speech signals was proportional to the input signal's instantaneous amplitude and frequency (Li et al., 2007). Similarly, in biological signals, muscle contraction and firing of associated MUAPs are accompanied by a rapid increase in signal amplitude and frequency. Therefore, TKEO can measure instantaneous energy changes in biological signals composed of time-varying amplitude and frequency. As such, TKEO is a widely accepted conditioning tool for biological signal processing, including the detection and classification of motor events from sEMG signals (Crotty et al., 2021; Li et al., 2007; Solnik et al., 2010).
The discrete TKEO Ψ proportional to the product of the instantaneous amplitude and frequency employed as a conditioning tool in the current study is defined as per equation 2.7

TKEO improves the signal-to-noise ratio by accentuating the amplitude and frequency properties of MUAP, making the action potential spikes sharper and narrower, as seen in Figure 2.12. Since the frequency of muscle contraction is higher than background noise, conditioning with TKEO, the muscle activity signal is more pronounced versus the background noise (Figure 2.12 B) (Crotty et al., 2021).
Therefore, the suppression of baseline noise and simultaneous amplification of the EMG burst due to muscular contraction reduces erroneous visual detection of the time of muscle

onset (Figure 2.12). Recognising that TKEO can markedly improve the method of visual detection by improving the EMG signal-to-noise ratio, previous research demonstrated that TKEO is most effective when used as a step in signal conditioning (Crotty et al., 2021; Li et al., 2007). Considering its properties and documented advantages in visually detecting the onset of muscle activity, TKEO was used in the current study as a conditioning tool prior to sEMG temporal analysis.

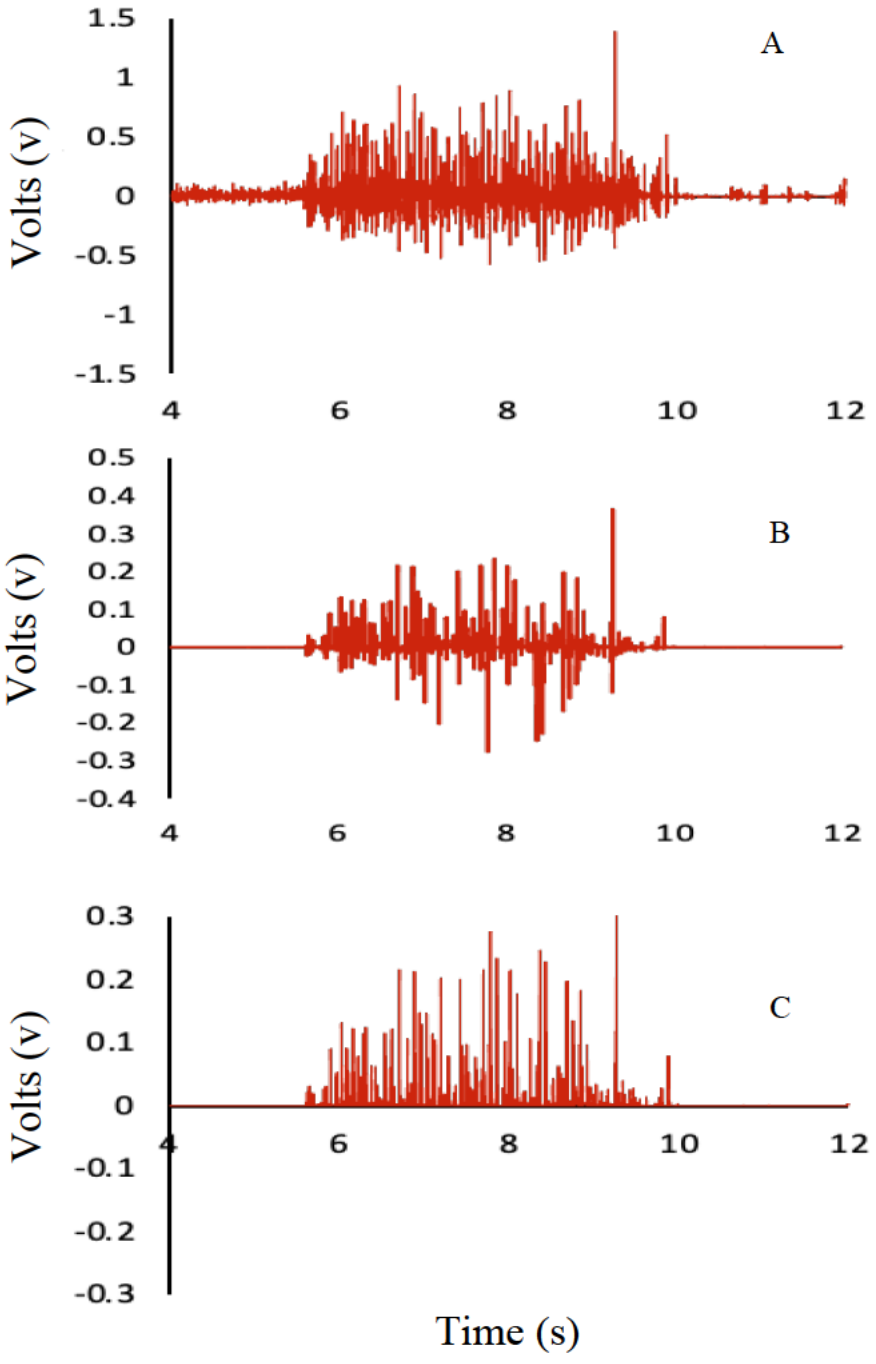

Figure 2.12 *(A)* It is an s*EMG signal obtained from the right bicep femoris of a participant during the IMTP. The trace has been band-pass filtered in both directions between 10 and 400 Hz using a 4th-order Butterworth digital filter and amplified by 1000. (B) Is the TKEO conditioned output of the trace suppressing the baseline noise in (A). (C) Full-wave rectification of the trace in (B) is the final step in signal processing before visual detection of muscular activity onset. From (A) to (C) the figure illustrates the suppression of noise, improving the SNR, thus facilitating more valid analysis.*

2.8.3 Visual detection of time of muscle onset

The automated methods used to identify the time of muscle onset (T_{mo}), generally rely on the baseline signal amplitude characteristics for deriving a threshold value above which T_{mo} may be assumed (section 2.8.1). As previously discussed, these include, TBM, AGLR and TKEO. However, the threshold value is sensitive to changes in the baseline amplitude. To elaborate, low levels of baseline amplitude reduce the threshold value, resulting in early-onset detection, while high baseline amplitude may result in late detection of the true onset (Allison, 2003; Crotty et al., 2021; Hodges & Bui, 1996). Threshold-dependent methods like such are robust only in the presence of a high signal-to-noise ratio (SNR) coupled with a high frequency of amplitude increases (Crotty et al., 2021; Hodges & Bui, 1996; Li et al., 2007; Li & Aruin, 2005).

The results of the established automated methods were derived from single-joint neuromuscular tests of arm raising (Allison, 2003), shoulder flexion, extension and abduction (Hodges & Bui, 1996), isometric ankle plantarflexion and dorsiflexion (Crotty et al., 2021) and isometric knee extension (Solnik et al., 2010). These tests were performed in a standing upright or in a seated position wherein movement artefacts due to manipulation of multiple joints is assumed to be negligible. Further contributors to relatively quiet baseline amplitude characteristics is the relative ease of maintaining focused control in movement and holding position of a single joint prior to the initiation of the test. However, in a multi-joint test such as the IMTP, a participant must hold joint angles replicating the highest force-producing position of a dynamic power clean (Haff et al., 1997). As such, the muscular activity of muscles responsible for holding position and pre-tension in other muscles is likely to display high levels of activity (noise) prior to the test onset.

The results highlighting the efficacy of TBM, AGLR and TKEO detection methods were obtained from analysing artificially simulated or reconstructed signals (Li et al., 2007; Li & Aruin, 2005; Solnik et al., 2008, 2010). When these methods were recently applied to experimental data consisting of fast explosive isometric contractions, the automated methods lacked the desired accuracy to be used interchangeably with visual detection (Crotty et al., 2021).

In contrast to the automated computer-based methods for determining the onset of muscle contraction, visual detection is more sensitive and accurate. This is primarily because visual detection is minimally influenced by either SNR or movement artefacts likely to be associated with the IMTP (Allison, 2003; Crotty et al., 2021; Hodges & Bui, 1996). Further, computer-based automated methods are often validated against visual detection (Allison,

2003; di Fabio, 1987; Hodges & Bui, 1996). Consequently, manual inspection of baseline muscle activity, determination of T_{mo} and characterisation of obtained sEMG signal forms a prerequisite to any automated method used in research.

2.9 Chapter summary

It is clear from the existing literature that despite the numerous studies using IMTP for neuromuscular performance analysis in athletes, there is no agreed methodology on the identification of a valid start-time. Therefore, it is reasonable to question the validity and reliability of time-dependent output variables reported in previous IMTP research. This highlights the need for investigating the theoretical validity of start-time methods that currently exist in the IMTP scientific literature. As such the thesis sought to develop a reliable method capable of validating the IMTP start-time. The physiological phenomenon of neural and muscular excitation precedes the expression of mechanical force production in motor tasks. The use of biomechanical instruments, sEMG and FP in conjunction allows concurrent assessment of neuromuscular excitation and mechanical force production respectively, in a given motor task. Therefore, it was proposed that, determining the onset of excitation in several muscles using sEMG could be used to validate a start-time method of an IMTP performed on a force platform or used in other studies that need knowledge of such variables. While onset times of muscular activity has been determined in single-joint isometric tests of neuromuscular function using sEMG, it is not the case for multi-joint isometric tests. To the author's knowledge, there are no reported studies investigating the onset of several muscles in a multi-joint isometric test using sEMG. Consequently, the reliability of determining the onset of muscle activity remains to be investigated.

With this the main aim of the thesis was to develop a reliable method for detecting the time of muscle onset (T_{mo}) in an IMTP. The objectives used to guide the research conducted in the present thesis are as follows

I. Select muscles, based on the literature, that are most likely to be activated during the performance of an IMTP
II. Develop a method for the identification of the instant corresponding to the time of muscle onset in the muscles identified in point I, during a maximal voluntary contraction (MVC) in an IMTP.
III. Assess the reliability of detecting the time of muscle onset in the method developed in II.
IV. Based on the results of III, recommend the muscles that can be used to represent the time of muscle onset during a MVC in an IMTP.

Chapter 3.0 Study 1: Selection of muscles and development of a software based visual detection method for determining the time of muscle onset in a multi-joint multi-muscle isometric activity

3.1 Introduction

The purpose of the present study was twofold. First, we aimed to select muscles guided by existing literature that are likely to be activated during the execution of an IMTP. Second, we endeavoured to develop an interactive visual detection tool, for identifying the time of muscle onset (T_{mo}) during a multi-muscle multi-joint test of neuromuscular performance, the IMTP. Thus, the study was designed to address objectives I and II of the thesis while explaining the methodological procedures and considerations associated with visually detecting the T_{mo} in an IMTP.

3.2 Selection of muscles assessed in an isometric midthigh pull

A search of the literature using the key words 'IMTP', 'EMG', 'sEMG' and 'sEMG in IMTP' revealed a lack of research on muscle activity assessment in an IMTP. Therefore, inferences regarding muscle selection were based on the biomechanical and neuromuscular principles of a dynamic power clean and variations of the deadlift (George. K., Beckham et al., 2012; Bird & Barrington-Higgs, 2010). Furthermore, attention was given to the isometric nature of the test, joint position, joint angles, and subsequent sites of sEMG sensor placement. The selection of muscles was also influenced by the expected joint angles, and muscle activity of the pull phase beyond the mid-thigh position in dynamic power cleans. While it is acknowledged that several muscles are likely to be active, this study prioritized key muscles across various muscle groups due to equipment constraints, particularly the number of individual sensors available.

In a power clean, the first pull is marked by slower, controlled movements associated with lifting the bar from the floor to the knees and realignment in preparation for the second pull. The second pull, however, is explosive, causing the ankles, legs, hips and back to thrust vertically at greater speed, producing a greater amount of force (Enoka, 1979; Garhammer, 1984; Souza et al., 2002).

3.2.1 Gastrocnemius Medialis

The gastrocnemius is responsible for the transfer of force into the ground during the initial phases (first pull) and plantar flexion in the later phases (second pull) of a power clean (Dryburgh & Psycharakis, 2016). Therefore, the ability of the gastrocnemius to transfer force is expected to contribute to the maximal isometric ground reaction force recorded at feet during an IMTP.

3.2.2 Hip extensors: Bicep Femoris and Gluteus Maximus

The kinematic pattern of the constant hip-joint extension during the first pull and rapid extension during the second pull in a power clean is correlated to greater weight lifted with respect to the lifter's body mass (Huyghe et al., 2021; Kipp et al., 2012). Further, the rapid hip extension during the second pull is an important contributor to success in weightlifting, given its role in achieving powerful triple extension of the lower extremity (Kipp et al., 2012). Therefore, the primary hip extensors, bicep femoris and gluteus maximus, of participants positioned such that their joint angles correspond to those at the start of the second pull were considered to be a good representation of the IMTP.

3.2.3 Knee extensor: Vastus lateralis

Knee extension plays an essential role in achieving powerful triple extension (ankle, knee, and hip extension) during the second pull phase of a power clean (Suchomel et al., 2016). The vastus lateralis is the primary muscle responsible for knee extension. It is one of the major muscle groups that generates a high amount of force throughout the pull phases of the lift (Dryburgh & Psycharakis, 2016). Further, EMG activity of the vastus lateralis has been reported to increase significantly with the load during the power clean (Dryburgh & Psycharakis, 2016). This suggests that with increased loads, individuals may rely more heavily on the ability of the vastus lateralis, especially during the pull phases of the lift. Given its kinematic and kinetic contribution during the key phases of a power clean, the vastus lateralis was assessed in the current study.

3.2.4 Trunk extensor: Erector Spinae longissimus

The erector spinae, amongst other back extensors, is the larger, superficial muscle that contributes to the static stabilisation of the trunk in the starting position of a dynamic mid-thigh pull (DeWeese et al., 2013; Richardson, 1994). From a technical aspect, practitioners recommend the continued engagement of the erector spinae throughout the second pull, kinematically contributing to the powerful vertical thrust associated with the triple extension (Suchomel et al., 2016). During the power clean, increased EMG activity with load primarily for the erector spinae, has been observed in a study which further supports these

recommendations (Dryburgh & Psycharakis, 2016). As such, the muscular activity of the erector spinae was assessed in the current study.

3.2.5 Upper limbs (forearms): Extensor Digitorum and Brachioradialis

During a power clean, the loaded barbell displaced, remains in contact with the upper limbs via a pronated grip throughout all phases of the lift. Technically, the upper extremity remains completely extended during the pull phases (Suchomel, Deweese, et al., 2016). From a neuromuscular perspective, the muscles of the upper extremity work isometrically in displacing the implement from the floor up to the point of triple extension. Biomechanically, the IMTP is based on a kinetic relationship such that the greater the amount of vertical pull force on the bar, the greater the VGRF recorded at the feet. Based on these principles, the bilateral muscle pairs of the forearm, the extensor digitorum (ED) and brachioradialis (BR) were assessed.

The static pronated grip is essential for coupling with the stationary horizontal bar and stabilising the wrist prior to initiating a maximal IMTP effort (Comfort et al., 2019). In a study assessing gripping tasks, the ED, displayed the highest EMG activity amongst other forearm extensors and flexors (Takala & Toivonen, 2013). Similar results were also reported for the weight-handling tasks performed with a pronated forearm (Takala & Toivonen, 2013). Therefore, the extensor digitorum (communis) was chosen for the current study.

Lastly, during elbow flexion tasks the greatest EMG activity was shown by the brachioradialis which is also primarily responsible for stabilising the elbow joint (Boland et al., 2008). Further, EMG activity of the brachioradialis during rotational tasks demonstrates its secondary function as a pronator (Boland et al., 2008; Pratt et al., 2020). Bending and flexing the elbow joint following the powerful triple extension in a power clean is an essential technical component for successfully executing the catch (Suchomel et al., 2016). A participant performing the IMTP can be viewed as attempting to overcome a resistance to execute the powerful triple extension followed by elbow flexion to catch the weighted barbell successfully. Therefore, considering the nature of the test, it was assumed that the brachioradialis would display high muscular activity by stabilising the elbow joint while maintaining the pronated forearm position.

To summarise, the myoelectric activity of 7 bilateral pairs of muscles was recorded using sEMG during a maximal IMTP effort (Figure 3.1). The muscles assessed were left and right: gastrocnemius medialis (GS), bicep femoris (BF), gluteus maximus (GM), vastus lateralis (VL), erector spinae longissimus (ESL), extensor digitorum (ED) and brachioradialis (BR).

● Gastrocnemius; ● Bicep Femoris; ● Gluteus Maximus; ● Vastus Lateralis;
● Erector Spinae; ● Extensor Digitorum; ● Brachioradialis

Figure 3.1 *Illustration of 7 pairs of muscles assessed in the current study. The colour-coded annotations are visual approximations of accurate sensor placements described in Tables 3.1 and 3.2. The images were taken from EMG works® Acquisition software, v4.8.0, Delsys INC, Boston, Massachusetts, USA. The images on the software are used as an interactive guide in assigning sensors to respective muscles.*

3.3 Methods

3.3.1 The isometric midthigh pull

The participants (N = 9, mean ±SD: 26.8 ± 2.8 years; 179.4 ± 5.6 cm; 89.6 ± 5.1 kg; weightlifting experience > 3 years) stood on the portable FP (type 9260AA6, Kistler Instruments Ltd., Farnborough, United Kingdom) positioned within a custom-built rig designed to implement an IMTP. The rig was equipped with a horizontal knurled hand-grip bar of the same dimensions as a standard weightlifting barbell (Bar diameter: 28 mm, IWF Weightlifting Training Bar, Eleiko, Sweden) positioned directly above the FP (Figure 3.2). The portable FP with built-in charge amplifiers and a vertical force range of 10 kN used to measure the VGRF was set at a sample length of 16-seconds. The sampling rate was set at 1000 Hz. The force-time histories were recorded on a laptop via a 16-bit analog-to-digital converter (Kistler Data Acquisition (DAQ) System, type 5691A, Kistler Instruments Ltd., Farnborough, United Kingdom). Force-time histories were digitally analysed using a data acquisition software, BioWare (Type 2812A, Version: 5.3.0.7).

Figure 3.2 *Anterior (left) and posterior (right) view of a participant in the IMTP position, equipped with sEMG sensors, prior to the initiation of the pull.*

Designed to mimic the start of the second pull during a power clean, the participants assumed a self-selected mid-thigh position with a flat trunk position and shoulders in line with the horizontal fixed bar. A hand-held goniometer (Smith & Nephew, Hull, United Kingdom) was used to ensure the knee was between 125-145° and hip joint angles was between 140-150°, in accordance with the recommended ranges (Comfort et al., 2019). Once in the optimal position, the bar height was adjusted and fixed in place. The use of weightlifting straps (AQF Sports, Worsley, United Kingdom) was standardised to avoid grip strength as a limiting factor during maximal efforts (Comfort et al., 2019; West et al., 2011).

Participants performed a standardised warm-up in preparation of the maximal IMTP efforts. The exercises are listed in order as 'Exercise name (n)', where 'n' is the number of repetitions: Cycling (5-minutes), body weight (BW) or 20 kg barbell (BB) squats (15), push ups (15), lunges (10, each side), Romanian deadlift (RDL) using the 20 kg BB (15), calf raises (20) and counter movement jumps (CMJ) (10). The warm-up designed by the author, also a Certified Strength and Conditioning Specialist (CSCS), was deemed sufficient to activate the muscles of interest. Assessment of the testing protocol revealed that the warm-up coupled with the submaximal IMTP efforts (50%, 75% and 90% of perceived max effort) negated the effects of post activation potentiation (PAP). This was confirmed via the visual inspection of IMTP MVC force-time histories, such that the peak force (PF) values in subsequent repeated trials were within the range of ±250 (N) of the first maximal effort (Comfort et al., 2019; Haff et al., 2005).

Following the standardised warm-up, participants performed 3 familiarisation submaximal trials at 50%, 75% and 90% of perceived maximal efforts, respectively. The rest period of 1-minute between the submaximal trials was used for verbal and visual feedback of the ground reaction force-time histories produced with reference to Figure 3.3 (Comfort et al., 2019). This was done to ensure participants were capable of holding onto the bar with minimal slack (elbows locked out) while maintaining a stable VGRF baseline, avoiding countermovement on the command to pull, and expressing a quick change of force from baseline to submaximal or maximal levels (Figure 3.3 A) (Comfort et al., 2019).

Following sufficient rest of three to five minutes from the submaximal trials, participants were cued to "pull as fast and hard as possible" prior to maximal efforts . For all maximal trials, participants were instructed to assume their respective IMTP position and remain as

still as possible with minimal slack on the bar for the first 5-seconds. A startling command to 'PULL' was given following the quiescent (still) phase of the test and immediately reinforced with strong verbal encouragement. Participants performed a maximal effort pull lasting approximately 5-seconds after the pull initiation.

A software-based timing device was used to ensure that the command to 'PULL' was given between the 5th and 6th second of the 16 s sample time. This was an important step to guide visual detection analytical procedures performed on sEMG data recorded simultaneously.

All force-time histories were visually inspected in accordance with the recommended inclusion criteria for a 'satisfactory' trial (Comfort et al., 2019) (Figure 3.3 A). In the case of unsatisfactory trials repeated trials were performed after recovery (Figures 3.3 B and C). Effects of fatigue were tracked by ensuring subsequent repeated trials were in the range of ±250 (N) of the first three maximal efforts (Comfort et al., 2019).

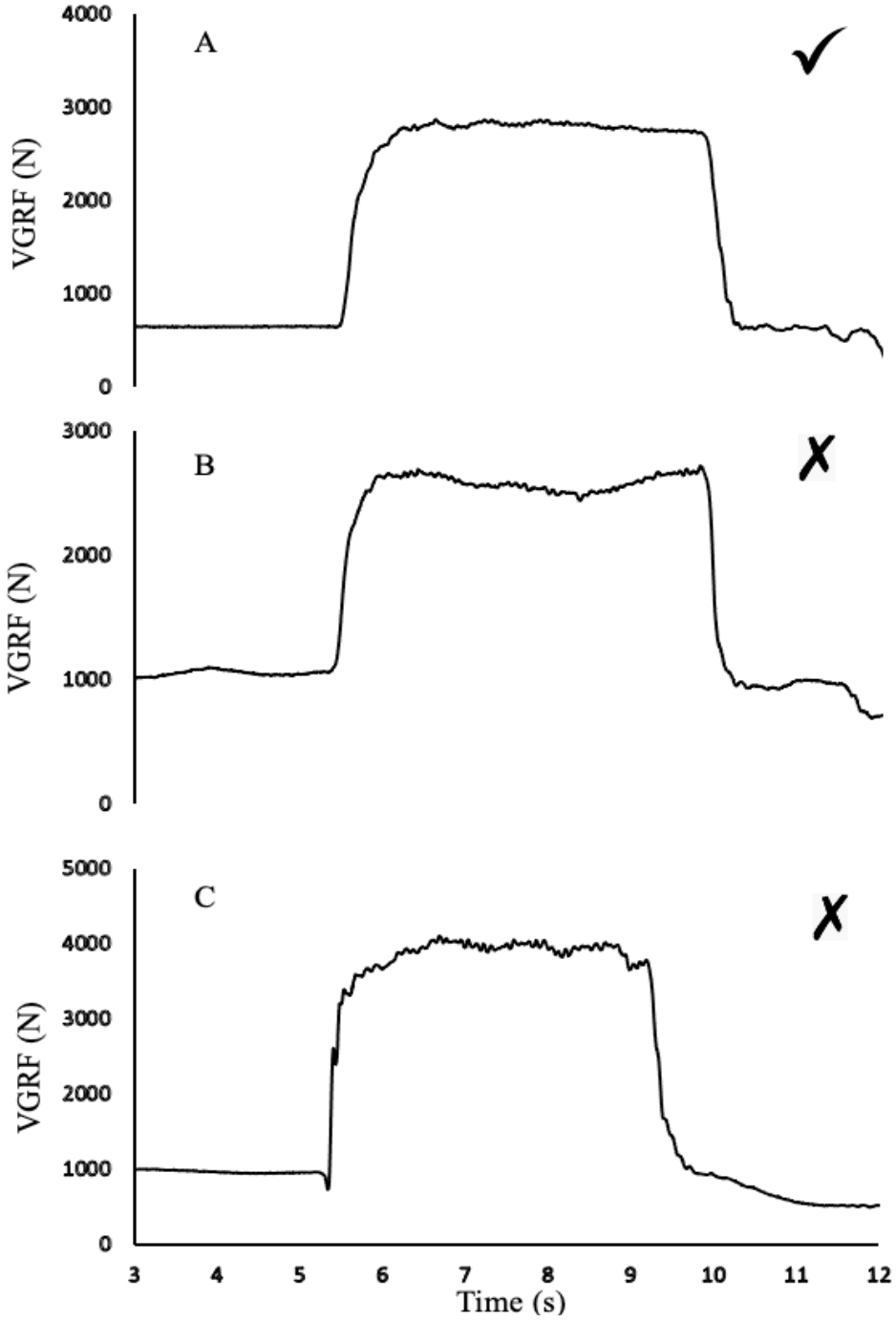

Figure 3.3 *Examples of acceptable (A) and unacceptable (B, C) IMTP force-time histories (A) The acceptable trace is characterised here by a stable baseline, no countermovement and early expression of peak force. (B) Force-time history with unstable baseline and peak force expressed at the end of the maximal effort. (C) Force-time history with countermovement just before the initiation of the pull.*

3.3.2 Determination of mechanical force onset in the isometric midthigh pull

A stable baseline is necessary for identifying the start of the pull and has been well documented (Comfort et al., 2019). When an IMTP is performed, due to the position, there is, in some participants, a tendency to push or pull on the bar prior to the commencement of the pull. While it is difficult to avoid this situation without affecting the ecological validity of the test, the force-time history, in some cases, lacks sufficient stability and is not suitable for determining a reliable start time. Alternatively, the rate of change of force i.e. the first derivative, with respect to time (WRT), of force, provided a stable metric suitable for determining the standing baseline value and threshold above which the start point of the pull could be identified (Figure 3.4).

Therefore, the method used to determine the start of the maximal effort was adapted from that described by West et al. (2011). Force-time histories were filtered using a dual-pass Butterworth filter (low pass, 20-Hz cut-off) and then numerically differentiated using the central difference method (equation 3.1). The first 3 seconds of the 1st derivative of VGRF, was discarded to avoid the edge effects associated with digital filtering. The mean and SD were calculated using a spreadsheet (Microsoft EXCEL, Version 16.69.1) for the remaining two seconds of the still phase before the command to pull. The start-time of the IMTP was then defined as the instant, that the instantaneous first derivative of VGRF exceeded the mean of the 1st derivate of VGRF value during the two seconds of the still phase by 7 SDs. West et al. (2011) used a mean value plus 5 SD; however, a pilot analysis showed that plus 7 SDs gave more consistent results.

$$\frac{dF_z}{dt}(t) = \frac{F_z\,(t + 1\ sample) - F_z\,(t - 1\ sample)}{2 \cdot \Delta t} \qquad 3.1$$

Where, Δt = sampling interval (1/ Sampling rate) and $(dF\_z)\ /\ dt$ = first derivative.

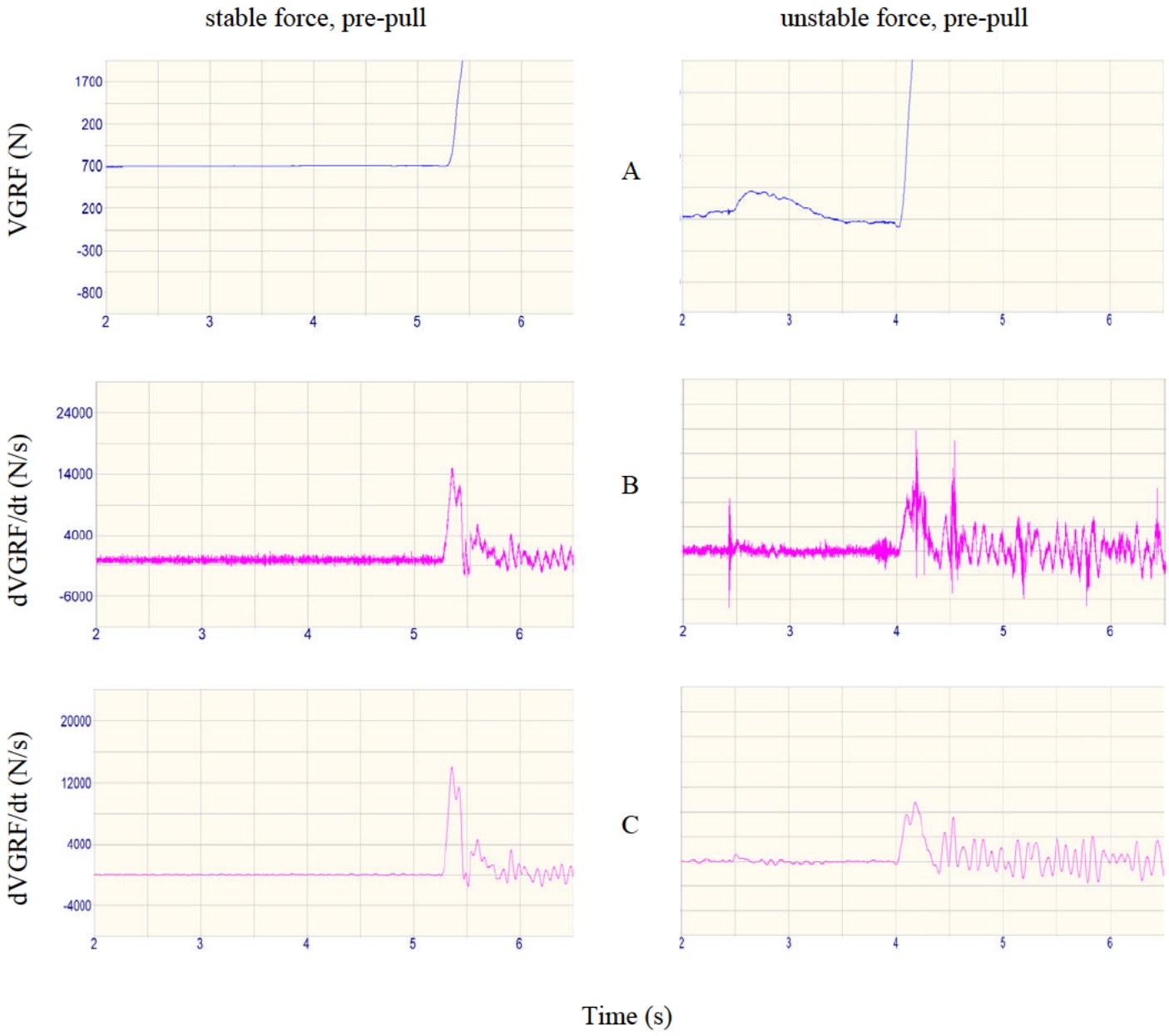

Figure 3.4 *Two typical force/time histories of IMTP, showing the period prior to initiation of the pull and the start of the pull, illustrating the filtered and un-filtered 1st derivative. (A) illustrates examples of a stable period and an unstable period prior to the initiation of the pull. (B) shows the corresponding 1st derivative of VGRF determined from raw, unfiltered data. (C) shows the corresponding 1st derivative of VGRF from filtered data (dual pass Butterworth low pass filter with cut-off frequency of 20 Hz). VGRF = Vertical ground reaction force.*

3.3.3 Surface electromyography data collection

An array of electrodes (dimensions in mm: 27 x 37 x 15; (Delsys INC, Boston, Massachusetts, USA) with 4 silver (99.9% Ag) bar contacts (inter-electrode spacing: 10 mm) were placed on the muscle belly in the direction of the underlying muscle fibres, used to measure the propagation of action potentials (AP) discharged by the motor neurons during the IMTP.

3.3.3.1 Sensors and Skin Preparation

EMG sensors (Delsys INC, Boston, Massachusetts, USA) were used to detect EMG signals at the surface of the skin. The sensors (dimensions in mm: 27 x 37 x 15) with 4 silver (99.9% Ag) bar contacts (inter-electrode spacing: 10 mm) were aligned in the direction of the underlying muscle fibres. With reference to the recommended and adapted electrode locations described in Tables 3.1 and 3.2, the sensors were attached to the skin over the belly of the muscles using Delsys Adhesive Sensor Interface. The sampling rate of 2000 Hz for 16s was used for the study. The raw sEMG signals were recorded using a data acquisition software (EMG works® v4.8.0, Delsys INC, Boston, Massachusetts, USA). The software controls and converts the Delsys Trigno Base Station analogue outputs to digital signals.

Prior to affixing the sEMG sensors to the surface of the skin, appropriate skin preparation steps are necessary to ensure signal quality. Following anthropometric measurements (Section 4.2.3), the muscles of interest were marked with a permanent marker with reference to the adapted methods described in Table 3.1 and 3.2. Before warm-up, excessive hair around the areas of the marked points on the muscles was dry shaved. After the warm-up, alcohol wipes (Medisave Professional 70% Alcohol IPA Pre-Injection Swabs, Dorset, United Kingdom) were used to remove any sweat, residual hair, dry dermis and skin oils.

3.3.3.2 Muscles of interest

Surface EMG data were recorded bilaterally from 7 muscle pairs, left and right: GS, BF, GM, VL, ESL, ED, BR. (Figure 3.1). The locations for attaching the sEMG electrodes were determined using the recommendations of the Biomedical Health and Research Program (BIOMED II) of the European Union in the Surface Electromyography for the Non-Invasive Assessment of Muscles (SENIAM) (Hermens et al., 1999, 2000). However, SENIAM recommendations for electrode placement on forearm muscles do not exist. Consequently, electrode locations for both pairs of forearm muscles, ED and BR, were adapted from previous studies (Merlo et al., 2021; Pratt et al., 2020; Santos et al., 2020; Zipp, 1982). SENIAM recommendations for electrode placement and adapted participant position to suit the field-based methods employed for the current study are described in Tables 3.1 and 3.2.

Table 3.1 *Specifications for sensor location as per the SENIAM recommendations.*

	SENIAM Recommendations		Adapted Technique
Muscles	Sensor location	Participant position	Participant Position
Gastrocnemius (Medialis)	The most prominent bulge of the muscle	Lying on the belly with the face down. The knee extended, and the foot projected over the end of the table.	Plantar flexion was performed by the participant standing on their toes one leg at a time.
Bicep Femoris (long head)	50% on the line between the ischial tuberosity and the lateral epicondyle of the tibia.	Lying on the belly with the face and the thigh down on the table. The knees flexed (to less than 90°) with the thigh in slight lateral rotation and the leg in slight lateral rotation with respect to the thigh.	Index finger pressing against the point halfway on the line between the ischial tuberosity and the lateral epicondyle of the tibia. On locating this point, the standing participant was asked to perform a standing knee flexion up to 90°.
Vastus Lateralis	Electrodes need to be placed at 2/3 on the line from the anterior spina iliaca superior to the lateral side of the patella.	Sitting on a table with the knees in slight flexion and the upper body slightly bend backwards	Participants were asked to step forward with one leg and tense their quadriceps by completely extending the respective knee and dorsiflexing the respective ankle.
Gluteus Maximus	50% on the line between the sacral vertebrae and the greater trochanter on the most significant prominence of the middle of the buttocks	Prone position, lying down on a table	Participant standing upright in a relaxed position.
Erector Spinae (longissimus)	Two fingers width lateral from the L1 vertebrae on the erector spinae longissimus	Prone with the lumbar vertebral columns slightly flexed.	Standing upright with lumbar vertebral columns flexed slightly.

Table 3.2 *Specifications for sensor location based on previous research, for forearm muscles that are not included in the SENIAM recommendations.*

	Recommendations adapted from previous studies.		Adapted Techniques
Muscles	Electrode location	Participant position	Participant position.
Extensor Digitorum	$1/4^{th}$ distance on the line from the lateral epicondyle of the humerus to the midpoint between the styloid processes of radius and the ulna (Zipp, 1982)	Sitting, with the upper arm abducted laterally, forearm on the table and pronated palm (Zipp, 1982)	Standing upright, with arms relaxed and elbows extended. The thumb was pressed against the point of electrode location. Once located, the participant was instructed to grip as hard as possible by clenching their fist.
Brachioradialis	Approximately 25-30% of the distance on the line from the lateral supracondylar ridge on the humerus to the styloid process of the radius (Merlo et al., 2021)	Sitting, with the upper arm abducted laterally, forearm on the table with the thumb pointing upwards in the neutral plane (halfway between supination and pronation) (Merlo et al., 2021)	Standing upright with arms relaxed and elbows extended. Pinch and grasp the electrode location on the muscle. Participants were instructed to grip as hard as possible by clenching their fists while attempting to flex their elbows against the resistance offered by the researcher.

3.3.4 Surface electromyography data analysis

Muscle activity data recorded using the sEMG data acquisition software (EMG works® v4.8.0, Delsys Inc, Boston, Massachusetts, USA) was exported to EMG works® Analysis (EMG works Analysis v4, Delsys INC, Boston, Massachusetts, USA) for the initial assessment. First, the 'Remove Mean' function was used to remove any DC offset (mean amplitude displacement from zero). Using the 'Filter IIR' function, the EMG signals were bandpass filtered between 10 Hz and 400 Hz using a 4^{th}-order dual pass Butterworth digital filter.

The filtered signal was then exported to EXCEL, and a custom MATLAB programme (R2021b, MathWorks, Massachusetts, USA) script was written to perform further analysis. i.e., detection of T_{mo}. All sEMG traces and T_{mo} were evaluated using manual visual detection in MATLAB. The filtered signal was imported onto MATLAB, which was amplified (gain = 1000) prior to further conditioning using TKEO. All EMG traces were full-wave rectified after conditioning with TKEO.

3.3.5 Synchronisation of surface electromyography and force platforms

Muscular contraction and VGRF were recorded simultaneously during the IMTP using sEMG and force platforms, respectively. The sEMG and force platform data recordings were synchronised using the Delsys Trigger Module (SP-U02, Delsys INC, Boston, Massachusetts, USA). The primary-secondary triggering strategy was employed, wherein the start of a primary data acquisition system controls the start of the secondary data acquisition system. The sEMG data acquisition software (EMG works® v4.8.0, Delsys Inc, Boston, Massachusetts, USA) used to control the EMG base station (Trigno™, Delsys Inc, Boston, Massachusetts, USA) was the primary acquisition system connected to the secondary acquisition system (Kistler Data Acquisition (DAQ box) System, type 5691A, Kistler Instruments Ltd., Farnborough, United Kingdom) (Figure 3.5). For the current study, initial testing showed that a trigger signal above 3 Volts (V) from the sEMG system was sufficient to trigger the force platform (Figure 3.5). Perfect synchrony of both systems was imperative, given that the analysis performed was in the time domain.

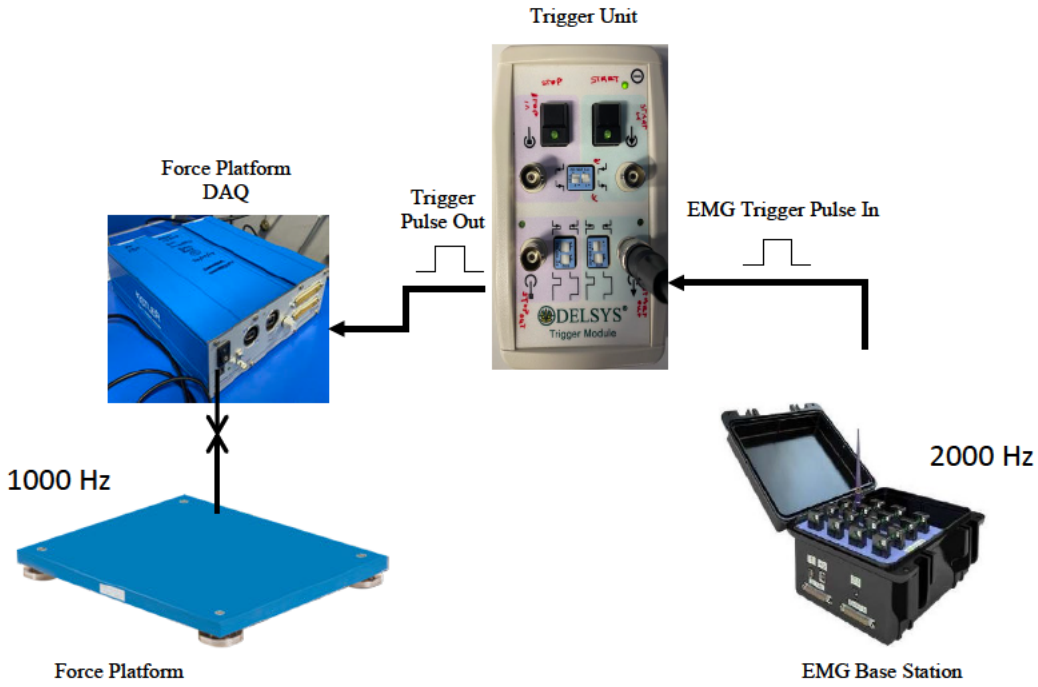

Figure 3.5 *Illustrates the equipment set-up, with the EMG systems (sensors and base station) working as the primary acquisition systems responsible for triggering the secondary acquisition systems, the force platforms via the data acquisition (DAQ) box.*

3.3.6 Development of a software-based method for detecting the time of muscle onset in an IMTP

Baseline noise patterns are likely to vary depending on the respective roles of the muscles in a multi-muscle multi-joint isometric test of neuromuscular function. Considering this and the stochastic characteristics of sEMG signals, the findings and recommendations reported by Crotty et al. (2021) and methods applied by Tillin et al. (2010) were adapted for the multi-joint maximal IMTP test. As such, manual visual detection following TKEO conditioning was deemed to be the appropriate method for determining the T_{mo} in the current study.

Precise visual detection of T_{mo} requires an appropriate scale on the x and y axes such that observed values read off the graph are of sufficient resolution (in terms of precision) to be useful to their intended purposes. Determining the T_{mo} from an sEMG signal, the resolution should be sufficiently high to establish the pattern of background noise and identify the instant that voluntary muscle activity has started to an appropriate temporal resolution (Tillin et al., 2010). As such, previously applied zoom scales were adapted for the current study (Crotty et al., 2021; Tillin et al., 2010). Multiple iterations were performed before formulating the 2-step visual detection method to determine T_{mo} to the nearest 0.001 s.

3.3.7 Time of muscle onset: Definition and programme Iterations

Time of muscle onset (T_{mo}) was defined as the last trough (the last point at the base of the first peak) before the signal deflected away from baseline noise (Crotty et al., 2021; Tillin et al., 2010). With reference to figure 3.6, selecting the estimated onset point (red dot) at the trough or minimum before the 2-mV maximum, indicating a distinct deflection resulting from voluntary contractions is a key criterion. Selecting the onset point at the trough of a signal deflection ensures easier and more consistent identification among raters, while also maintaining the standardization of the signal onset definition. A programme in MATLAB (R2021a, MathWorks, Massachusetts, USA) was developed to view the sEMG data such that a cursor could be used to identify the time an event occurred in the region on interest, Appendix D, E1 and E2. The basic MATLAB programme was referred to as the first iteration of the instrument.

In the first iteration of the programme, all sEMG traces were viewed with a set resolution, x-axis scale of 1000 ms (between the 5th and 6th second of the test), and y-axis scale of 2 mV as

illustrated in Figure 3.6 (Appendix E1, E2). However, the fixed resolution of the x-axis was not high enough as the T_{mo} could only be identified with an uncertainty of ± 10 ms (Figure 3.6). As such, the first iteration lacked the required precision, necessitating the development of a second iteration of the MATLAB programme with enhanced x-axis resolution.

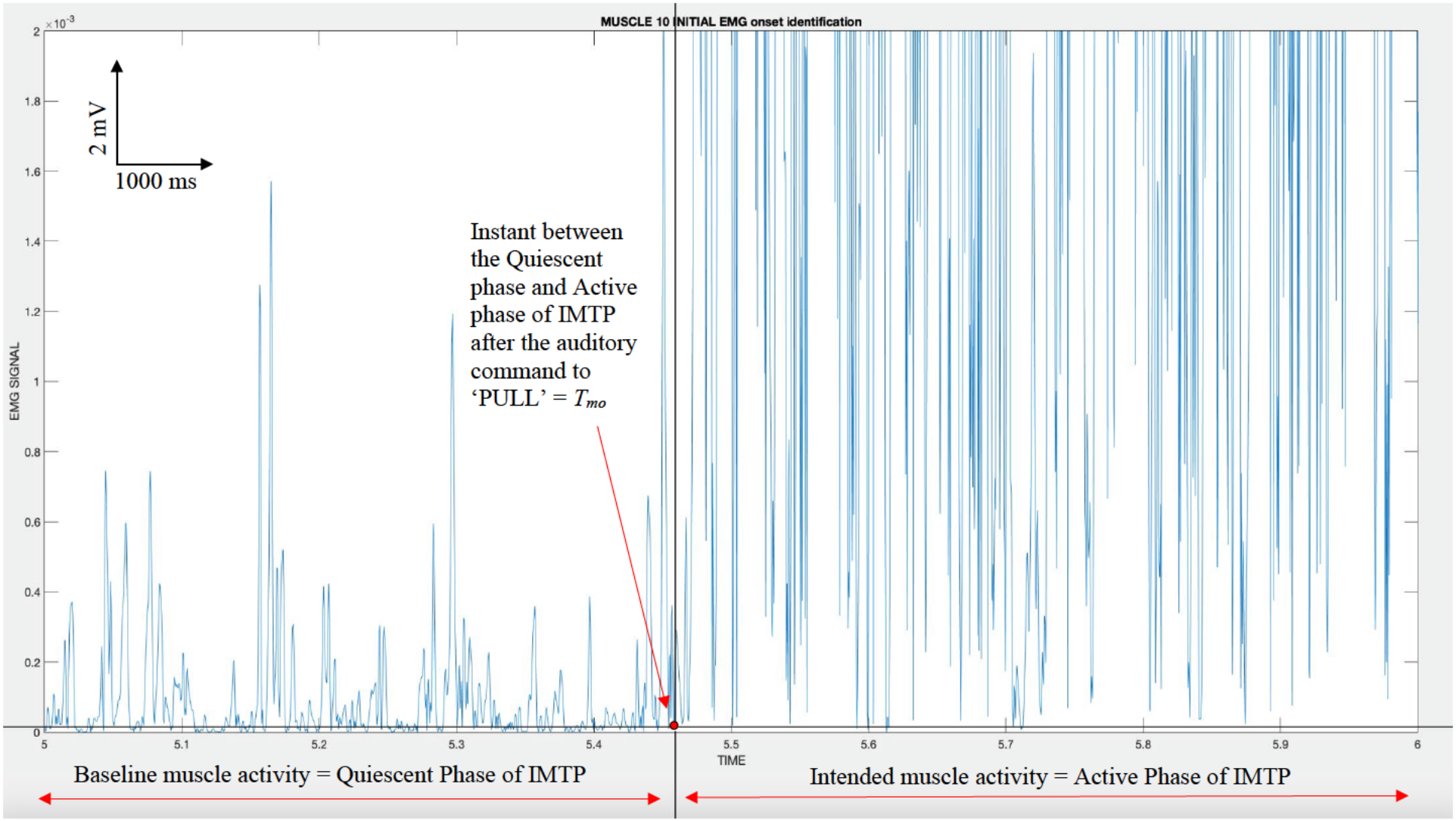

Figure 3.6 *Illustrates an example of the first iteration of the MATLAB programme.* T_{mo} detected with a full scale of 2 mV along the y-axis and 1000 ms along the x-axis. The window displays 2000 individual data samples (2000 Hz).

In the second iteration of the MATLAB programme, sEMG traces for all muscles were viewed with a y-axis scale of 2 mV and an x-axis scale of 1000 ms (Figure 3.6). The window displaying 2000 data samples similar to the previous iteration was used to recognise the baseline noise pattern and identify the region of interest (approximately T_{mo}) along the x-axis (Figure 3.6, 3.7A). When the region of interest had been identified, a second trace was displayed with a magnified x-axis, such that the final onset point was located in a window with a y-axis scale of 2mV and an x-axis scale of 50 ms (100 data samples) (Figure 3.7 B). The region of interest was centred in the higher resolution window of a full scale of 50 ms, with 25 ms on each side (initial marking ± 25 ms) (Figure 3.7 B). Therefore, by increasing the resolution of the scale on the x-axis, an operator was able to identify individual data samples with a precision of 0.5 ms (Appendix E1,E3).

3.3.7.1 Categorisation of surface electromyography traces

The selected muscles displayed varying baseline activity observed in respective sEMG traces, likely to be attributable to their distinct roles during the quiescent phase of the IMTP.
As such, sEMG traces were grouped under three distinct categories to aid the detection of T_{mo}. These categories were determined based on the baseline noise observed with the resolution of the initial data window (Figure 3.6, 3.7 A). The y-axis had a scale of 2mV and the x-axis was scaled at of 1000 ms.

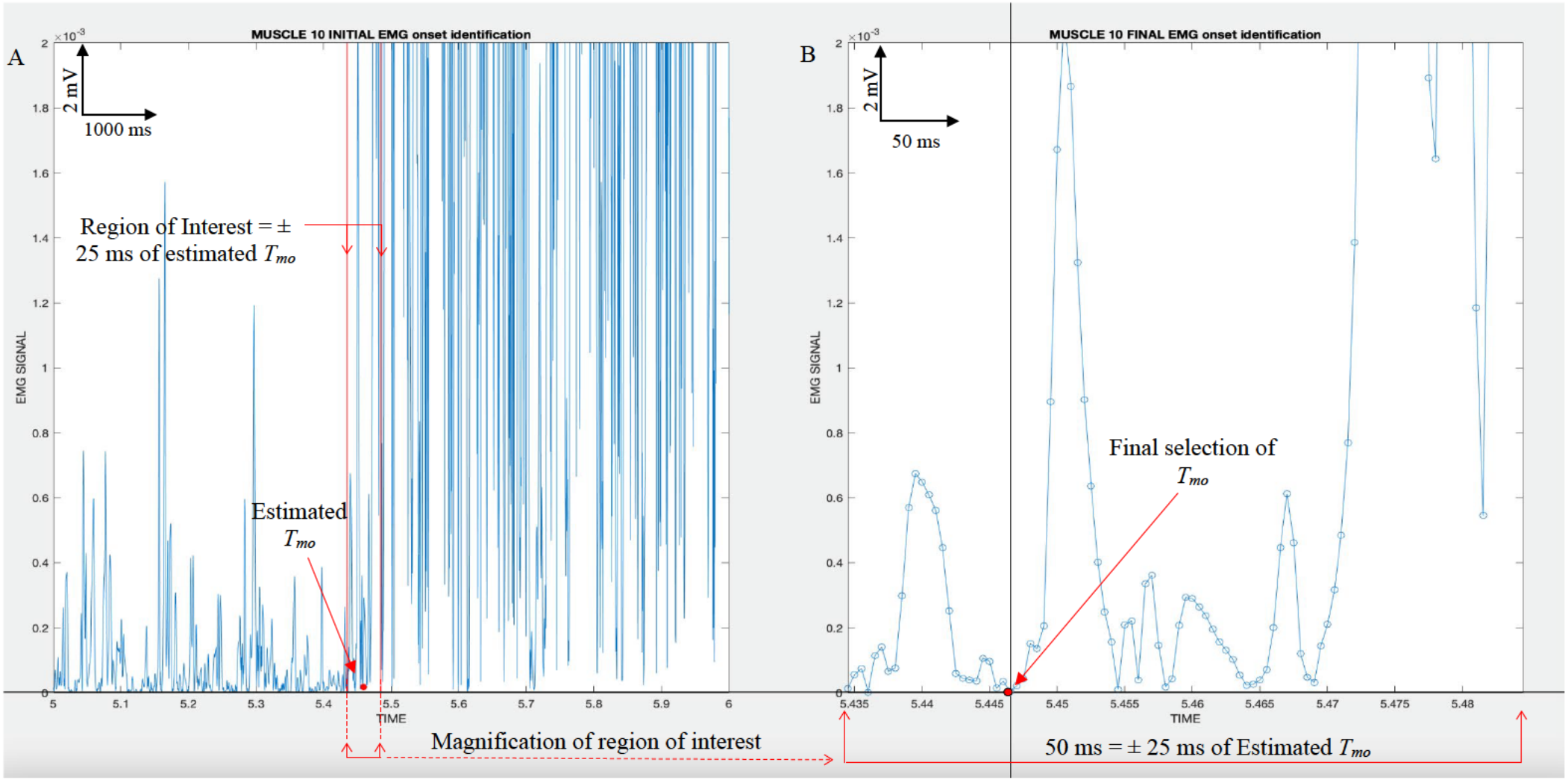

Figure 3.7 *Illustrates an example of the second iteration of the MATLAB programme. (A) Represents the initial window viewed with a y-axis scale of 2mV and an x-axis scale of 1000 ms used to identify the region of interest, illustrated here with two red vertical lines and a red dot marked as an estimation of T_{mo} (B) Displays the final selection of T_{mo}, detected at higher resolution (red dot) with a y-axis scale of 2mV and an x-axis full scale of 50 ms. Note: The region bordered by the two red lines, ± 25 ms of the estimated T_{mo} in (A), is displayed in (B) for the final selection of T_{mo}*

3.4 Results

The development of a software-based T_{mo} detection method considered 14 muscles (7 muscle pairs) whilst the participants performed an IMTP. The resulting MATLAB programme in the second iteration and its constituent categories were collectively termed as the '2-step visual detection' method. In the first step, all sEMG traces were viewed with a y-axis scale of 2 mV and an x-axis scale of 1000 ms. This scale provided operators with a good resolution from which the pattern of baseline muscle activity during the quiescent phase could be established and the region of interest interpolated. In the second step sEMG traces were viewed with a higher resolution, y-axis scale of 2mV and an x-axis scale of 50 ms for the detection of T_{mo} with a precision of 0.5 ms (Appendix E, E3).

To aid the 2-step visual detection method, all sEMG traces obtained from the selected muscles were classified under one of three distinct categories. The sEMG traces classified under Category 1 and Category 2 were primarily based on the baseline amplitude characteristics of the muscles. Category 3 was composed of signals with high amplitude baseline noise, such that the visual detection of muscle onset was based on the frequency variation of the signal between the quiescent state and the active state.

T_{mo} for traces classed under Category 1 and Category 2 was defined as the last trough (the last point at the base of the first peak) before the signal deflected away from baseline noise (Figure 3.2 and 3.3). In the case of Category 3, further refinements were made to the definition of T_{mo}, based on sEMG signal's frequency-content as some sEMG signals had no discernible baseline due to a constant high amplitude, Figure 3.10 A. However, it was visually evident that there was a clear change in frequency of the signal that corresponded to the T_{mo} as identified on Category 1 muscles. As such, T_{mo} in sEMG traces classified under Category 3 was defined as the point at the trough (base) of the first spike of the sustained deflected signal, displaying a distinctively frequency-dense area as opposed to the baseline muscle activity, Figure 3.10.

3.4.1 Category 1

Category 1 consisted of sEMG traces, with minimal baseline noise and an apparent deflection of the signal (Figure 3.8 A and B). The region of interest is displayed in Figure 3.8 A, with two vertical red lines, 25 ms on either side (± 25 ms) of the estimated T_{mo} (red dot). This region was displayed as a full scale of 50 ms along the x-axis in Figure 3.8 B, for the final selection of a point representative of T_{mo}.

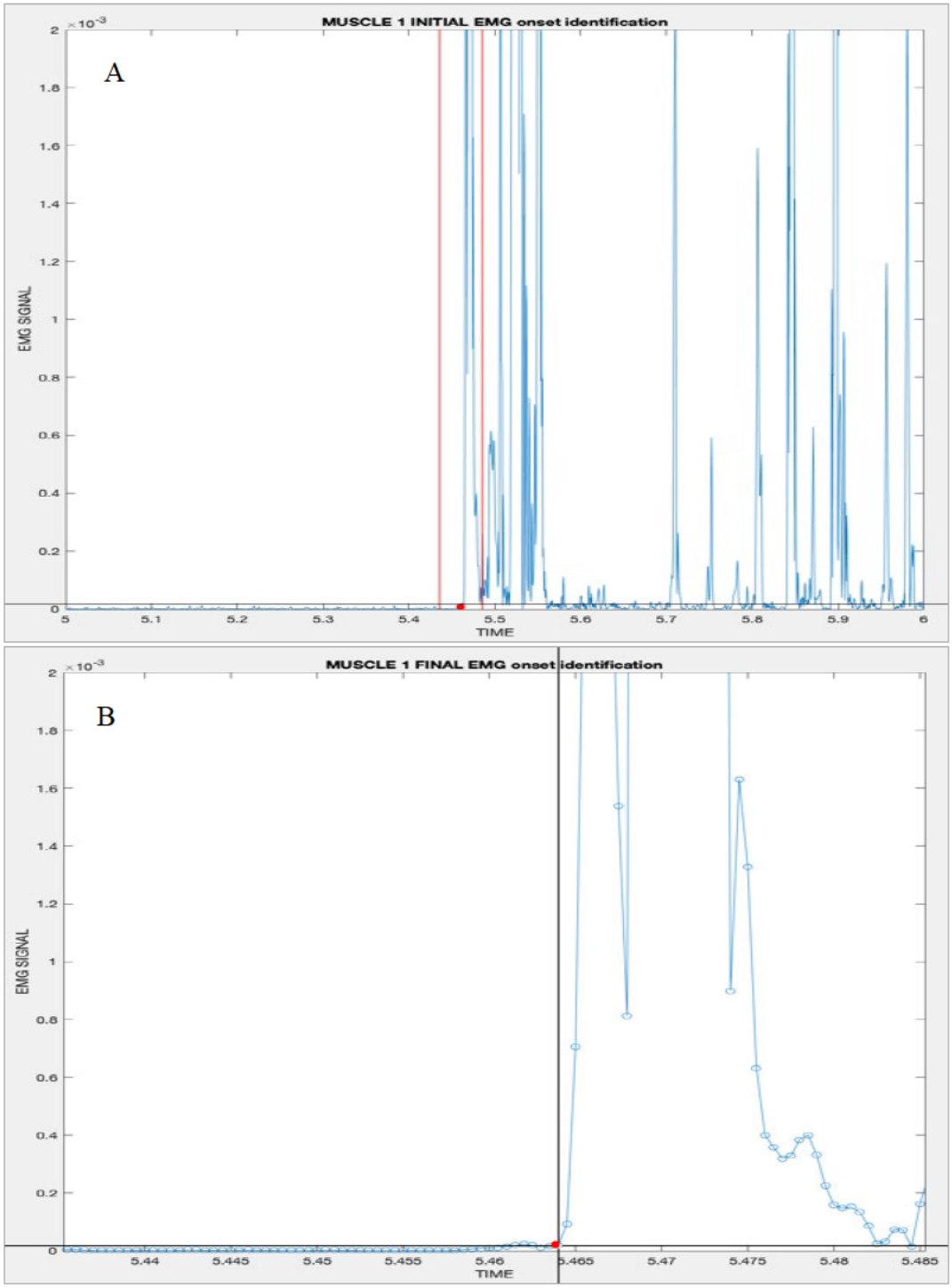

Figure 3.8 *Illustrates an sEMG trace with minimal baseline noise, classed under Category 1. (A) Represents the initial window viewed with a y-axis scale of 2mV and an x-axis scale of 1000 ms used to identify the region of interest, illustrated here with two red vertical lines and a red dot marked as an estimation of* T_{mo} *(B) Displays the final point detected at higher resolution (red dot) with a y-axis scale of 2mV and an x-axis full scale of 50 ms.*
Note: The region bordered by the two red lines, $\pm$ *25 ms of the estimated* T_{mo} *in (A), is displayed in (B) for the final selection of* T_{mo}

3.4.2 Category 2

Category 2 is composed of signals with distinctively high baseline noise as compared to those in Category 1, yet a visible deflection of the signal can be observed (Figure 3.9 A and B). The region of interest is displayed in Figure 3.9 A, with two vertical red lines, 25 ms on either side (± 25 ms) of the estimated T_{mo} (red dot). This region was displayed as a full scale of 50 ms along the x-axis in Figure 3.9 B, for the final selection of a point representative of T_{mo}

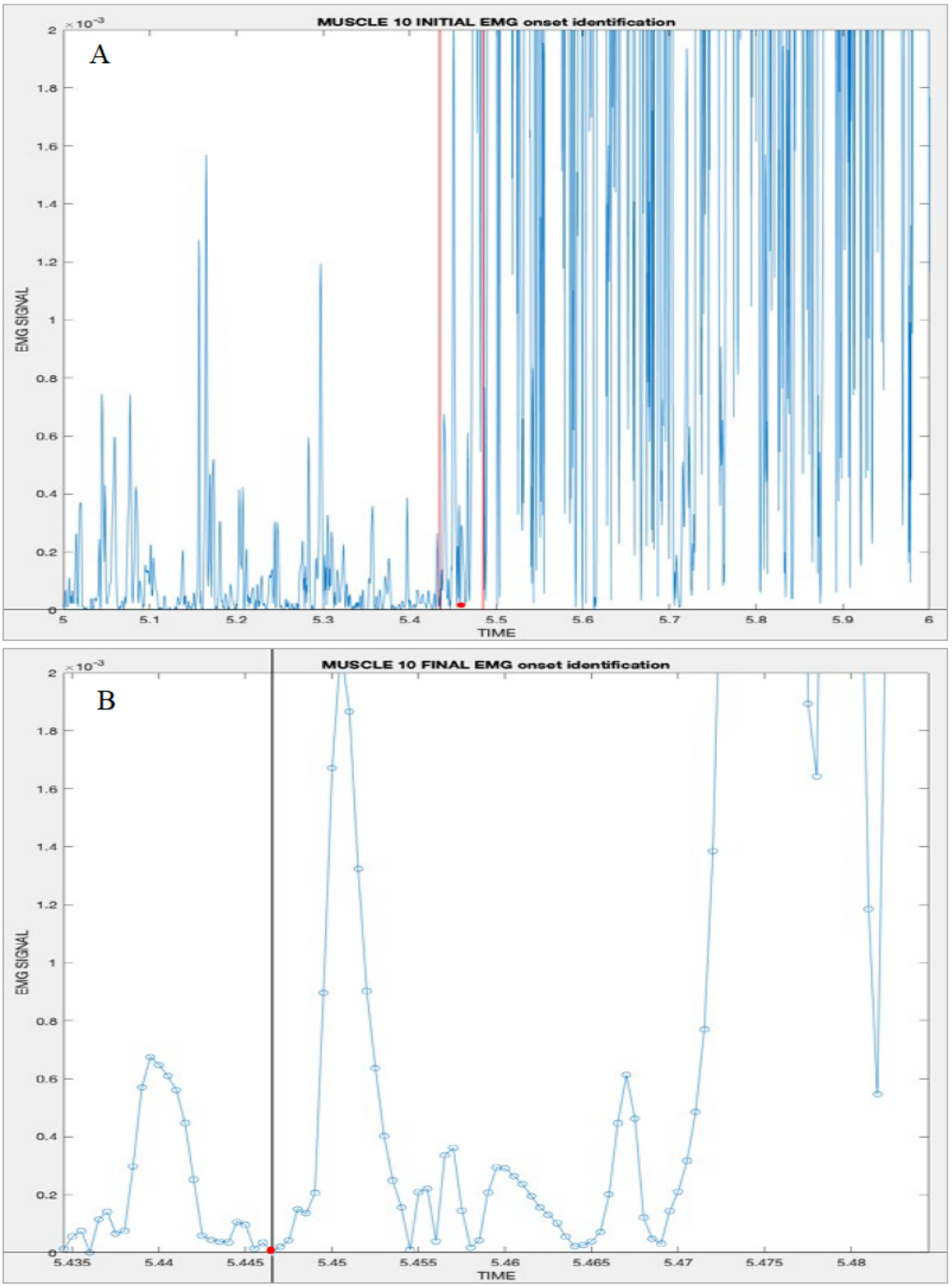

Figure 3.9 *Illustrates an sEMG trace with relatively higher baseline noise, classed under Category 2. (A) Represents the initial window viewed with a y-axis scale of 2mV and an x-axis scale of 1000 ms used to pick the region of interest, illustrated here with two red vertical lines and a red dot marked as an estimation of* T_{mo} *(B) Displays the final point detected at higher resolution (red dot) with a y-axis scale of 2mV and an x-axis full scale of 50 ms.*
Note: The region bordered by the two red lines, $\pm$ *25 ms of the estimated* T_{mo} *in (A), is displayed in (B) for the final selection of* T_{mo}

3.4.3 Category 3

Category 3 comprised sEMG traces that displayed high amplitude baseline activity. For such traces, the T_{mo} was re-defined, and the frequency characteristics of the signal were considered. As such, T_{mo} was defined as the point at the trough (base) of the first spike of the sustained deflected signal, displaying a distinctively frequency-dense area as opposed to the baseline muscle activity (Figure 3.10 A and B).

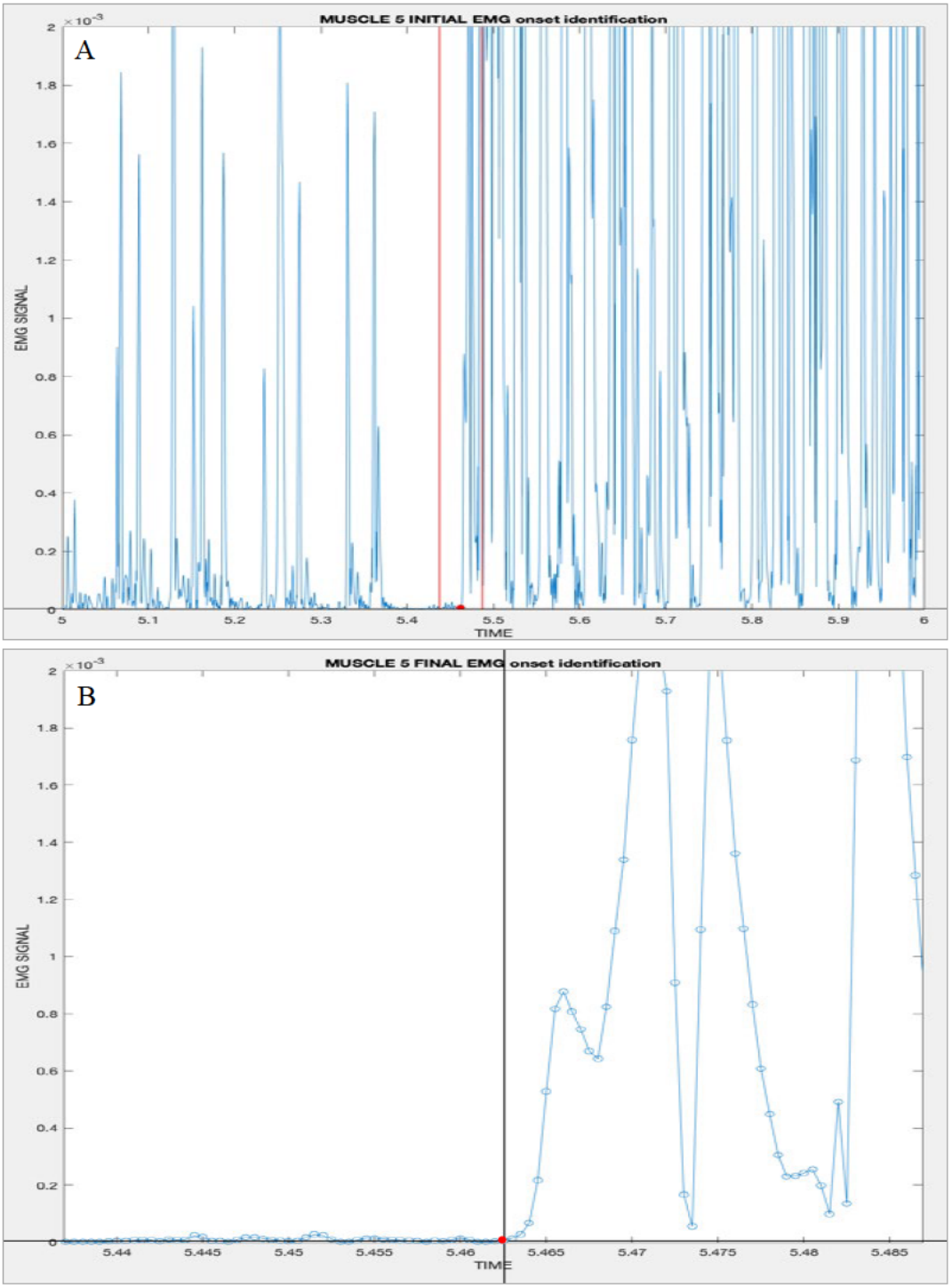

Figure 3.10 *Illustrates the type of traces classed under Category 3(A) Represents the initial window viewed with a y-axis scale of 2mV and an x-axis scale of 1000 ms used to pick the region of interest, illustrated here with two red vertical lines and a red dot marked as an estimation of* T_{mo} *(B) Displays the final point detected at higher resolution (red dot) with a y-axis scale of 2mV and an x-axis full scale of 50 ms.*

Note: The region bordered by the two red lines, $\pm$ *25 ms of the estimated* T_{mo} *in (A), is displayed in (B) for the final selection of* T_{mo} *as per the refined definition.*

3.5 Discussion and recommendation

Visually identifying an instant that differentiates between the quiescent state and active state, representing the T_{mo} during a maximal isometric effort can be challenging. However, it is reasonable to assume that activation patterns tend to vary based on the role of the muscles during the quiescent state and active state of an isometric multi-joint test. Further, the postural weight bearing and joint positional demands during the anticipatory quiescent phase may give rise to movement artefacts, making the detection of T_{mo} more challenging. Therefore, considering the standardised IMTP test procedures (Comfort et al., 2019; West et al., 2011), and taking into account the varying activation patterns observed in the muscles identified this study, we recommend the use of the 2-step visual detection for determining the T_{mo} in an IMTP.

3.5.1 Determining the time of muscle onset

As per the test conditions, participants were required to stay still in the IMTP position for the first 5 s of the 16 s sample time. This period of inactivity with participants in postural weight bearing IMTP position was referred to as the quiescent phase of the test. The quiescent phase, lasting approximately 5 s, preceded a starling command to "PULL" and thus the initiation of maximal isometric effort. As such, the initiation of the pull was always recorded between the 5^{th} and 6^{th} second of the test.

The startling command to "PULL" activates the cell hairs located on the auditory area of the inner ear, the cochlea. The axons originating from the activated hair cells bundle together to form the cochlear nerve, a sensory nerve that transmits auditory information to the brain (Johansson et al., 1983). The auditory stimulus results in an activation signal originating in the CNS, transmitted through the motor unit and transformed into contractile activity (Duchateau et al., 2006). T_{mo} can therefore be judged as the instant between the quiescent phase and active phase of the IMTP test, after the auditory command to "PULL". This instant was located to the nearest 0.001 s by analysing the sEMG traces of 14 muscles being monitored using the 2-step visual detection method.

The T_{mo}, was defined as the last trough (last point at the base of the first peak) before the signal deflected from baseline noise. The baseline noise refers to the signal obtained from the

muscles during the positional and postural weight bearing quiescent state. The deflection of the signal refers to the rapid increase in amplitude, reflective of the active state of the muscle during maximal voluntary isometric effort. Locating the T_{mo} requires an examiner or a rater to recognize the baseline noise patterns and differentiate it from the active state. The baseline muscle activity signal obtained during the quiescent state of the IMTP was observed to vary between muscles based on their respective roles. Therefore, all sEMG traces were classified under 3 distinctive categories based on the baseline muscle activity patterns.

The definition of T_{mo} was based on the amplitude characteristics of the signal and only applicable to muscle traces classified under Category 1 and Category 2 (Figure 3.8; 3.9). Muscles classified under Category 3, consisted of sEMG traces displaying high amplitude baseline activity with unevenly spaced spikes (signal deflection) (Figure 3.10). As such, recognition of the baseline noise during the quiescent state and differentiating it from the active state was based on both the amplitude and frequency content of signal. Considering the frequency characteristics of sEMG traces in Category 3 the definition of T_{mo} was amended such that, the T_{mo} was detected at the trough (base) of the first spike of the sustained deflected signal, displaying a distinctively frequency-dense region as opposed to the baseline muscle activity (Figure 3.10). While it is beyond the scope of this thesis, the categories can also be described mathematically. This would involve averaging the baseline amplitude in sEMG traces classified under Category 1 and 2 and quantifying the frequency content of the signal in traces classified under Category 3.

3.5.2 Iterations of the MATLAB programme

The first iteration of the MATLAB programme involved the detection of T_{mo} with a constant y-axis scale of 2 mV and an x-axis scale of 1000 ms. The key limitation of the first iteration was associated with selecting a point amongst 2000 (2000 Hz) individual data samples displayed in the window, i.e., the portion of the graph being viewed was 1 s in duration, therefore there were 2000 discrete samples when sampling at 2000 Hz (Figure 3.6; 3.11 A). Consequently, in sEMG traces with low baseline noise, the potential variation in the selected point was estimated to be in the order of ~ ± 5 ms. Whereas, for higher baseline noise the variation in the selected point was estimated to be in the order of ~ ± 10 ms (Figure 3.11). This specifically affected the precision of T_{mo} detection in muscles that displayed nosier baseline patterns. Figure 3.11 A illustrates a rater's selection of an instant representative of T_{mo} marked on 3 different occasions with a scale of 2 mV along the y-axis and 1000 ms along the x-axis. Figure 3.11 B illustrates the same graph in Figure 3.11 A with the 3 selected samples, viewed at a higher resolution, displaying a full scale of 50 ms along the x-axis. The example in figure 3.11 demonstrates the accuracy of the system up to 50 ms however the precision of the selected point was affected in the order of ~ ± 10 ms.

Despite the limitations, the first iteration of the MATLAB programme was instrumental in the observational study of sEMG traces and recognising differences in baseline noise patterns between muscle pairs and, in some cases, within muscle pairs. To the author's knowledge, methodological considerations with respect to visually detecting the T_{mo} in a multi-muscle multi-joint test does not exist within the scientific literature. As such, the first iteration provided a good starting point for the visual analysis of sEMG traces recorded during an IMTP.

Recognising the limitations of the first iteration, i.e., limited temporal precision, the second iteration of the MATLAB programme was performed to standardise a zoom scale along the x-axis, such that each trace was viewed at a higher resolution. Additionally, all sEMG traces were categorised in 3 distinct categories based on their baseline activity patterns. In the second iteration, the first step took place at same x-axis scale (1000 ms) as the first iteration. However, the purpose of this step was to approximately mark the T_{mo} so that the area around that point could be enlarged. The area was enlarged such that, the marked point was centred at a higher resolution, with a full scale of 50 ms, along the x-axis. The second step therefore, involved the final selection of a point representative of T_{mo} amongst 100 data samples with a precision of 0.5 ms as opposed to the 2000 data samples in the first iteration. The resolution

along the y-axis (2mV) remained constant across both steps. Implementing such a method, by increasing the resolution of the scale on the x-axis, allows an operator to identify samples with a precision of 0.5 ms. This was the 2-step visual detection method, wherein sEMG traces were viewed and T_{mo} detected at a higher resolution only along the x-axis as opposed to previously applied methods (Crotty et al., 2021; Tillin et al., 2010).

3.5.3 Methodological considerations in comparison to previous research on single-joint tests of neuromuscular function

Tillin et al. (2010), visually detected the T_{mo} in sEMG traces, initially viewed at a constant y-axis scale of 10 mV and an x-axis scale of 500 ms. The T_{mo} was then verified at a higher resolution, such that the traces were viewed at a y-axis scale of 6 mV and an x-axis scale of 25 ms. The sEMG traces were obtained from the knee extensor muscles during a series of isometric knee extensions of the dominant leg. Participants were secured to a strength testing chair with a waist belt and shoulder straps and the hip and knee angles were fixed.

Similar methods and scales were used by Crotty et al. (2021) to visually detect the T_{mo} in a series of isometric plantarflexion of the right leg. Participants laying prone on a calibrated dynamometer were secured in a similar manner and the ankle was fastened using two straps.

In contrast to these previous methods, each sEMG trace in the present study were marked twice, differing in resolutions only along the x-axis. Selecting the point of onset using a wider resolution and verification of the marked point at a higher resolution maybe sufficient for single joint tests of neuromuscular function. This is especially when these tests are performed laying or sitting on an adjustable strength chair since the postural and weight bearing demands on the target muscles are near negligible.

Further, securing participants and respective joint angles as done by Tillin et al. (2010) and Crotty et al. (2021), helps minimise any pre-tension in the target muscles and movement in other body parts. As such, sEMG traces do not require categorization, with most traces characteristically similar to the ones classified under Category 1 (Figure 3.8) in the present study.

On the contrary, the postural and weight bearing quiescent phase of an IMTP is susceptible to movement artefacts and anticipatory pre-tension in muscles, often detected as noise. Further, the level of noise in the target muscles was affected by their respective functions in both the quiescent and active phases of the test. Therefore, acknowledging the multi-muscle multi-joint nature of the test in the current study, categorization of sEMG traces was imperative.

The sEMG traces obtained from the 14 muscles during an IMTP were categorised primarily based on their amplitude characteristics along the y-axis, aiding in temporal analysis along the x-axis. This is of particular importance from a visual perspective since, magnifying both the x-axis and y-axis to achieve a higher resolution window, is likely to change the visual characteristics of the sEMG trace, especially in traces with lower SNR (high levels of noise). Therefore, considering the varying levels of noise associated with each muscle tested in the present study, it was deemed reasonable to retain the amplitude characteristics of the traces in the initial window while magnifying the x-axis in the final window.

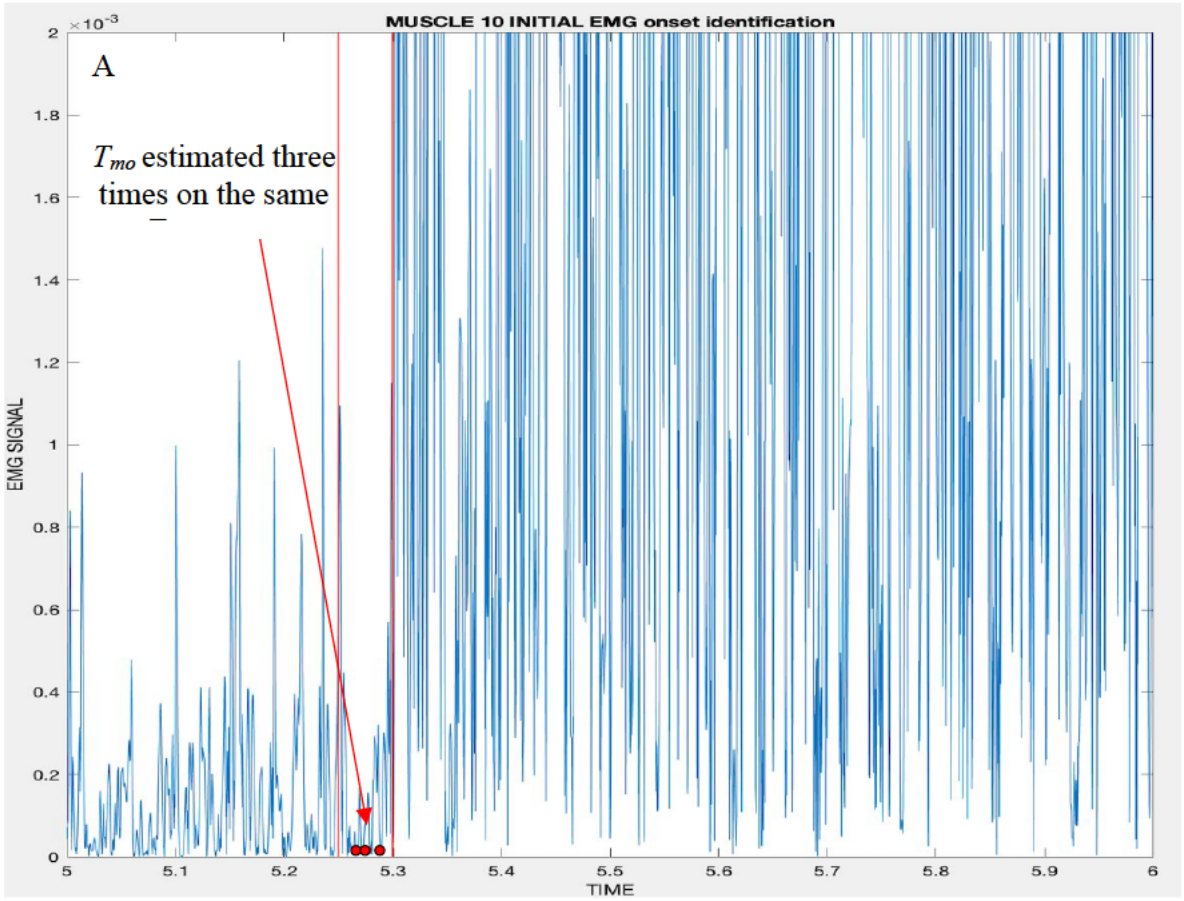
MUSCLE 10 INITIAL EMG onset identification
A
T_{mo} estimated three times on the same
EMG SIGNAL
TIME

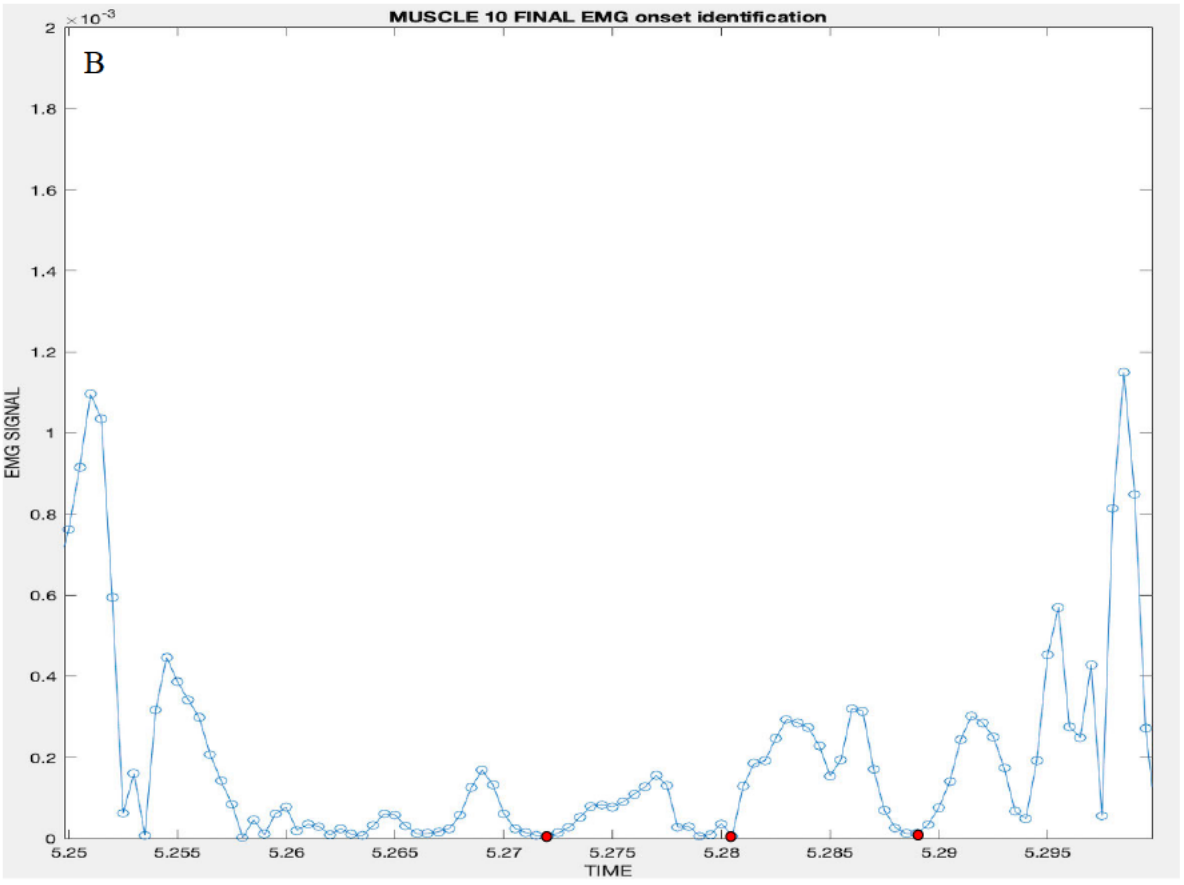
MUSCLE 10 FINAL EMG onset identification
B
EMG SIGNAL
TIME

Figure 3.11 *Illustrates an EMG trace with relatively high baseline noise. (A) Represents the initial window viewed with a y-axis scale of 2mV and an x-axis scale of 1000 ms, displaying 2000 data samples. (B) Is the expanded scale along the x-axis such that the same window in (A) is viewed with a higher resolution, y-axis scale of 2mV and an x-axis scale of 50 ms, displaying 100 data samples.*

3.6 Summary

In this study, key methodological considerations, and procedures with respect to the assessment of muscle activity, specifically T_{mo} using sEMG during an IMTP are reported. The study successfully addressed the first objective of the thesis by identifying seven pairs of muscles, based on the literature that are most likely to be activated during the performance of an IMTP. Further, the study was also successful in the development of a software-based visual detection tool, the 2-step visual detection method, for determining T_{mo} in a multi-joint multi-muscle isometric activity.

The 2-step visual detection method was a product of multiple MATLAB iterations, developed to identify T_{mo} in sEMG traces at two different resolutions with the help of three distinctive categories. In an IMTP, T_{mo} was judged as the instant between the quiescent phase and active phase of the test, after the auditory command to "PULL". This instant was located to the nearest 0.001 s by analysing the sEMG traces of the selected muscles using the 2-step visual detection method.

The development of the 2-step visual detection method addresses the second objective of the thesis. However, its reliability for assessing the T_{mo} in muscles of participants performing an IMTP needs to be established before its use as a tool to validate existing IMTP start-time methods.

Chapter 4.0 Study 2: Reliability of a software based visual detection method for determining the time of muscle onset recorded using surface electromyography in an isometric midthigh pull

4.1 Introduction

To the author's knowledge, assessment of muscle activity, particularly identification of T_{mo} in an IMTP remains to be investigated. In line with this, in the previous chapter a method for identifying T_{mo} in a multi-muscle, multi-joint isometric activity, the IMTP, was developed. It is reasonable to consider the method valid as it uses techniques previously used to detect muscle onset time for isometric contraction in single-joint activities (Crotty et al., 2021; Tillin et al., 2012). However, before this method is used as means to validate an IMTP start-time, its reliability for the assessment of T_{mo} in muscles of participants performing the test needs to be established.

With this, the purpose of the study was to assess the reliability of the 2-step visual detection method developed in Chapter 3, for determining the T_{mo} in 7 pairs of muscles in an IMTP. Thus, the study was designed to address objectives III and IV of the thesis, concluding with recommendations on muscles that can be used to represent T_{mo} during a MVC in an IMTP.

4.2 Methods

The method of data collection and analysis in the assessment of muscle activity recorded using sEMG in an isometric test of neuromuscular function, the IMTP are identical to Chapter 3, and described in Section 3.3. The data for the assessment of reliability was produced using the 2-step visual detection method developed in Chapter 3.

4.2.1 Experimental approach: Overview

The study was designed to assess the reliability of visually detecting T_{mo} in an isometric midthigh pull (IMTP) using surface electromyography (sEMG). The 2-step visual detection tool developed in Chapter 3 was used in the present study to identify $T_{mo.}$ Figure 4.1 illustrates the standardised testing day layout employed for data collection. Participants arrived at the testing location having refrained from fatiguing exercise and caffeine consumption for 24 hours before testing day. Following the arrival, anthropometric measurements and respective bar height of the IMTP rig were determined (Section 3.3.1; 4.3.3). Skin preparation of EMG sensor sites (Section 3.3.3.1) was interspersed by a standardised warm-up (section 3.3.1). The area on the muscles of interest were located, marked and dry shaven before the warm-up (Section 3.3.3.1). Following the warm-up, alcohol wipes were used to remove any sweat, residual hair, dry dermis and skin oils. The sensors were then affixed to their pre-assigned locations oriented in line with the underlying

muscle fibres. The participants were then expected to perform three familiarisation submaximal trials in preparation of subsequent maximal efforts (Section 3.3.1).

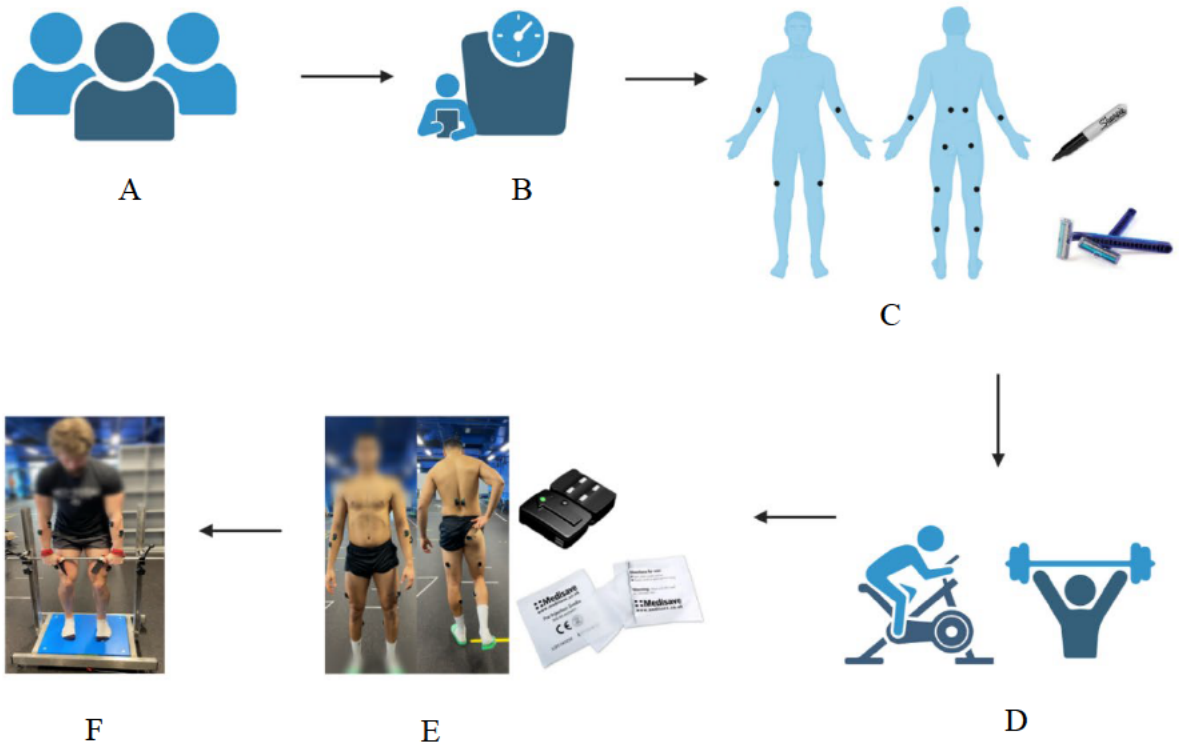

Figure 4.1 *Illustrates the testing day layout. (A) Participant arrival (B) Collection of anthropometric measurements and determination of IMTP rig bar height. (C) EMG sensor location, marking and dry shaving performed as a part of skin preparation. (D) Standardised warm-up. (E) Wiping EMG sensor sites and affixing the pre-assigned EMG electrodes to the respective muscles of interest. (F) Performance of submaximal and maximal IMTP trials.*

4.2.2 Experimental design and participant Recruitment

Participants (N = 9, mean ±SD: 26.8 ± 2.8 years; 179.4 ± 5.6 cm; 89.6 ± 5.1 kg) provided written informed consent to participate in the study, which was approved by the Swansea University Ethics Committee (Appendix A,B,C). Participants were recruited on the basis that they had engaged in structured weight-training programme and had more than 3 years of experience in weightlifting exercises, specifically the power clean.

4.2.3 Determination of anthropometric measurements

Body height was measured using a portable stadiometer (Seca 213, Hamburg, Germany) to the nearest 0.1 cm. Body weight was measured in newtons (N), with participants standing still and upright on a portable force platform (FP) (type 9260AA6, Kistler Instruments Ltd., Farnborough, United Kingdom) sampling at 1000 Hz, for approximately 5 s. The average value between the 3rd and 4th second of the recorded vertical component of the ground reaction force (VGRF) was noted to the nearest 0.1 N. BW was divided by 9.81 $m \cdot s^{-2}$ (acceleration due to gravity) to calculate the body mass (BM) of the participant to the nearest 0.1 kg.

4.2.4 Experimental conditions

The sEMG data collected during the IMTP was performed under 3 conditions, designated as; ‘ON’, ‘OFF’ and ‘WL’. The ON and OFF conditions were performed by the same participant on two separate occasions interspersed by a recovery period of 72-hours. The third condition involved the other 8 weightlifters (WL), that performed a minimum of 3 trials each on the same day.

4.2.4.1 Condition 1: ON

In this condition one male participant (Age: 29 years; weight: 88.3 kg; height: 183.8 m and weightlifting experience > 3 years) performed a minimum of 8 acceptable IMTP trials, Figure 3.3 A. with a rest period of 3-5 minutes between each subsequent pull. The sEMG sensors were stuck to the surface of the skin of the participant over the belly of the 14 muscles, Figure 3.1 and 3.2, Table 3.1 and 3.2 and Section 3.3.3, prior to the first IMTP trial. These sensors remained in place, on the muscles of the participant until the conclusion of the test condition. The ‘ON’ condition was designed for the visual assessment of muscle activation

patterns in terms of SNR, during IMTP test-retest trials for the same individual and its effect on reliability.

4.2.4.2 Condition 2: OFF

On a separate occasion, the same participant in the ON condition, arrived for their second visit and performed a minimum of 8 acceptable IMTP trails, Figure 3.3 A, with a rest period of 3-5 minutes between each subsequent pull. The sEMG sensors were stuck to the surface of the skin of the participant over the belly of the 14 muscles, Figure 3.1 and 3.2, Table 3.1 and 3.2 and section 3.3.3, prior to the first IMTP trial. All 14 electrodes were removed after each trial. During the rest period, prior to subsequent trials new self-adhesive electrode tapes were used to prepare the sensors and re-attached approximately to their original position. The OFF test-retest condition was designed to visually assess whether sensor placement performed by a trained individual had an effect on muscle activation patterns, in terms of SNR and the reliability.

4.2.4.3 Condition 3: WL

In this condition 8 male participants (mean ±SD: 26.5 ± 2.9 years; 178.9 ± 5.7 cm; 89.8 ± 5.4 kg) with a background in weightlifting (> 3 years) were recruited. The participants arrived at the testing location and were lead across the testing session displayed in Figure 4.1. Each participant performed a minimum of 3 acceptable IMTP trials (Figure 3.3 A), with a rest period of 3-5 minutes between trials. This condition was designed to assess the reliability in a group of participants as opposed to an individual in the previous two conditions. The condition further allowed the assessment of whether muscle activation patterns of individual or bilaterally paired muscles were similar across weightlifting trained individuals.

Collectively, such a study design allowed the assessment of reliability in visually detecting multi-muscle activity across 3 conditions during a maximal multi-joint isometric activity. The data further allows investigations into the most reliable muscles or muscle pairs across conditions, capable of directing future research considerations.

4.2.4.4 Sample size

While the sample population may appear small with N = 1, in ‘ON’ and ‘OFF’ and N = 8 in, ‘WL’, the true dataset consists of the total number of onset points (sEMG traces) acquired as a result of the current study design. A total of 336 sEMG traces were acquired by analysing

14 muscles (seven pairs) across three conditions with eight trials in 'ON' and 'OFF' and eight participants in 'WL' condition (3 x 14 x 8 = 336). Therefore, the true 'N' in the current study is 336 onset points, which is significantly higher than previous studies investigating the reliability of visual detecting the T_{mo} (Crotty et al., 2021; Tillin et al., 2010).

4.2.5 Isometric midthigh pull output variables

The VGRF was analysed to determine the absolute PF, the time to PF and the average RFD. The absolute PF was calculated by subtracting the participant's BW (N) from the PF produced during the trial. The time difference between the pull initiation (0 s) and time at absolute PF was used to determine the time to PF. Absolute PF divided by the time to PF was used to calculate the average RFD

4.2.6 Selection of isometric midthigh pull trial

Each IMTP trial underwent visual inspection and objective selection criteria. For the 8 WL participants, 3 satisfactory trials were obtained (Figure 3.3 A) . While for the one participant recruited for both the ON and OFF conditions, 8 satisfactory trials were obtained in each condition (Figure 3.3 A). Objectively, the trial with the highest average RFD value of the 3 trials for the 8 WL was used to select the respective sEMG data for further analysis. Similarly, from each of the two other conditions the 8 pulls with the highest average RFD were chosen from the ON condition and the 8 pulls with highest average RFD were chosen from the OFF condition. The selected pulls were then used to select the respective sEMG data for further analysis. The rationale for the selection process was that RFD during explosive contractions is associated with a greater number of motor units recruited and motor neurons discharged at frequencies significantly greater than sustained contractions (Del Vecchio et al., 2019; Enoka & Duchateau, 2017). Therefore, it was assumed that the trial with peak forces achieved in the least amount of time expressed as, average RFD, would best display visually clear points (data samples) of muscle activity onset recorded synchronously using sEMG.

4.2.7 Surface electromyography data analysis

The full-wave rectified sEMG traces for all muscles under each condition were viewed on MATLAB between the 5th and 6th second of the test (Section 3.3.4). The T_{mo} was selected using the 2-step visual detection method. Methodological considerations for selecting the T_{mo} using the 2-step visual detection method are reported in Chapter 3, Sections 3.3.6, 3.3.7 and 3.4.

4.2.8 Statistical analysis

The reliability of visual onset detection was evaluated for 14 muscles across 3 conditions: ON, OFF and WL. Standard deviation (SD) of differences (variation) between two independent sets of muscle onset times was used as the measure of reliability in the assessment of how close two successive readings were for the same muscle across all conditions.

The intra-rater reliability was evaluated by calculating the standard deviation (SD) of the differences in pairs of T_{mo} identified by rater 1 with 5 days between trials. Inter-rater reliability was evaluated by calculating the SD of differences in pairs of T_{mo} identified by both raters, 1 and 2. To account for potential bias and learning effect, the order of markings were randomised in each condition for both raters and the sEMG traces of all muscles remained unlabelled.

4.2.9 Reliability criteria

To the authors knowledge, there is no pre-set criteria for reliability of visually detecting the onset of multiple muscles in a maximal multi-multi joint isometric test. Based on a recent study, automated methods of EMG onset detection were validated against manual visual detection using a criterion of correspondence of 3 ms (Crotty et al., 2021). As such, automated methods exceeding visual detection by uncertainty of 3 ms, were deemed invalid. The criteria of 3 ms was used for single-joint isometric tests with minimal positional demand and postural weight bearing was negligible. Thus, for a multi-muscle multi-joint test, where muscles are also activated for postural control, it is reasonable to propose a visual detection reliability criterion of correspondence $\leq$ 5 ms. The proposed increase in criterion magnitude is reasonable as sEMG traces are suspectable to increased noise during the quiescent phase of an IMTP due to three key factors; postural weight bearing, movement artefacts about the hip, knee and ankle joints and anticipatory pre-tension in muscles. Brown and Frank (1987), studied the onset of tibialis anterior, lateral gastrocnemius, anterior and posterior deltoid using visual detection during a two-choice reaction-time task involving pushing or pulling on a handle as quickly as possible. Investigating the influence of event anticipation on postural actions accompanying voluntary movement, each experimenter made an independent estimate of onset times and trials with differences exceeding 5 ms were discarded (Brown & Frank, 1987). However, to account for variations inherent in the current experimental setup and data collection methods, we set a reliability criterion of a SD of differences $\geq$ 5 ms for the identification of $T_{mo.}$ The study by Brown and Frank (1987), involving multi-joint postural

assessments provides some support for the reliability criteria adopted in the current study (Hodges & Bui, 1996).

The T_{mo} was detected on a chart with vertical scale of 2 mV (full scale) on the y-axis and 50 ms (full scale) along the x-axis. Each markable point along the x-axis is 0.5 ms, (i.e., 10 discrete, markable, samples between each 5 ms tick mark).

A time of 0.5 ms was the sampling time of the data acquisition system, corresponding to a sample frequency of 2000 Hz. Therefore, from a visual assessment aspect a variation of ≤ 5 ms (10 data samples) as the criteria for reliability in the current study was deemed a reasonable uncertainty to aim for.

Intra-rater and inter-rater data analysis was performed on EXCEL, with the mean, SD and associated error (standard error of mean (SE)) of differences between markings reported for each muscle (n = 14) across all conditions. A total of 336 onsets (14 muscles x 3 conditions x 8 pulls/participants per condition) were marked on each occasion, equating to 672 onsets for Rater 1, for intra-rater reliability and 336 for Rater 2, for inter-rater reliability.

4.3 Results

The purpose of this study was to assess the reliability of visually detecting T_{mo} in 14 muscles during a maximal multi-joint isometric test, the IMTP. The 2-step visual detection method was used to obtain the relevant data for reliability analysis. The results are reported as the mean, SD and associated error (SE) of differences in visually detected T_{mo} marked by the same rater (intra-rater) and two raters (inter-rater).

4.3.1 Intra-rater reliability

Rater 1 performed the intra-rater analysis. As per the criteria described in section 4.2.9, the SD of the differences between the first and second markings must be less than or equal to 5 ms or visual detection difference of 10 data samples. The variation (SD) in differences between the two sets of markings for all 14 muscles across the 3 experimental condition was ≤ 5 ms. The gastrocnemius (GS) on both sides of the body had the least variation across all conditions, ≤ 1 ms, Figure 4.2; Table 4.1.

4.3.2 Inter-rater reliability

Rater 2 completed a set of markings for inter-rater analysis. Similar criteria to the intra-rater analysis were maintained, in order to elicit which muscles produced the least variation (≤ 5 ms) in differences between the markings of Rater 1 and Rater 2, Figure 4.3; Table 4.2, across the 3 conditions.

In the ON condition, where sEMG sensors remained stuck to the selected muscles, the variation in markings calculated as the SD of differences was ≤ 5 ms for all muscles on the right side of the body (n = 7) (Figure 4.8; Table 4.4). Of the 7 muscles on the left side of the body, gluteus maximus (GM), extensor digitorum (ED) and brachioradialis (BR) were the 3 muscles with a variation greater than 5 ms (Figure 4.3; Table 4.2). The gastrocnemius (GS) on both sides of the body had the least variation ≤ 1 ms (Figure 4.3; Table 4.2).

In the OFF condition, where sEMG sensors were removed and re-attached before each subsequent trial, left and right GS, bicep femoris (BF) and erector spinae longissimus (ESL) had a variation of ≤ 5 ms (Figure 4.8; Table 4.4). For vastus lateralis (VL) only the left side had a variation of ≤ 5 ms (Figure 4.8; Table 4.4). The gastrocnemius (GS) on both sides of the body had the least variation ≤ 1 ms (Figure 4.3; Table 4.2).

In the WL condition, consisting of 8 participants proficient in weightlifting, variation (SD) in differences between markings for muscles of the forearm, ED and BR on both sides of the body was greater than 5 ms (Figure 4.3; Table 4.2). Left and right, GS, BF, VL, GM and ESL had a variation of ≤ 5 ms, with the least variation observed for GS (≤ 1 ms) (Figure 4.3; Table 4.2).

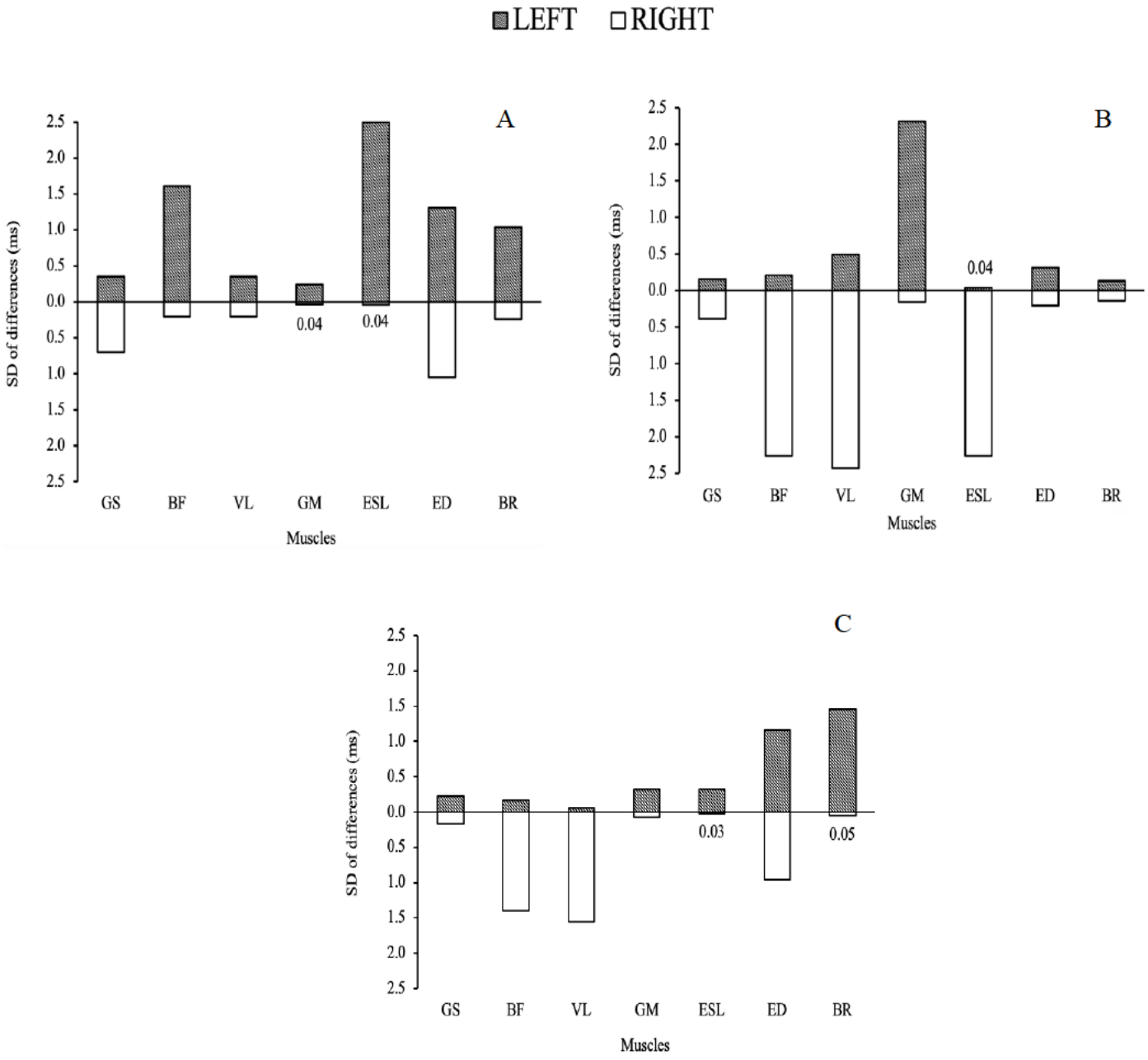

GS = Gastrocnemius Medialis, BF = Bicep Femoris, VL = Vastus Lateralis, GM = Gluteus Maximus, ESL = Erector Spinae Longissimus, ED = Extensor Digitorum, BR = Brachioradialis.

Figure 4.2 *Standard deviation (SD) of differences (milliseconds (ms)) in visually detected T_{mo} twice by rater 1 (intra-rater) for 14 muscles in each of the 3 conditions: (A) ON (N = 8), (B) OFF (N = 8) and (C) WL (N = 8).*

Table 4.1 *Mean, SD and associated error (SE) calculated for differences in T_{mo} detected by Rater 1 on two separate occasions for intra-rater analysis.*

	ON (ms)			OFF (ms)			WL (ms)		
Muscles	Mean	SD	SE	Mean	SD	SE	Mean	SD	SE
Left GS	0.3	0.4	0.1	0.1	0.2	0.1	0.2	0.2	0.1
Right GS	0.5	0.7	0.2	0.2	0.4	0.1	0.1	0.2	0.1
GS	0.4	0.5	0.2	0.1	0.3	0.1	0.1	0.2	0.1
Left BF	0.7	1.6	0.6	0.1	0.2	0.1	0.1	0.2	0.1
Right BF	0.1	0.2	0.1	0.9	2.3	0.8	0.5	1.4	0.5
BF	0.4	0.9	0.3	0.5	1.2	0.4	0.3	0.8	0.3
Left VL	0.2	0.4	0.1	0.3	0.5	0.2	0.1	0.1	0.0
Right VL	0.2	0.2	0.1	1.0	2.4	0.9	0.7	1.6	0.6
VL	0.2	0.3	0.1	0.7	1.5	0.5	0.4	0.8	0.3
Left GM	0.2	0.2	0.1	1.7	2.3	0.8	0.3	0.3	0.1
Right GM	0.1	0.0	0.0	0.1	0.2	0.1	0.1	0.1	0.0
GM	0.1	0.1	0.0	0.9	1.2	0.4	0.2	0.2	0.1
Left ESL	1.4	2.6	0.9	0.1	0.0	0.0	0.2	0.3	0.1
Right ESL	0.1	0.0	0.0	1.0	2.3	0.8	0.0	0.0	0.0
ESL	0.7	1.3	0.5	0.5	1.1	0.4	0.1	0.2	0.1
Left ED	0.6	1.3	0.5	0.2	0.3	0.1	0.5	1.2	0.4
Right ED	0.5	1.0	0.4	0.1	0.2	0.1	0.5	1.0	0.3
ED	0.6	1.2	0.4	0.2	0.3	0.1	0.5	1.1	0.4
Left BR	0.5	1.0	0.4	0.1	0.1	0.0	0.6	1.5	0.5
Right BR	0.2	0.2	0.1	0.1	0.1	0.0	0.1	0.0	0.0
BR	0.4	0.6	0.2	0.1	0.1	0.0	0.4	0.8	0.3

SE = Standard error of mean; SD = Standard Deviation.

Muscles: GS = Gastrocnemius Medialis, BF = Bicep Femoris, VL = Vastus Lateralis, GM = Gluteus Maximus, ESL = Erector Spinae Longissimus, ED = Extensor Digitorum, BR = Brachioradialis

†*Data presented as mean, SD and SE of differences in visually detected T_{mo} marked twice by Rater 1 for 14 muscles. Data also presented as mean, SD and SE of differences between the first and second visually detected T_{mo} for the 7 experimental bilateral muscle pairs.*

ON (N = 8) = Condition 1; OFF (N = 8) = Condition 2; WL (N = 8) = Condition 3

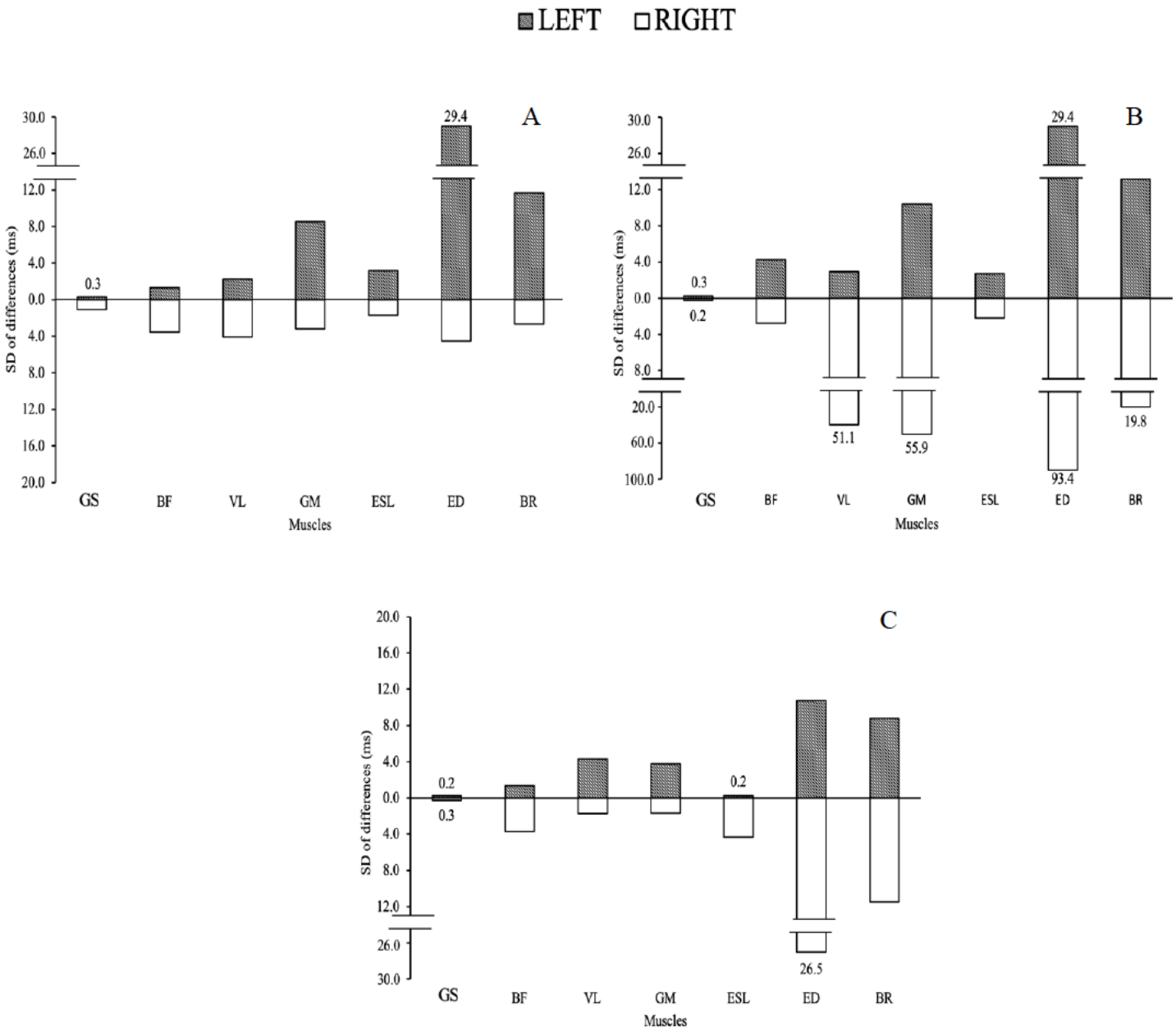

GS = Gastrocnemius Medialis, BF = Bicep Femoris, VL = Vastus Lateralis, GM = Gluteus Maximus, ESL = Erector Spinae Longissimus, ED = Extensor Digitorum, BR = Brachioradialis.

Figure 4.3 *Standard deviation (SD) of differences (milliseconds (ms)) in visually detected T_{mo} marked twice by rater 1 and rater 2 (intra-rater) for 14 muscles in each of the 3 conditions: (A) ON (N = 8), (B) OFF (N = 8) and (C) WL (N = 8).*

Table 4.2 *Mean, SD and associated error (SE) calculated for differences in T_{mo} detected by Rater 1 and Rater 2 for inter-rater analysis.*

	ON (ms)			OFF (ms)			WL (ms)		
Muscles	Mean	SD	SE	Mean	SD	SE	Mean	SD	SE
Left GS	0.3	*0.3	0.1	0.3	*0.3	0.1	0.2	*0.2	0.1
Right GS	0.7	*1.0	0.4	0.3	*0.2	0.1	0.2	*0.3	0.1
GS	0.5	*0.7	0.2	0.3	*0.2	0.1	0.2	*0.3	0.1
Left BF	1.5	*1.3	0.5	2.4	*4.2	1.5	0.8	*1.4	0.5
Right BF	2.3	*3.5	1.3	1.7	*2.8	1.0	2.1	*3.7	1.3
BF	1.9	*2.4	0.9	2.1	*3.5	1.2	1.4	*2.5	0.9
Left VL	1.0	*2.2	0.8	2.2	*3.0	1.0	2.1	*4.3	1.5
Right VL	2.2	*4.1	1.4	22.2	51.1	18.1	1.6	*1.7	0.6
VL	1.6	*3.2	1.1	12.2	27.0	9.6	1.9	*3.0	1.1
Left GM	4.5	8.5	3.0	6.8	10.4	3.7	1.7	*3.8	1.3
Right GM	1.8	*3.2	1.1	21.7	55.9	19.8	0.8	*1.7	0.6
GM	3.2	5.9	2.1	14.3	33.1	11.7	1.3	*2.7	1.0
Left ESL	2.4	*3.2	1.12	1.4	*2.7	0.96	0.3	*0.2	0.1
Right ESL	1.7	*1.7	0.6	1.1	*2.2	0.8	2.8	*4.3	1.5
ESL	2.0	*2.4	0.9	1.2	*2.5	0.9	1.6	*2.3	0.8
Left ED	17.6	29.4	10.4	15.7	29.4	10.4	7.5	10.7	3.8
Right ED	1.9	*4.5	1.6	53.6	93.4	33.0	26.6	26.5	9.4
ED	9.7	17.0	6.0	34.6	61.4	21.7	17.0	18.6	6.6
Left BR	12.9	11.7	4.1	11.6	13.2	4.7	9.2	8.8	3.1
Right BR	1.8	*2.7	0.9	12.7	19.8	7.0	7.5	11.5	4.1
BR	7.3	7.2	2.5	12.2	16.5	5.8	8.4	10.1	3.6

SE = Standard error of mean; SD = Standard Deviation.

Muscles: GS = Gastrocnemius Medialis, BF = Bicep Femoris, VL = Vastus Lateralis, GM = Gluteus Maximus, ESL = Erector Spinae Longissimus, ED = Extensor Digitorum, BR = Brachioradialis.

**Standard deviation (SD) of differences ≤ 5 ms*

†*Data presented as mean, SD and SE of differences in visually detected T_{mo} marked by rater 1 and rater 2 for 14 muscles. Data also presented as mean, SD and SE of differences in visually detected T_{mo} marked by the two raters for the 7 experimental bilateral muscle pairs.*

ON (N = 8) = Condition 1; OFF (N = 8) = Condition 2; WL (N = 8) = Condition 3

4.4 Discussion

The IMTP is a multi-joint multi-muscle test designed to approximate the body in the power position replicating the beginning of the second pull during the weightlifting exercises, power cleans and snatch (Haff et al., 1997). The IMTP was first presented to the scientific and coaching community in 1997, and it has since been used extensively in neuromuscular performance research among athletes across various disciplines (Haff et al., 1997; Stone et al., 2019). Despite its widespread use in research and by practitioners, the method of identifying a IMTP start-time (i.e.an instant between the end of the quiescent phase and the start of the active pulling phase) remains to be validated and subsequently standardised (Section 2.7.4 and Table 2.1). The validation and standardisation of a start-time is especially important in time-dependent variables such as RFD given its diagnostic ability of addressing performance in time-constrained tasks in sports (Suchomel, Nimphius, et al., 2016), return-to-sport decisions following injuries (Angelozzi et al., 2012), and as a marker of exercise-induced neuromuscular fatigue (Farup et al., 2016; Oliveira et al., 2016; Peñailillo et al., 2015; Thorlund et al., 2008).

The expression of mechanical force is preceded by a physiological phenomenon of neural and muscular excitation. Acknowledging this principle, it was proposed that the time of muscle onset during an IMTP recorded using surface electromyography (sEMG) would serve as an appropriate tool for identifying the start of this phenomenon and consequently, for validating the onset (start-time) of mechanical force production.

Consequently, the primary purpose of the current study was to assess the reliability of visually detecting the T_{mo} in 14 muscles (7 bilateral pairs) (Figure 3.1) during a MVC in an IMTP. The sEMG data collected during the IMTP was performed under 3 experimental conditions, designated as; 'ON', 'OFF' and 'WL' (Section 4.2.4). The 2-step visual detection method and its constituent categories established in Chapter 3 were applied by both raters to determine the T_{mo}. Inter-rater and intra-rater analysis were carried out to establish the most reliable muscles in terms of temporal agreement of muscle onset times, that could be used in the future to validate a IMTP start-time method. The results of this study demonstrate, 3 muscle pairs (left and right) GS, BF and ESL to be the most reliable muscles for the identification of T_{mo} during an IMTP across the three experimental conditions.

4.4.1 Discussion of the statistical method used in the study

Prior to discussing the results, it is important to highlight the statistical analysis employed in this study.

Commonly applied measure of reliability, intraclass correlation coefficient (ICC) has previously been used along with typical error (TE) to evaluate the reliability of visual onset detection in an isometric ankle plantarflexion test (Crotty et al., 2021). The study reported excellent intra-rater (TE = 0.3 ms; ICC = 1.000) and inter-rater (TE = 1.1 ms; ICC = 1.000) reliability, however the absolute variation between markings was unknown. Whilst, ICC is a quantitative measure, it does not allow the quantification of error is terms of absolute values. Consider the example in Table 4.3, the sample data set represents T_{mo} marked by Rater 1 and Rater 2 and the differences between their markings. The rational-whole number in this example is '5' since the command to pull was consistently given after 5 s of quiescent state. Consequently, the onset of muscle activity was always recorded between the 5^{th} and 6^{th} second of the IMTP trial. Performing ICC (Two-way mixed, Absolute agreement) in SPSS (v28), on the sample data demonstrated excellent reliability, 0.900 ($p < 0.001$). However, when the SD of differences is calculated on excel for the same data, a variation of 55.9 ms is observed. Although statistically insignificant, a variation of 55.9 ms is crucial from a physiological performance aspect especially during time constrained tasks in sports (Suchomel et al., 2016). The example in Table 4.3 illustrates the lack of ability of ICC to quantify errors in units of the original variables i.e., time (difference). Therefore, previously applied methods, ICC and hence TE (TE = SD $\sqrt{(1 - ICC)}$) are not appropriate statistical measures for assessing the reliability of visual onset detection (Crotty et al., 2021; Gupta et al., 2014; Tillin et al., 2010). Further, TE, wouldn't work if ICC = 1, as reported previously (Crotty et al., 2021).

Intra-rater reliability was assessed by calculating the SD of differences between the first and second set of markings performed by Rater 1 (Figure 4.2; Table 4.1). Inter-rater reliability was assessed by calculating the SD of differences between the markings performed by the two raters (Figure 4.3; Table 4.2). The method of calculating the absolute variation in markings, reported as the SD of differences in this study is a novel approach, however it allows decisions to be made about the applied use of muscle timings as it returns an absolute value of difference, in the units of the variable. Therefore, the results of the present study are not comparable to those reported in previous literature, assessing the reliability of visual detection of muscle activity onset in single-joint tests of neuromuscular function (Crotty et al., 2021; Gupta et al., 2014; Tillin et al., 2010).

Table 4.3 Sample data, T_{mo} detected by the two raters for the same muscle across 8 trials for inter-rater analysis

PULL No.	Experimental Muscle: Condition OFF		
	R1 T_{mo} (s)	R2 T_{mo} (s)	Diff (s)
PULL 1	5.489	5.489	0.000
PULL 2	5.260	5.264	0.004
PULL 3	5.333	5.330	0.003
PULL 4	5.650	5.650	0.000
PULL 5	5.497	5.499	0.002
PULL 6	5.483	5.483	0.000
PULL 7	5.404	5.564	0.160
PULL 8	5.423	5.427	0.004

T_{mo} = Time of muscle onset

R1 T_{mo} = T_{mo} determined by Rater 1

R2 T_{mo} = T_{mo} determined by Rater 2

Diff = Difference in T_{mo} between raters 1 and 2 for respective pulls.

4.4.2 Interpretation of the results

Intra-rater and inter-rater reliability of visually detecting the T_{mo} for 14 muscles during an IMTP was assessed using a pre-set criteria of ≤ 5 ms, variations above which were deemed unreliable.

Rater 1 determined the onset times in 336 sEMG traces obtained from 14 muscles, across three conditions consisting of 8 trials or participants in each. The differences in onset times determined on two occasions separated by 5 days were quantified for each muscle in each trial across all conditions. The SD of differences between the first and second markings performed by Rater 1 for all 14 muscles was ≤ 3 ms across all conditions (Figure 4.2; Table 4.1). The results of the intra-rater analysis therefore indicate that all 14 muscles were reliable, with left and right GS demonstrating the least variation (≤ 1 ms; Figure 4.2; Table 4.1).

Rater 2 determined the onset times in 336 sEMG traces (14 muscles x 3 conditions x 8 trials or participants in each condition). The differences in onset times determined by the two raters were quantified for each muscle in each trial across all conditions respectively. The SD of differences (variation) in T_{mo} was calculated to assess the inter-rater reliability for each muscle in the three experimental conditions. For a bilateral muscle pair to be deemed reliable, unilateral (left and right) variation in onset times between the markings of the two raters were required to be less than or equal to the pre-set criteria of 5 ms in each condition. The SD of differences in the ON condition was ≤ 5 ms for left and right GS, BF, VL and ESL (Figure 4.3; Table 4.2). Similarly, in the OFF condition, GS, BF and ESL were the three muscle pairs deemed reliable (Figure 4.3; Table 4.2). In the WL condition, 4 muscle pairs, GS, BF, GM and ESL were found to be reliable (Figure 4.3; Table 4.2). The muscles of the forearms, bilateral ED and BR were the least reliable across all conditions (Figure 4.3; Table 4.2). Collectively, GS, BF, ESL were identified as the 3 muscles for which T_{mo} could be measured reliably across the three experimental conditions (Figure 4.3; Table 4.2). The activity of muscles during the IMTP and explanation for associated results of reliability are further discussed in section 4.4.4.

4.4.3 Visual detection training time

There were considerable differences in the results of the intra-rater reliability compared to the inter-rater reliability analysis. The results of the intra-rater reliability indicate all 7 muscle pairs (14 experimental muscles) were reliable. These findings were in contrast to the results of the inter-rater reliability analysis, indicating only three muscle pairs, GS, BF and ESL to be reliable.

It is likely that, contrasting results are primarily due to the difference in the amount of training undertaken by both raters. Rater 1, also the lead researcher on the project, gained adequate experience in implementing definitions for each muscle category during the development of the 2-step visual detection method. Consequently, Rater 1 underwent sufficient training in visually detecting the onset of muscle activity during an IMTP. Additionally, Rater 1 was responsible for the experimental data collection, thus well versed with the associated intricacies of the methodological procedures. Rater 2 on the other hand, had expertise in signal processing with minimal training in manual visual detection of muscle onset during an IMTP.

While acknowledging these differences in training time as a key limitation, such a study design fits the purpose of the overall project. In the present case, results of the intra-rater analysis confirm the reliability of the 2-step visual detection method and its constituent categories established in Chapter 3. While the results of inter-rater reliability can be interpreted as a filter used to elicit the most reliable muscle pairs, fulfilling the purpose of the study. It would be reasonable to assume that, addressing the limitation by employing raters with knowledge in sEMG signal processing and similar amount of training in detecting the T_{mo}, would only improve the results of the current study. Furthermore, using ICC and TE as measures of reliability as used in previous similar studies (Crotty et al., 2021; Tillin et al., 2010), would yield results that identify all experimental muscles reliable in the current study regardless of the differences in training time.

Summarising, bilateral muscle pairs with a variation in T_{mo} of ≤ 5 ms in both intra-rater and inter-rater analysis were identified as reliable for future applications. The results of intra-rater reliability indicate all 7 muscle pairs (14 muscles) were reliable. While only 3 muscle pairs, GS, BF and ESL were identified as reliable from the results of inter-rater reliability. Therefore, the muscle pairs that would be recommended in the future for validating a start-time method in an IMTP are GS, BF and ESL.

4.4.4 Muscle activity and categorisation of sEMG traces

Briefly, visual detection of an onset point requires a rater to inspect the amplitude characteristics of the signal and differentiate between the baseline noise and active state of a muscle (Crotty et al., 2021; Tillin et al., 2010).

In the present case, baseline noise refers to the signal obtained during the quiescent phase of the test (the first 5 s of measurement, before the command to 'pull' is given). The active state of the muscle refers to the spike in signal amplitude detected after the command to "PULL". The activity onset was therefore judged as the instant between the quiescent phase and active phase of the IMTP test, after the auditory command to "PULL" (Section 3.5.1). The baseline muscle activity signal obtained during the quiescent state of the IMTP was observed to vary between muscles, in terms of signal amplitude, based on their respective roles during the test. The observed variations are possibly due to the differences in postural and weight bearing demands placed on the muscles. Further, pre-tension due to anticipation of the command to 'PULL' and subsequent maximal effort is likely to vary across muscles, contributing to their respective baseline activity signal. Acknowledging these differences, categorization of sEMG traces in the 2-step visual detection method was based on the baseline signal amplitude and frequency characteristics of muscles during the quiescent phase of the test (section 3.4).

4.4.4.1 Multi-muscle activity during the quiescent and active phases of an IMTP

The current study highlighted that the baseline activity of a muscle during the quiescent phase of an IMTP is likely to affect the reliable identification of $T_{mo.}$ As such, this subsection will discuss the activity of all muscle pairs assessed in the current study with reference to their functions described in section 3.2. Further, it will attempt to provide an explanation for the results of the current study based on the activity of muscles during the quiescent phase of an IMTP via the visual inspection of respective sEMG traces.

The gastrocnemius medialis (GS) is responsible for the transfer of force into the ground during the initial phases (first pull) and plantar flexion in the later phases (second pull) of a power clean (Dryburgh & Psycharakis, 2016). The positioning in an IMTP is achieved primarily by flexion around the knee (125-145°) and hip joints (140-150°) (Comfort et al., 2019). Knee joint flexion, reduces the angle between the leg and the dorsum of the foot, also termed as dorsiflexion. The muscles in the anterior compartment of the lower leg, tibialis

anterior, extensor digitorum longus, extensor hallucis longus and fibularis tertius are collectively responsible for dorsiflexion of the foot (Juneja & Hubbard, 2020). As such, these muscles act as agonists (that is, maintaining postural stability) during the quiescent phase when the knee is flexed to assume the optimal IMTP position. Conversely, the GS in the posterior compartment acts as the antagonist (Figure 4.4). The amplitude spike in sEMG traces of GS after the command to 'PULL' represents the onset of contraction in order to develop force at the feet, measured externally as the VGRF (Figure 3.3, 4.5; Section 3.4.1). Thus, sEMG traces of GS recorded in the current study, demonstrate its function as an antagonist during the quiescent phase and agonist during the active phase of the test (Figure 4.4).

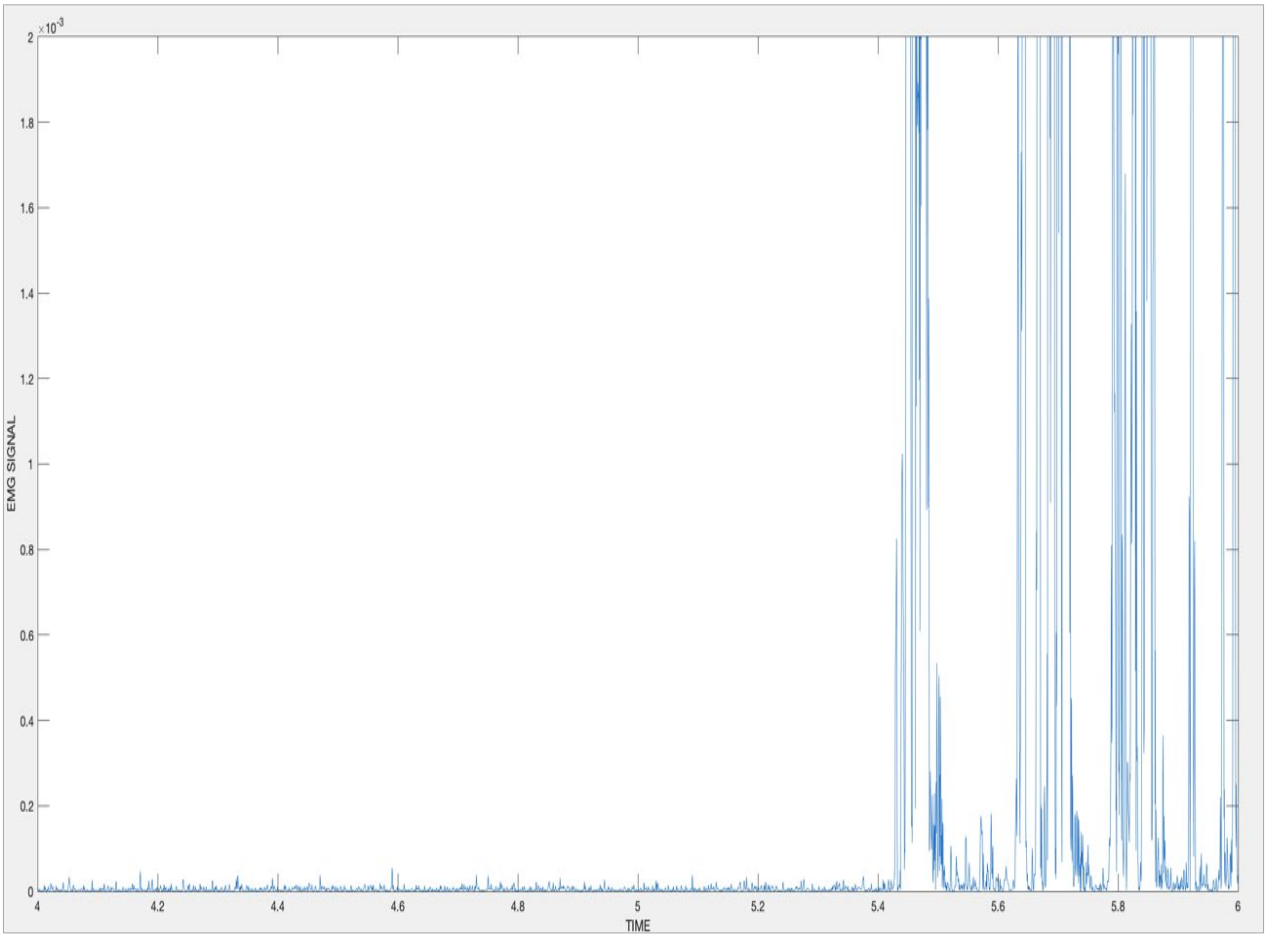

Figure 4.4 *sEMG trace obtained from the gastrocnemius medialis (GS) after signal processing. The figure illustrates the function of GS as an antagonist during the quiescent phase of the IMTP. The graph is scaled at 2mV along the y-axis and 2 s (2000 ms) along the x-axis. The bigger scale along the x-axis (4 s to 6 s) was used to demonstrate the activity of GM approximately one second prior to the command to 'PULL'. The command to 'PULL' was given after 5 s of the quiescent phase such that all muscle onsets and subsequent mechanical force production were recorded between the 5th and 6th second of the test.*

Similar agonist-antagonist relationship was observed in the sEMG traces of muscles of the upper leg, BF and VL during the quiescent phase of the test (Figure 4.5 A and B). The vastus lateralis, amongst the four muscles of the quadriceps is the primary muscle responsible for knee extension (Biondi & Varacallo, 2019). The hamstring muscle group, composed of semitendinosus, semimembranosus and BF play a prominent role in hip extension and knee flexion (Rodgers & Raja, 2020). Once in the IMTP position VL acts as the agonist during the quiescent phase due to the positional and postural weight bearing demands placed on the muscle (Figure 4.5 B). In contrast, the BF is relatively relaxed, acting as an antagonist (Figure 4.5 A). However, in some cases, the BF in the quiescent phase of the test may demonstrate comparatively higher baseline amplitude than GS, likely due to its role as a hip extensor. After the command to "PULL", a participant performing the IMTP can be viewed as attempting to overcome a resistance to execute the powerful triple extension. A key determinant of success in weightlifting exercises, triple extension is achieved by explosively extending the ankle, knee and hip joints at the end of the second pull. As such, both BF and VL act as agonist during the active phase of the test, functioning as hip and knee extensors respectively (Figure 4.5 A and B). The sEMG traces obtained from both BF and VL demonstrate their agonistic properties during the active state of the IMTP, observed as a spike in signal amplitude and increase in frequency of motor unit firing respectively (Figure 4.5 A and B).

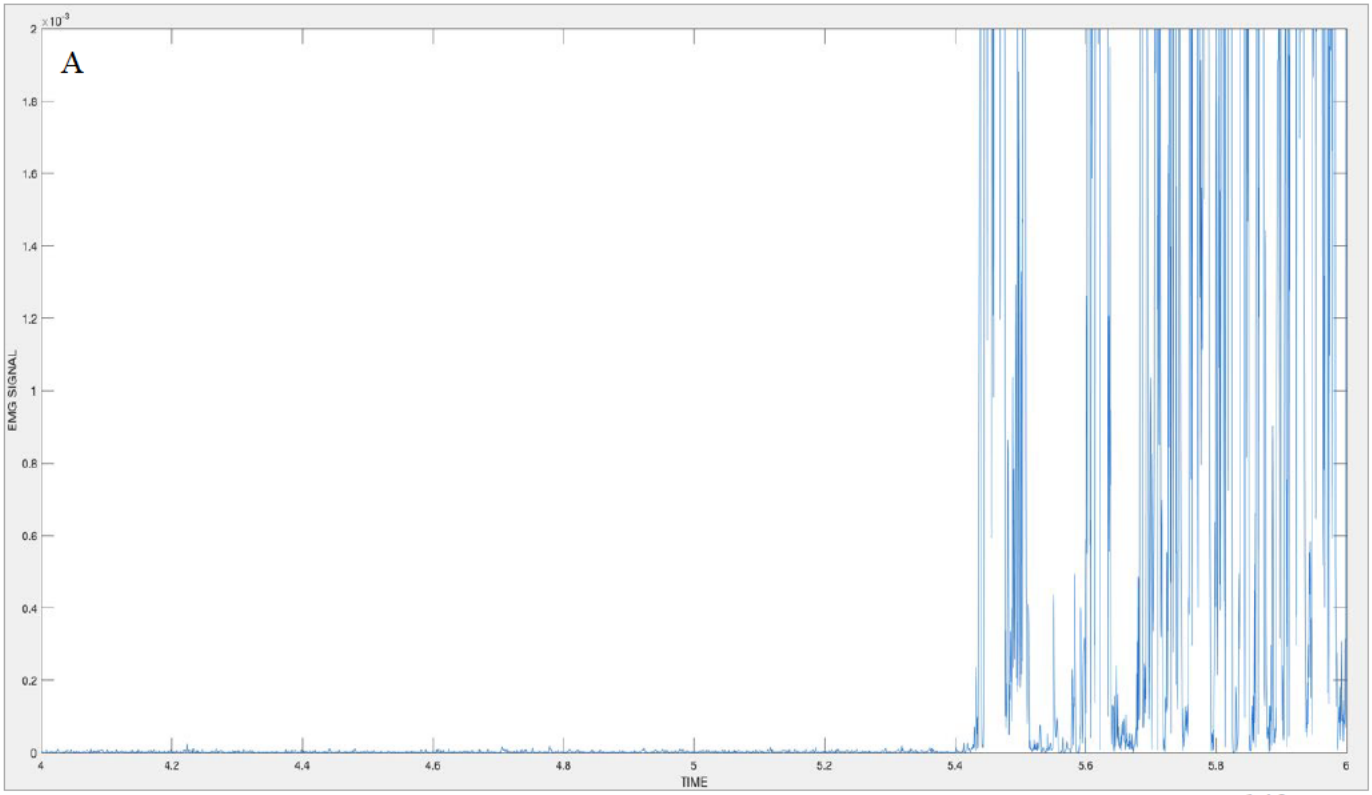

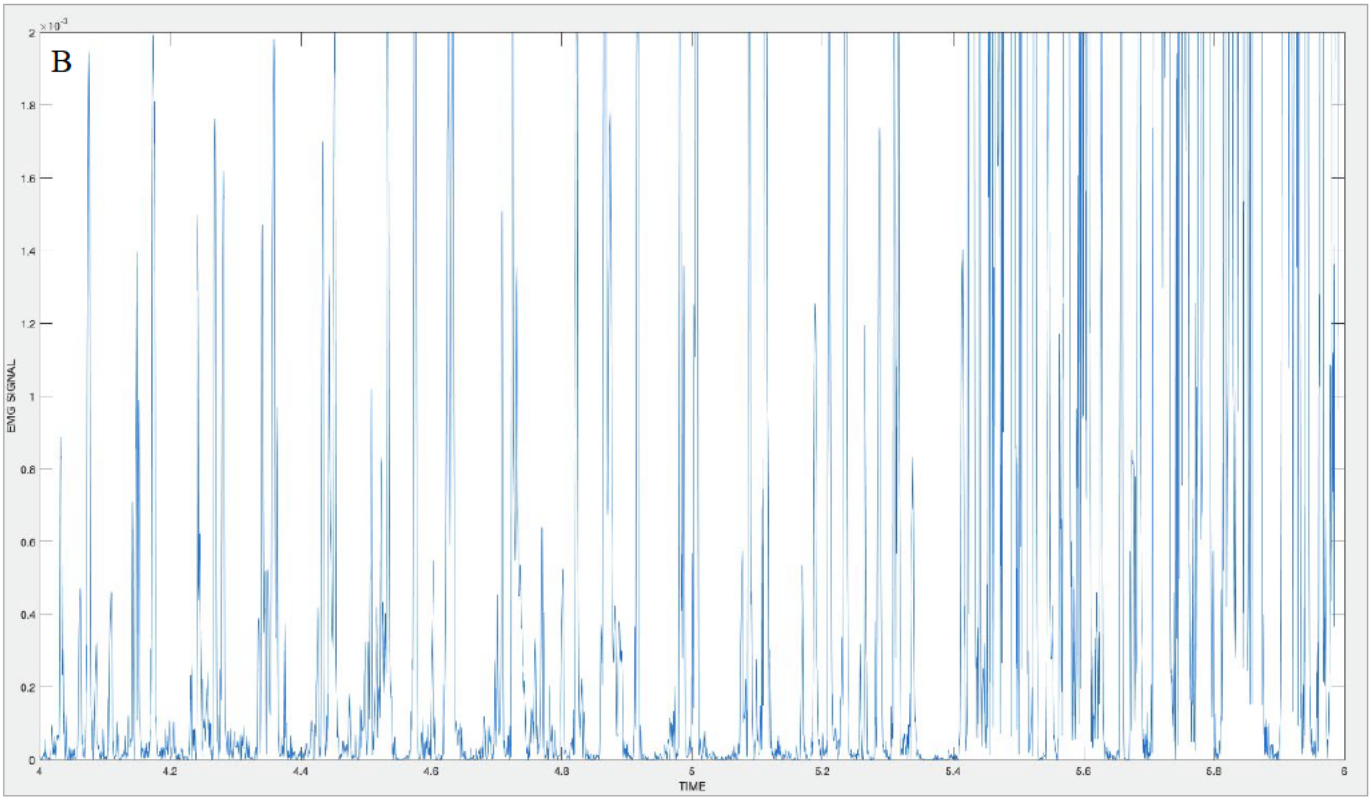

Figure 4.5 *sEMG traces obtained from (A) Bicep Femoris (BF) and (B) Vastus Lateralis (VL) after signal processing. The figure illustrates the function of BF as an antagonist and VL as an agonist during the quiescent phase of the IMTP. The graph is scaled at 2mV along the y-axis and 2 s (2000 ms) along the x-axis. The bigger scale along the x-axis (4 s to 6 s) was used to demonstrate the activity of both the BF and VL approximately one second prior to the command to 'PULL'. The command to 'PULL' was given after 5 s of the quiescent phase such that all muscle onsets and subsequent mechanical force production were recorded between the 5th and 6th second of the test.*

Note: sEMG traces like the one in (B) were categorised in 'Category 3' and the onset was detected by visually analysing the change in frequency content of the signal. In (B) the frequency pattern can be distinguished before and after 5.4 s

In an IMTP, both GS and BF function as antagonists during the quiescent phase and agonists during the active phase of the test. This was demonstrated in their respective sEMG traces during the test, with minimal baseline noise and large amplitude spike after the command to 'PULL', thus making onset detection straightforward. As such, sEMG traces obtained from both left and right, GS and BF were classified under Category 1 of the 2-step visual detection method (Figure 3.2; section 3.4.1). The straightforward procedure of visually detecting the T_{mo} in traces classified under Category 1 may explain the results of the inter-rater reliability for both the GS and BF (Figure 3.8; Section 3.4.1).

The VL, acts as an agonist in both the quiescent and active phase of the IMTP. The tension developed due to the postural and weight-bearing demands placed on the muscle were reflected in the sEMG traces displaying high amplitude baseline activity (Figure 4.10 B). Consequently, sEMG traces of the VL were predominantly classified under Category 3 with some traces in Category 2 (Figure 3.9; 3.10, Section 3.4.2; 3.4.3). The VL muscle was identified as unreliable only in the OFF condition, affecting the overall reliability of the muscle. The possible explanation for these results lies in the experimental design of the study. Unlike the GS or BF, the underlying muscle fibres of the VL run at an angle, which makes the sensor placement a challenging task (Biondi & Varacallo, 2019). In the ON condition, the EMG sensors remained attached to the sensor site over the belly of the muscle until the cessation of the test condition (Section 4.2.4.1). As such, skin preparation procedures, sensor site location and subsequent sensor placement was only performed once, in the allocated time before the first trial. Similarly, in the WL condition, each participant was allocated an hour testing slot within which, there was sufficient time set aside for skin preparation, sensor site location and placement (section 4.2.4.3). In the OFF condition however, there were only 3-5 minutes during the recovery period, for skin re-preparation, retaping EMG sensors with self-adhesive interface and sensor placement (section 4.2.4.2). Additionally, the height of the horizontal bar may coincide with that of the VL sensor location (Figure 3.2). As such, the sEMG traces of the VL may be susceptible to interference from the horizontal bar and the straps used to grip the bar, resulting in noise. Although, VL was identified as reliable in two of the three experimental conditions, future studies should consider its function and sEMG sensor location in an IMTP.

Similar to BF, GM is a primary hip extensor associated with powerful triple extension of the lower extremity, a key determinant of success in weightlifting (Elzanie & Borger, 2019;

Huyghe et al., 2021; Kipp et al., 2012). The sEMG traces of the GM, were composed of high baseline amplitude during the quiescent phase of an IMTP. This may be reflective of the tension development in the muscle due to postural weight-bearing of the anatomical trunk and positional demands of the lower extremity (Elzanie & Borger, 2019). During the active phase, after the command to "PULL'' the increment in signal amplitude was gradual unlike the spike observed in BF, resulting in low SNR. Therefore, sEMG traces of the GM were classified under Category 2 of the 2-step visual detection method (Figure 3.9, section 3.4.2). Due to low SNR, the complexity of visually detecting the onset of muscle activity in traces classified in Category 2 is comparatively much higher than those in Category 1. Consequently, visual inspection of traces in Category 2 requires sufficient training in differentiating baseline noise from the signal obtained during the active phase of the desired activity. Differences in training time, with Rater 2 lacking sufficient experience in visually detecting the T_{mo} may explain the results of inter-rater reliability, identifying GM as an unreliable muscle. Additionally, neuromuscular assessment of GM using EMGs is associated with practical limitations that must be considered prior to testing. Similar to the VL, the underlying muscle fibres of the GM run at an angle and requires careful alignment of the sensors (Elzanie & Borger, 2019). The SENIAM recommendations for palpation and sensor site location techniques for the GM may pose a risk to participant comfort. As such, the placement of sensors on the GM is accompanied by participants pulling respective layers of clothing (undergarments and shorts) over the top of the sensors. Although necessary to assure participant comfort, the layers of clothing may interfere with the self-adhesive interface affecting the accuracy of the sensor placement. Therefore, it would be reasonable to suspect that the high levels of baseline amplitude in the GM is due to the sensor site and its function in an IMTP. Research in muscle activity during a conventional barbell deadlift suggests GM activity occurs towards the end stages of the lifting phase peaking at 83% of the lift height (del Vecchio, 2018). Similarity in the movement pattern of the lifting phases in a deadlift and power cleans up to the point of triple extension, would suggest higher GM activity at hip-joint angles above 150° in an IMTP. This further explains the low levels of GM activation amplitude observed in the sEMG traces recorded during an IMTP at the recommended hip-joint angles, 140-150°.

The ESL, amongst other back extensors, is the larger, superficial muscle that contributes to the static stabilisation of the trunk in the starting position of a dynamic mid-thigh pull

(DeWeese et al., 2013; Richardson, 1994). Kinematically, the ESL contributes to the powerful vertical thrust associated with the triple extension (Suchomel et al., 2016).
The EMG activity of the ESL during a dynamic power clean has previously been reported to increase with load (Dryburgh & Psycharakis, 2016). Given the role of ESL in weightlifting performance, practitioners cue their athletes to engage their ESL throughout the pull phases of a power clean (Suchomel et al., 2016). Engagement of the ESL in the starting position of a power clean is achieved when the scapulae are depressed and retracted while maintaining a neutral or slightly arched spine (Caulfield & Berninger, 2016). Participants in the current study engaged their ESL in a similar technical manner during the quiescent phase of an IMTP, maintaining a neutral spine with the scapulae depressed and retracted. The amplitude and frequency characteristics of the ESL sEMG signal during an IMTP was reflective of its function in dynamic weightlifting exercises. The sEMG trace during the quiescent phase was composed of unevenly spaced amplitude spikes interspersed by instances of low amplitude activity. The frequency of these high amplitude spikes in the signal were irregular, as opposed to the active phase of the test composed of both high amplitude and high frequency (Figure 3.4).
Consequently, all ESL sEMG traces were classified in Category 3 and the onset time was determined by visually inspecting the amplitude and frequency characteristics of sEMG signal (Figure 3.10, section 3.4.3). Time of ESL onset after the command to "PULL'' was identified at the trough (base) of the first spike of the sustained high-amplitude signal, displaying a distinctively frequency-dense area as opposed to the baseline muscle activity. Traditionally, the visual detection of T_{mo} is based on visually differentiating between the amplitude characteristics of baseline noise and activation signal. Determining the T_{mo} in sEMG traces classified under Category 3 by only considering its amplitude characteristics is likely to heighten the complexity of visual detection resulting in misinterpretation of the onset time (Figure 3.10). Therefore, raters were instructed to consider both the amplitude and frequency characteristics of sEMG traces classified in Category 3 (Figure 3.10, section 3.4.3). The definition amendments, description and instructions associated with Category 3, reduced the complexity of visually detecting the onset of ESL activity in an IMTP. The complexity of visual detection was reduced to a level such that, despite the limited experience of Rater 2, ESL was identified as a reliable muscle.

The implement (barbell and added load) displaced during a power clean remains in contact with the upper limbs via a pronated grip throughout all phases of the lift. Technically, the

upper extremity remains completely extended during the pull phases, functioning isometrically up to the point of triple extension (Suchomel et al., 2016). In an IMTP, the test is initiated at the hands gripping the horizontal bar via a pronated grip with completely extended elbow joints. Consequently, grip strength levels essential for coupling with the stationary horizontal bar is an integral technical aspect and a performance limiting factor in an IMTP (Comfort et al., 2019). In the current study the onset of muscle activity in two pairs of superficial muscles in the extensor compartment of the forearm, ED and BR were assessed. High baseline amplitude was observed for both muscles during the quiescent phase of an IMTP reflective of their function in dynamic tasks. The high level of grip strength demand on the ED is likely the cause of high baseline amplitude during the quiescent phase of an IMTP (Takala & Toivonen, 2013). Similarly, high baseline amplitude observed in sEMG traces of the BR is reflective of its function in stabilising the extended elbow joint while maintaining the pronated forearm position (Boland et al., 2008; Pratt et al., 2020). As such, sEMG traces of both muscles were predominantly classified under Category 2 with some traces spread across the other two categories of the 2-step visual detection method (Section 3.4).

The results of inter-rater reliability in the current study identified both muscles, ED and BR as unreliable (Figure 4.3, Table 4.2). The large variation in the T_{mo} is likely due to the difference in training time with, limited experience of Rater 2. The results also suggest that the experience of Rater 2 had an effect on the reliability of sEMG traces in Category 2 namely the GM, ED and BR.

Mistrials, due to minute changes in ankle, knee or hip joint angles during the quiescent phase of an IMTP are detectable, given the sensitivity of the force platform. Since, changes in joint angles affect muscular activity, the sEMG traces of mistrials recorded synchronously are also discarded. The sEMG traces alone are not suitable for detecting mistrials since it requires offline analysis in which the recorded traces need to be exported to a different software. While changes in ankle, knee or hip joints are detectable during the test using a force platform, the movement in digits of the hands gripping the bar remain undetected. The primary function of ED is the extension of the medial four fingers (digits 2,3, 4 and 5). Therefore, in acceptable trials (Figure 3.3 A), extension in any of these flexed digits gripping the bar, either due to anticipation or adjusting the weightlifting strap, is likely to affect the baseline noise and signal amplitude.

The anatomy of the forearm, function of both ED and BR in an IMTP and associated experimental limitations, explain the results of the current study, identifying both muscles as unreliable.

Chapter 5.0: Thesis Conclusion

5.1 Limitations and future considerations

The methodological considerations associated with the assessment of multi-muscle multi-joint activity using sEMG during the IMTP were addressed in Study 1. The 2-step visual detection method developed for the identification of the time of muscle onset (T_{mo}) in an IMTP was the result of multiple MATLAB programme iterations. The sEMG traces were viewed at two different resolutions that were adapted from previous studies, investigating T_{mo} in single-joint tests of neuromuscular function (Crotty et al., 2021; Tillin et al., 2010). In the first step all sEMG traces were viewed with a y-axis scale of 2 mV and an x-axis scale of 1000 ms. This fixed initial resolution did not account for variations in muscle activity, specifically differences in baseline amplitude, during the quiescent phase of an IMTP. In the second step, T_{mo} was identified at a higher resolution for the x-axis (only), by increasing the scale to a full scale of 50 ms. The y-axis scale (2 mV) was fixed across both steps to retain the high amplitude baseline characteristics of sEMG traces that were significantly off-scale and to standardise viewing conditions in terms of amplitude deviation used to identify T_{mo}. Four of the 7 muscle pairs benefitted from this approach however, this may have impacted the accuracy and precision of T_{mo} detection in traces where both, baseline noise and activity signal amplitude were relatively low contributing to a poor SNR. Therefore, key limitations were observed and acknowledged in both steps of the 2-step visual detection method. To counter these limitations, future researchers should investigate the use of muscle-specific resolutions based on their respective baseline activity recorded using sEMG. Another important limitation of the study was with respect to the definition of T_{mo}. The widely accepted definition of T_{mo}, in terms of sEMG is dependent on the amplitude of the signal (Crotty et al., 2021; Tillin et al., 2010). However, in the current study, amendments in the definition were necessary for three out of 7 muscle pairs, to account for the magnitude of either the amplitude of the signal or the frequency of the signal to identify T_{mo}. This amended definition was novel and therefore lacked evidence for its validity. As such, the amended definition warrants further investigation and discussion.

Study 2 investigated the reliability of the methodology developed in Study 1. This was achieved by measuring the inter and intra-rater reliabilities of onset times in the seven pairs of selected muscles across three experimental conditions. A limitation of the study was the differences in training time between the two Raters. Rater 1, the lead investigator, was responsible for data collection and formulation of the MATLAB code used in the subsequent

development of the 2-step visual detection method. Consequently Rater 1, received sufficient training in visually detecting the T_{mo} during an IMTP. Rater 2 on the other hand, was knowledgeable in signal processing with relatively less training in visually detecting the T_{mo} during an IMTP. These differences in terms of familiarity and amount of exposure to the sEMG traces are likely to give rise to subjective bias, an inherent limitation associated with manual visual detection of T_{mo}. Further, inferring the results of the study it has become evident that more training may be needed for independent raters. Therefore, this fundamental limitation, could be portrayed as a strength of the study, providing insight into the appropriate level of training that is necessary to become reliable as a 'Rater'. Accordingly, it is recommended that future studies of reliability, employ two independent raters that undergo similar amount of exposure to sEMG traces and training in detecting the T_{mo} during an IMTP. In addition to subjective bias, visual detection is also considered to be time-consuming and susceptible to errors within and between raters especially in signals with low SNR. However, visual detection was deemed appropriate for the detection of T_{mo} in the current study, where three pairs of muscles were found to be reliable between both raters. These results serve as a pre-requisite for future research into muscle activity during an IMTP. Inspection of muscle activity via sEMG traces over the course of Study 2, revealed that GS and BF were the only two muscle pairs with near negligible baseline noise prior to $T_{mo.}$ Given this, automated methods of T_{mo} detection, can be effectively applied to these two muscle pairs, with further investigation, potentially accounting for limitations associated with visual detection in future studies.

The anatomy of the forearm is highly complex, composed of 19 closely packed muscles that function together to move the elbow, forearm, wrist and digits of the hand (Mitchell & Whited, 2019; Rodrigues et al., 2019). The EMG sensors used in the current study were 27 mm in length, 37mm in height and 15 mm in breadth with an inter-electrode spacing of 10 mm (4 silver (99.9% Ag) bar contacts. The observed high baseline amplitude and frequency in the sEMG traces of ED and BR muscles may be attributed to equipment incompatibility, in terms of the size of the sensors relative to the muscles of the forearms. Consequently, both ED and BR are highly susceptible to crosstalk from surrounding muscles. Assessment of these forearm muscles may be of particular interest to researchers in the future since the test is initiated at the hands. Furthermore, biomechanically the IMTP follows a linear kinetic relationship between the pull force on the bar and the VGRF recorded at the feet. With this, it is recommended that future studies use smaller electrodes, developed specially for the

muscles of the forearm, such as the Trigno Duo Sensor with 2-channel mini dual-head (25 x 12 x 7 mm) EMG sensors (Delsys INC, Boston, Massachusetts, USA).

The current study implemented a comprehensive warm-up protocol to mitigate the potential effects of potentiation. However, the protocol was tested with only one participant. Therefore, it remains uncertain whether the warm-up protocol was equally effective for all participants. Further, there appears to be no studies reporting on the effect of warm-up on the reliability of IMTP performance in repeated trials. Whilst it is recognised as a limitation of the IMTP testing protocol in the current study, it is also a limitation in all other studies. Given its widespread use more research may be required on the effects and subsequent standardisation of IMTP warm-up protocols amongst a range of athletes.

5.2 Conclusion

This is the first study to conduct a thorough analysis of the time of muscle onset (T_{mo}) in a multi-muscle multi-joint isometric test of neuromuscular function, the IMTP. The IMTP is a test widely used in research and in practice for neuromuscular assessment of athletes, usually in terms of PF and RFD. The reliability and validity of PF has been well documented, however the same is not the case for time dependent variables such as RFD. This is primarily due to the lack of agreement between studies in terms of the definition and subsequent determination of a valid and reliable start-time, determined from the VGRF-time history. However, before the validity of such a start-time can be investigated, there has to be a clearly defined and valid temporal reference point from which to judge the validity of said start-time. Given the physiological phenomenon of neural and muscular excitation preceding mechanical force production, use of sEMG analysis, to investigate muscle timings was proposed for identifying the T_{mo} (reference point) to validate a start-time method of an IMTP performed on a FP. Consequently, the main aim of the thesis was to develop a reliable method of detecting the T_{mo} during an IMTP. The research objectives, as outlined in section 1.4, guided the research conducted in this thesis, which was divided into two studies. First, seven pairs of muscles, likely to be active in an IMTP were identified from the literature in Study 1. Inferences regarding their selection were based on the biomechanical and neuromuscular principles of a dynamic power clean and variations of the deadlift. The selected muscles were, left and right gastrocnemius medialis (GS), bicep femoris (BF), gluteus maximus (GM), vastus lateralis (VL), erector spinae longissimus (ESL), extensor digitorum (ED) and

brachioradialis (BR). Study 1, focused on the methodological considerations associated with the development of a novel method for identifying the T_{mo} during a standard trial in an IMTP. Following the critical evaluation of the existing literature, the method of visual detection was deemed appropriate to fulfil the purpose of the study. As such a visual detection tool was developed to analyse sEMG traces at two different resolutions, termed as the 2-step visual detection method. In total, 336 sEMG traces obtained as a result of the experimental set up, were divided into three distinctive categories based on the baseline amplitude and frequency characteristics of the signals. Study 2 investigated the inter and intra-rater reliability of the methodology developed in Study 1, under three experimental conditions, 'ON', 'OFF', 'WL'. SD of differences between the T_{mo} as determined by Rater 1 on two separate occasions identified all 7 pairs of muscles as reliable (≤ 5 ms) in each condition. In contrast, SD of differences between the T_{mo} determined by Rater 1 and Rater 2 identified 3 muscle pairs, GS, BF & ESL as reliable, demonstrating variations of ≤ 5 ms across the three experimental conditions. Near negligible baseline noise was observed in sEMG traces of GS and BF, owing to their antagonistic muscle actions during the quiescent phase of an IMTP, prior to the $T_{mo.}$ Therefore, the straightforward procedure of visually detecting the sEMG onset in such traces, explains the results of the inter-rater reliability for both GS and BF. Interestingly, ESL was identified as a reliable muscle despite the high amplitude baseline activity and low SNR. The sEMG traces obtained for ESL were reflective of its function as an agonist in both quiescent and active phases of an IMTP. Consequently, the T_{mo} in all ESL sEMG traces was identified using the amended definition of T_{mo}, accounting for both the amplitude and frequency characteristics of the signal. Although novel, it can be inferred that the definition amendments facilitated the reliable detection of ESL onset in an IMTP despite the limited experience of Rater 2.

5.2.1 Recommendations and practical implications

The primary aim of the thesis was the development of a reliable method for detecting the time of muscle onset (T_{mo}) in an IMTP. This aim achieved through four objectives outlined in the thesis. The T_{mo} was identified in seven pairs of selected muscles using the 2-step visual detection method. Three of the seven muscle pairs, GS, BF and ESL were found to be reliable. Having met the reliability standards of the study, these muscle pairs are recommended for future temporal investigations, undertaken with sEMG in the IMTP. It is further recommended that future studies of reliability employ two independent raters, that undergo similar amounts of training in detecting the T_{mo} in selected muscles during an IMTP.

Inspection of muscle activity of the reliable muscle pairs revealed that GS and BF were the only two muscle pairs with near negligible baseline noise prior to $T_{mo.}$ Automated methods of detecting T_{mo}, that rely on the baseline noise can therefore be applied to GS and BF, potentially accounting for limitations associated with visual detection in future studies. With respect to sEMG, it is recommended that researchers carefully assess the suitability of the available equipment and the target muscles of interest to avoid limitations identified in the present thesis, namely excessive crosstalk and baseline noise. This is the first study to conduct a thorough analysis of the time of muscle onset (T_{mo}) in a multi-muscle multi-joint isometric test of neuromuscular function, the IMTP. The results of the thesis can be applied in the future to validate new and existing start-time methods, subsequently standardising IMTP testing and analysis protocols.

References

Aagaard, P., Simonsen, E. B., Andersen, J. L., Magnusson, P., & Dyhre-Poulsen, P. (2002). Increased rate of force development and neural drive of human skeletal muscle following resistance training. *Journal of Applied Physiology*, *93*(4). https://doi.org/10.1152/japplphysiol.00283.2002

Abe, T., Kawakami, Y., Ikegawa, S., Kanehisa, H., & Fukunaga, T. (1992). Isometric and isokinetic knee joint performance in Japanese alpine ski racers. *Journal of Sports Medicine and Physical Fitness*, *32*(4).

Abernethy, P., Wilson, G., & Logan, P. (1995). Strength and Power Assessment: Issues, Controversies and Challenges. In *Sports Medicine* (Vol. 19, Issue 6). https://doi.org/10.2165/00007256-199519060-00004

Allison, G. T. (2003). Trunk muscle onset detection technique for EMG signals with ECG artefact. *Journal of Electromyography and Kinesiology*, *13*(3). https://doi.org/10.1016/S1050-6411(03)00019-1

Altman, D. G., & Bland, J. M. (2005). Standard deviations and standard errors. *BMJ*, *331*(7521). https://doi.org/10.1136/bmj.331.7521.903

Anderson, M. A., Gieck, J. H., Perrin, D., Weltman, A., Rutt, R., & Denegar, C. (1991). Data preparation. The relationships among isometric, isotonic, and isokinetic concentric and eccentric quadriceps and hamstring force and three components of athletic performance. *Journal of Orthopaedic and Sports Physical Therapy*, *14*(3). https://doi.org/10.2519/jospt.1991.14.3.114

Angelozzi, M., Madama, M., Corsica, C., Calvisi, V., Properzi, G., McCaw, S. T., & Cacchio, A. (2012). Rate of force development as an adjunctive outcome measure for return-to-sport decisions after anterior cruciate ligament reconstruction. *Journal of Orthopaedic and Sports Physical Therapy*, *42*(9). https://doi.org/10.2519/jospt.2012.3780

Apolinário, I. F., & Diniz, P. S. R. (2014). Introduction to Signal Processing Theory. In R. Chellappa & S. Theodoridis (Eds.), *Academic Press Library in Signal Processing* (Vol. 1, pp. 3–28). Academic Press. https://doi.org/10.1016/b978-0-12-396502-8.00001-2

Atha, J. (1981). Strengthening muscle. *Exercise and Sport Sciences Reviews*, *9*(1). https://doi.org/10.1249/00003677-198101000-00001

Atkinson, G., & Nevill, A. M. (1998). Statistical methods for assessing measurement error (reliability) in variables relevant to sports medicine. *Sports Medicine*, *26*(4). https://doi.org/10.2165/00007256-199826040-00002

Baena-Raya, A., Díez-Fernández, D. M., García-Ramos, A., Soriano-Maldonado, A., & Rodríguez-Pérez, M. A. (2021). Concurrent validity and reliability of a functional electromechanical dynamometer to assess isometric mid-thigh pull performance. *Proceedings of the Institution of Mechanical Engineers, Part P: Journal of Sports Engineering and Technology*. https://doi.org/10.1177/17543371211030180

Baker, D., Wilson, G., & Carlyon, B. (1994). Generality versus specificity: a comparison of dynamic and isometric measures of strength and speed-strength. *European Journal of Applied Physiology and Occupational Physiology*, *68*(4). https://doi.org/10.1007/BF00571456

Bartolomei, S., Rovai, C., Lanzoni, I. M., & Di Michele, R. (2022). Relationships Between Muscle Architecture, Deadlift Performance, and Maximal Isometric Force Produced at the Midthigh and Midshin Pull in Resistance-Trained Individuals. *Journal of Strength and Conditioning Research*, *36*(2). https://doi.org/10.1519/JSC.0000000000003455

Bartolomei, S., Sadres, E., Church, D. D., Arroyo, E., Iii, J. A. G., Varanoske, A. N., Wang, R., Beyer, K. S., Oliveira, L. P., Stout, J. R., & Hoffman, J. R. (2017). Comparison of the recovery response from high-intensity and high-volume resistance exercise in trained men. *European Journal of Applied Physiology*, *117*(7). https://doi.org/10.1007/s00421-017-3598-9

Batterham, A. M., & George, K. P. (2003). Reliability in evidence-based clinical practice: A primer for allied health professionals. In *Physical Therapy in Sport* (Vol. 4, Issue 3). https://doi.org/10.1016/S1466-853X(03)00076-2

Baumgartner, T. A., & Chung, H. (2001). Confidence limits for intraclass reliability coefficients. *Measurement in Physical Education and Exercise Science*, *5*(3). https://doi.org/10.1207/S15327841MPEE0503_4

Beckham, G. K. , Suchomel, T. J. , Bailey, C. A. , Sole, C. J. , &, & Grazer, J. L. (2014). The relationship of the reactive strength index-modified and measures of force development in the isometric mid-thigh pull. *32nd International Conference of Biomechanics in Sports*, 501–504.

Beckham, G. K., Sato, K., Santana, H. A. P., Mizuguchi, S., Gregory Haff, G., & Stone, M. H. (2018). Effect of body position on force production during the isometric midthigh pull. *Journal of Strength and Conditioning Research*, *32*(1). https://doi.org/10.1519/JSC.0000000000001968

Beckham, G., Mizuguchi, S., Carter, C., Sato, K., Ramsey, M., Lamont, H., Hornsby, G., Haff, G., & Stone, M. (2013). Relationships of isometric mid-thigh pull variables to weightlifting performance. *Journal of Sports Medicine and Physical Fitness*, *53*(5).

Beckham, George. K. , Lamont, Hugh. S. , Sato, K., W. Ramsey, M., G., G. H., & H. Stone, M. (2012). Isometric Strength of Powerlifters in Key Positions of the Conventional Deadlift. *Journal of Trainology*, *1*(2). https://doi.org/10.17338/trainology.1.2_32

Bellumori, M., Jaric, S., & Knight, C. A. (2011). The rate of force development scaling factor (RFD-SF): Protocol, reliability, and muscle comparisons. *Experimental Brain Research*, *212*(3). https://doi.org/10.1007/s00221-011-2735-7

Biondi, N. L., & Varacallo, M. (2019). Anatomy, Bony Pelvis and Lower Limb, Vastus Lateralis Muscle. In *StatPearls*.

Bird, S., & Barrington-Higgs, B. (2010). Exploring the deadlift. *Strength and Conditioning Journal*, *32*(2). https://doi.org/10.1519/SSC.0b013e3181d59582

Blazevich, A. J., Wilson, C. J., Alcaraz, P. E., & Rubio-Arias, J. A. (2020). Effects of Resistance Training Movement Pattern and Velocity on Isometric Muscular Rate of Force Development: A Systematic Review with Meta-analysis and Meta-regression. In *Sports Medicine* (Vol. 50, Issue 5). https://doi.org/10.1007/s40279-019-01239-x

Boland, M. R., Spigelman, T., & Uhl, T. L. (2008). The Function of Brachioradialis. *Journal of Hand Surgery*, *33*(10). https://doi.org/10.1016/j.jhsa.2008.07.019

Brady, C. J., Harrison, A. J., & Comyns, T. M. (2018). A review of the reliability of biomechanical variables produced during the isometric mid-thigh pull and isometric squat and the reporting of normative data. In *Sports Biomechanics* (Vol. 19, Issue 1). https://doi.org/10.1080/14763141.2018.1452968

Brady, C. J., Harrison, A. J., Flanagan, E. P., Gregory Haff, G., & Comyns, T. M. (2020). The relationship between isometric strength and sprint acceleration in sprinters. *International Journal of Sports Physiology and Performance*, *15*(1). https://doi.org/10.1123/ijspp.2019-0151

Brown, J. E., & Frank, J. S. (1987). Influence of event anticipation on postural actions accompanying voluntary movement. *Experimental Brain Research*, *67*(3). https://doi.org/10.1007/BF00247295

Bruton, A., Conway, J. H., & Holgate, S. T. (2000). Reliability: What is it, and how is it measured? *Physiotherapy*, *86*(2). https://doi.org/10.1016/S0031-9406(05)61211-4

Caulfield, S., & Berninger, D. (2016). Exercise Technique for Free Weight and Machine Training. In G. G. Haff & N. T. Triplett (Eds.), *Essentials of Strength Training and Conditioning* (4th ed., pp. 351–408). Human Kinetics.

Cavalcanti Garcia, M. A., & Vieira, T. M. (2011). Surface electromyography: Why, when and how to use it. *Revista Andaluza de Medicina Del Deporte*, *4*(1).

Challis, J. H. (2008). Data processing and error estimation. In C. J. Payton & R. M. Bartlett (Eds.), *Biomechanical Evaluation of Movement in Sport and Exercise: The British Association of Sport and Exercise Sciences Guidelines* (pp. 129–152). Routledge. https://doi.org/10.4324/9780203935750

Cholewicki, J., Silfies, S. P., Shah, R. A., Greene, H. S., Reeves, N. P., Alvi, K., & Goldberg, B. (2005). Delayed trunk muscle reflex responses increase the risk of low back injuries. *Spine*, *30*(23). https://doi.org/10.1097/01.brs.0000188273.27463.bc

Clarke, H. H. (1948). Objective Strength Tests of Affected Muscle Groups Involved in Orthopedic Disabilities. *Research Quarterly. American Association for Health, Physical Education and Recreation*, *19*(2), 118–147. https://doi.org/10.1080/10671188.1948.10620983

Comfort, P., Dos'Santos, T., Beckham, G. K., Stone, M. H., Guppy, S. N., & Haff, G. G. (2019). Standardization and methodological considerations for the isometric midthigh pull. *Strength and Conditioning Journal*, *41*(2). https://doi.org/10.1519/SSC.0000000000000433

Comfort, P., Jones, P. A., McMahon, J. J., & Newton, R. (2015). Effect of knee and trunk angle on kinetic variables during the isometric midthigh pull: Test-retest reliability. *International Journal of Sports Physiology and Performance*, *10*(1). https://doi.org/10.1123/ijspp.2014-0077

Comfort, P., Jones, P. A., Thomas, C., Dos'Santos, T., McMahon, J. J., & Suchomel, T. J. (2022). Changes in Early and Maximal Isometric Force Production in Response to Moderate- and High-Load Strength and Power Training. *Journal of Strength and Conditioning Research*, *36*(3). https://doi.org/10.1519/JSC.0000000000003544

Considine, W. J., & Sullivan, W. J. (1973). Relationship of selected tests of leg strength and leg power on college men. *Research Quarterly of the American Association for Health, Physical Education and Recreation*, *44*(4). https://doi.org/10.1080/10671188.1973.10615220

Cook, E. W., & Miller, G. A. (1992). Digital Filtering: Background and Tutorial for Psychophysiologists. *Psychophysiology*, *29*(3). https://doi.org/10.1111/j.1469-8986.1992.tb01709.x

Cormie, P., McGuigan, M. R., & Newton, R. U. (2011). Developing maximal neuromuscular power: Part 2 training considerations for improving maximal power production. *Sports Medicine*, *41*(2). https://doi.org/10.2165/11538500-000000000-00000

Crotty, E. D., Furlong, L. A. M., Hayes, K., & Harrison, A. J. (2021). Onset detection in surface electromyographic signals across isometric explosive and ramped contractions: A comparison of computer-based methods. *Physiological Measurement*, *42*(3). https://doi.org/10.1088/1361-6579/abef56

Currell, K., & Jeukendrup, A. E. (2008). Validity, reliability and sensitivity of measures of sporting performance. In *Sports Medicine* (Vol. 38, Issue 4). https://doi.org/10.2165/00007256-200838040-00003

De Luca, C. J. (1997). The use of surface electromyography in biomechanics. *Journal of Applied Biomechanics*, *13*(2). https://doi.org/10.1123/jab.13.2.135

de Witt, J. K., English, K. L., Crowell, J. B., Kalogera, K. L., Guilliams, M. E., Nieschwitz, B. E., Hanson, A. M., & Ploutz-Snyder, L. L. (2018). Isometric midthigh pull reliability and relationship to deadlift one repetition maximum. *Journal of Strength and Conditioning Research*, *32*(2). https://doi.org/10.1519/jsc.0000000000001605

Del Vecchio, A., Negro, F., Holobar, A., Casolo, A., Folland, J. P., Felici, F., & Farina, D. (2019). You are as fast as your motor neurons: speed of recruitment and maximal discharge of motor neurons determine the maximal rate of force development in humans. *Journal of Physiology*, *597*(9). https://doi.org/10.1113/JP277396

Derrick, T. R. (2014). Signal Processing. In D. G. E. Robertson, G. E. Caldwell, J. Hamill, G. Kamen, & S. N. Whittlesey (Eds.), *Research Methods in Biomechanics* (2nd ed., pp. 279–290). Human Kinetics. https://doi.org/10.5040/9781492595809

DeWeese, B. H., Serrano, A. J., Scruggs, S. K., & Burton, J. D. (2013). The midthigh pull: Proper application and progressions of a weightlifting movement derivative. *Strength and Conditioning Journal*, *35*(6). https://doi.org/10.1519/SSC.0b013e318297c77b

Di Fabio, R. P. (1987). Reliability of computerized surface electromyography for determining the onset of muscle activity. *Physical Therapy*, *67*(1). https://doi.org/10.1093/ptj/67.1.43

Disselhorst-Klug, C., Schmitz-Rode, T., & Rau, G. (2009). Surface electromyography and muscle force: Limits in sEMG-force relationship and new approaches for applications. In *Clinical Biomechanics* (Vol. 24, Issue 3). https://doi.org/10.1016/j.clinbiomech.2008.08.003

Dos'Santos, T., Jones, P. A., Comfort, P., & Thomas, C. (2017). Effect of different onset thresholds on isometric midthigh pull force-time variables. *Journal of Strength and Conditioning Research*, *31*(12). https://doi.org/10.1519/JSC.0000000000001765

Dos'Santos, T., Jones, P. A., Kelly, J., McMahon, J. J., Comfort, P., & Thomas, C. (2016). Effect of sampling frequency on isometric midthigh-pull kinetics. *International Journal of Sports Physiology and Performance*, *14*(4), 255–260. https://doi.org/10.1123/ijspp.2019-2015-0222

Dos'Santos, T., Thomas, C., Comfort, P., McMahon, J. J., Jones, P. A., Oakley, N. P., & Young, A. L. (2018). Between-session reliability of isometric midthigh pull kinetics and maximal power clean performance in male youth soccer players. *Journal of Strength and Conditioning Research*, *32*(12). https://doi.org/10.1519/jsc.0000000000001830

Dos'Santos, T., Thomas, C., Jones, P. A., McMahon, J. J., & Comfort, P. (2017). The effect of hip joint angle on isometric midthigh pull kinetics. *Journal of Strength and Conditioning Research*, *31*(10). https://doi.org/10.1519/JSC.0000000000002098

Dryburgh, I., & Psycharakis, S. G. (2016). Muscle activation under different loading conditions during the power clean. *International Journal of Performance Analysis in Sport*, *16*(2). https://doi.org/10.1080/24748668.2016.11868901

Duchateau, J., & Baudry, S. (2011). Training Adaptation of the Neuromuscular System. In P. V. Komi (Ed.), *Neuromuscular Aspects of Sport Performance* (Vol. 17, pp. 216–253). John Wiley & Sons. https://doi.org/10.1002/9781444324822

Duchateau, J., Semmler, J. G., & Enoka, R. M. (2006). Training adaptations in the behavior of human motor units. In *Journal of Applied Physiology* (Vol. 101, Issue 6). https://doi.org/10.1152/japplphysiol.00543.2006

Dylan G. SuarezKevin M. CarrollJake A. SlatonKyle G. RochauMichael W. DavisMichael H. Stone. (2020). Utility of a Shortened Isometric Midthigh Pull Protocol for Assessing Rapid Force Production in Athletes. *Journal of Strength and Conditioning Research* .

Elzanie, A., & Borger, J. (2019). Anatomy, Bony Pelvis and Lower Limb, Gluteus Maximus Muscle. In *StatPearls*.

Enoka, R. M. (1979). The pull in olympic weightlifting. *Medicine and Science in Sports*, *11*(2).

Enoka, R. M. (1995). Neuromechanical Basis of Kinesiology, 2nd Edition. *Medicine & Science in Sports & Exercise*, *27*(11). https://doi.org/10.1249/00005768-199511000-00018

Enoka, R. M., & Duchateau, J. (2017). Rate coding and the control of muscle force. *Cold Spring Harbor Perspectives in Medicine*, *7*(10). https://doi.org/10.1101/cshperspect.a029702

Enoka, R. M., & Duchateau, J. (2018). Muscle Function: Strength, Speed, and Fatigability. Strength, Speed, and Fatigability. In *Muscle and Exercise Physiology*. https://doi.org/10.1016/B978-0-12-814593-7.00007-4

Escabí, M. A. (2005). Biosignal Processing. In J. D. Enderle, S. M. Blanchard, & J. D. Bronzino (Eds.), *Introduction to Biomedical Engineering* (2nd ed., pp. 549–625). Elsevier. https://doi.org/10.1016/B978-0-12-238662-6.50012-4

Farup, J., Rahbek, S. K., Bjerre, J., de Paoli, F., & Vissing, K. (2016). Associated decrements in rate of force development and neural drive after maximal eccentric exercise. *Scandinavian Journal of Medicine and Science in Sports*, *26*(5). https://doi.org/10.1111/sms.12481

Faude, O., Rössler, R., Petushek, E. J., Roth, R., Zahner, L., & Donath, L. (2017). Neuromuscular adaptations to multimodal injury prevention programs in youth sports: A systematic review with meta-analysis of randomized controlled trials. In *Frontiers in Physiology* (Vol. 8, Issue OCT). https://doi.org/10.3389/fphys.2017.00791

Garhammer, J. (1984). Bridging the gap: Kinesiological evaluation. *National Strength and Conditioning Association Journal*, *6*(3). https://doi.org/10.1519/0744-0049(1984)006<0040:P>2.3.CO;2

Garhammer, J. (1993). A review of power output studies of olympic and powerlifting: Methodology, performance prediction, and evaluation tests. In *Journal of Strength and Conditioning Research* (Vol. 7, Issue 2). https://doi.org/10.1519/00124278-199305000-00002

Guppy, S. N., Brady, C. J., Kotani, Y., Stone, M. H., Medic, N., & Haff, G. G. (2018). The effect of altering body posture and barbell position on the between-session reliability of force-time curve characteristics in the isometric mid-thigh pull. *Sports*, *6*(4). https://doi.org/10.3390/sports6040162

Gupta, A., Mudie, K. L., & Clothier, P. J. (2014). The reliability of determining the onset of medial gastrocnemius muscle activity during a stretch-shorten-cycle action. *Journal of Electromyography and Kinesiology*, *24*(5). https://doi.org/10.1016/j.jelekin.2014.05.005

Haff, G. G., Carlock, J. M., Hartman, M. J., Kilgore, J. L., Kawamori, N., Jackson, J. R., Morris, R. T., Sands, W. A., & Stone, M. H. (2005). Force-time curve characteristics of dynamic and isometric muscle actions of elite women olympic weightlifters. *Journal of Strength and Conditioning Research*, *19*(4). https://doi.org/10.1519/R-15134.1

Haff, G. G., Jackson, J. R., Kawamori, N., Carlock, J. M., Hartman, M. J., Kilgore, J. L., Morris, R. T., Ramsey, M. W., Sands, W. A., & Stone, M. H. (2008). Force-time curve characteristics and hormonal alterations during an eleven-week training period in elite

women weightlifters. *Journal of Strength and Conditioning Research*, *22*(2). https://doi.org/10.1519/JSC.0b013e31816191be

Haff, G. G., Ruben, R. P., Lider, J., Twine, C., & Cormie, P. (2015). A comparison of methods for determining the rate of force development during isometric midthigh clean pulls. *Journal of Strength and Conditioning Research*, *29*(2). https://doi.org/10.1519/JSC.0000000000000705

Haff, G. G., Stone, M., O'Bryant, H. S., Harman, E., Dinan, C., Johnson, R., & Han, K. H. (1997). Force-time dependent characteristics of dynamic and isometric muscle actions. *Journal of Strength and Conditioning Research*, *11*(4). https://doi.org/10.1519/00124278-199711000-00014

Hakkinen, K. (1991). Force production characteristics of leg extensor, trunk flexor and extensor muscles in male and female basketball players. *Journal of Sports Medicine and Physical Fitness*, *31*(3).

Hawley, J. A., & Noakes, T. D. (1992). Peak power output predicts maximal oxygen uptake and performance time in trained cyclists. *European Journal of Applied Physiology and Occupational Physiology*, *65*(1). https://doi.org/10.1007/BF01466278

Hermens, H. J., Freriks, B., Disselhorst-Klug, C., & Rau, G. (2000). Development of recommendations for SEMG sensors and sensor placement procedures. *Journal of Electromyography and Kinesiology*, *10*(5). https://doi.org/10.1016/S1050-6411(00)00027-4

Hermens, H. J., Freriks, B., Merletti, R., Stegeman, D., Blok, J., Rau, G., Disselhorst-Klug, C., & Hägg, G. (1999). European Recommendations for Surface ElectroMyoGraphy Results of the SENIAM project. *Roessingh Research and Development*, *8*(2).

Hettinger, T., & Müller, E. A. (1953). Muskelleistung und Muskeltraining. *Arbeitsphysiologie*, *15*(2). https://doi.org/10.1007/BF00934143

Hodges, P. W., & Bui, B. H. (1996). A comparison of computer-based methods for the determination of onset of muscle contraction using electromyography. *Electroencephalography and Clinical Neurophysiology - Electromyography and Motor Control*, *101*(6). https://doi.org/10.1016/S0921-884X(96)95190-5

Hoffman, J. R., Maresh, C. M., Newton, R. U., Rubin, M. R., French, D. N., Volek, J. S., Sutherland, J., Robertson, M., Gómez, A. L., Ratamess, N. A., Kang, J., & Kraemer, W. J. (2002). Performance, biochemical, and endocrine changes during a competitive football game. *Medicine and Science in Sports and Exercise*, *34*(11). https://doi.org/10.1097/00005768-200211000-00023

Hogarth, L., McKean, M., McKenzie, M., & Collings, T. (2021). Utility of an isometric midthigh pull test to assess lower body muscular strength in professional netball players. *International Journal of Sports Physiology and Performance*, *16*(5). https://doi.org/10.1123/ijspp.2019-0900

Hopkins, W. G. (2000a). Measures of reliability in sports medicine and science. In *Sports Medicine* (Vol. 30, Issue 1). https://doi.org/10.2165/00007256-200030010-00001

Hopkins, W. G. (2000b). Measures of Reliability in Sports Medicine and Science. *Sports Medicine*, *30*(5). https://doi.org/10.2165/00007256-200030050-00006

Hopkins, W. G. (2015). Spreadsheets for analysis of validity and reliability. *Sportscience*, *19*(19).

Hunter, S. K., Pereira, X. H. M., & Keenan, K. G. (2016). The aging neuromuscular system and motor performance. In *Journal of Applied Physiology* (Vol. 121, Issue 4). https://doi.org/10.1152/japplphysiol.00475.2016

Huyghe, T., Goriss, B., DeLosAngeles, E., & Bird, S. P. (2021). Exploring The Power Clean. *International Journal of Strength and Conditioning*, *1*(1). https://doi.org/10.47206/ijsc.v1i1.95

Jakobsen, J. R., & Krogsgaard, M. R. (2021). The Myotendinous Junction-A Vulnerable Companion in Sports. A Narrative Review. *Front. Physiol*, *12*, 635561. https://doi.org/10.3389/fphys.2021.635561

James, L. P., Roberts, L. A., Haff, G. G., Kelly, V. G., & Beckman, E. M. (2017). Validity and reliability of a portable isometric mid-thigh clean pull. *Journal of Strength and Conditioning Research*, *31*(5). https://doi.org/10.1519/JSC.0000000000001201

Jaric, S. (2002). Muscle strength testing: Use of normalisation for body size. In *Sports Medicine* (Vol. 32, Issue 10). https://doi.org/10.2165/00007256-200232100-00002

Jarić, S., Ristanović, D., & Corcos, D. M. (1989). The relationship between muscle kinetic parameters and kinematic variables in a complex movement. *European Journal of Applied Physiology and Occupational Physiology*, *59*(5). https://doi.org/10.1007/BF02389813

Johansson, C. A., Kent, B. E., & Shepard, K. F. (1983). Relationship between verbal command volume and magnitude of muscle contraction. *Physical Therapy*, *63*(8). https://doi.org/10.1093/ptj/63.8.1260

Juneja, P., & Hubbard, J. B. (2020). Anatomy, Bony Pelvis and Lower Limb, Tibialis Anterior Muscles. In *StatPearls*.

Karras, D. J. (1997). Statistical methodology: II. Reliability and validity assessment in study design, part B. In *Academic Emergency Medicine* (Vol. 4, Issue 2). https://doi.org/10.1111/j.1553-2712.1997.tb03723.x

Kawamori, N., Rossi, S. J., Justice, B. D., Haff, E. E., Pistilli, E. E., O'Bryant, H. S., Stone, M. H., & Haff, G. G. (2006). Peak Force and Rate of Force Development During Isometric and Dynamic Mid-Thigh Clean Pulls Performed at Various Intensities. *The Journal of Strength and Conditioning Research*, *20*(3), 483. https://doi.org/10.1519/18025.1

Khamoui, A. V., Brown, L. E., Nguyen, D., Uribe, B. P., Coburn, J. W., Noffal, G. J., & Tran, T. (2011). Relationship between force-time and velocity-time characteristics of dynamic and isometric muscle actions. *Journal of Strength and Conditioning Research*, *25*(1). https://doi.org/10.1519/JSC.0b013e3181b94a7b

Kim, K. H., & Kim, S. J. (2000). Neural spike sorting under nearly 0-dB signal-to-noise ratio using nonlinear energy operator and artificial neural-network classifier. *IEEE Transactions on Biomedical Engineering*, *47*(10). https://doi.org/10.1109/10.871415

Kim, K. H., & Kim, S. J. (2003). A wavelet-based method for action potential detection from extracellular neural signal recording with low signal-to-noise ratio. *IEEE Transactions on Biomedical Engineering*, *50*(8). https://doi.org/10.1109/TBME.2003.814523

Kipp, K., Redden, J., Sabick, M. B., & Harris, C. (2012). Weightlifting performance is related to kinematic and kinetic patterns of the hip and knee joints. *Journal of Strength and Conditioning Research*, *26*(7). https://doi.org/10.1519/JSC.0b013e318239c1d2

Komi, P. V. (1994). Strength and Power in Sport. *Medicine & Science in Sports & Exercise*, *26*(11). https://doi.org/10.1249/00005768-199411000-00021

Komi, P. V. (2011). From Isolated Actions to True Muscle Function. In *Neuromuscular Aspects of Sport Performance* (Vol. 17, pp. 1–14). John Wiley & Sons. https://doi.org/10.1002/9781444324822.ch1

Kraska, J. M., Ramsey, M. W., Haff, G. G., Fethke, N., Sands, W. A., Stone, M. E., & Stone, M. H. (2009). Relationship between strength characteristics and unweighted and weighted vertical jump height. *International Journal of Sports Physiology and Performance*, *4*(4). https://doi.org/10.1123/ijspp.4.4.461

Kumar, M. P. (2012). Accuracy & Precision and Conceptualisation to Estimation of Measurement Uncertainty in Quantitative Analysis of Quality Control Testing of Petroleum Products. *Conference Paper*, *June 2012*.

Lauersen, J. B., Bertelsen, D. M., & Andersen, L. B. (2014). The effectiveness of exercise interventions to prevent sports injuries: A systematic review and meta-analysis of randomised controlled trials. In *British Journal of Sports Medicine* (Vol. 48, Issue 11). https://doi.org/10.1136/bjsports-2013-092538

Leary, B. K., Statler, J., Hopkins, B., Fitzwater, R., Kesling, T., Lyon, J., Phillips, B., Bryner, R. W., Cormie, P., & Haff, G. G. (2012). The relationship between isometric force-time curve characteristics and club head speed in recreational golfers. *Journal of Strength and Conditioning Research*, *26*(10). https://doi.org/10.1519/JSC.0b013e31826791bf

Lee, A. S., Cholewicki, J., & Peter Reeves, N. (2007). The effect of background muscle activity on computerized detection of sEMG onset and offset. *Journal of Biomechanics*, *40*(15). https://doi.org/10.1016/j.jbiomech.2007.05.012

Li, X., & Aruin, A. S. (2005). Muscle activity onset time detection using Teager-Kaiser energy operator. *Annual International Conference of the IEEE Engineering in Medicine and Biology - Proceedings*, *7 VOLS*. https://doi.org/10.1109/iembs.2005.1616259

Li, X., Zhou, P., & Aruin, A. S. (2007). Teager-kaiser energy operation of surface EMG improves muscle activity onset detection. *Annals of Biomedical Engineering*, *35*(9). https://doi.org/10.1007/s10439-007-9320-z

Maffiuletti, N. A., Aagaard, P., Blazevich, A. J., Folland, J., Tillin, N., & Duchateau, J. (2016). Rate of force development: physiological and methodological considerations. In

European Journal of Applied Physiology (Vol. 116, Issue 6). https://doi.org/10.1007/s00421-016-3346-6

Mangine, G. T., Hoffman, J. R., Wang, R., Gonzalez, A. M., Townsend, J. R., Wells, A. J., Jajtner, A. R., Beyer, K. S., Boone, C. H., Miramonti, A. A., LaMonica, M. B., Fukuda, D. H., Ratamess, N. A., & Stout, J. R. (2016). Resistance training intensity and volume affect changes in rate of force development in resistance-trained men. *European Journal of Applied Physiology*, *116*(11–12). https://doi.org/10.1007/s00421-016-3488-6

Maragos, P., Quatieri, T. F., & Kaiser, J. F. (1993). On Amplitude and Frequency Demodulation Using Energy Operators. *IEEE Transactions on Signal Processing*, *41*(4). https://doi.org/10.1109/78.212729

Martin Bland, J., & Altman, D. G. (1986). STATISTICAL METHODS FOR ASSESSING AGREEMENT BETWEEN TWO METHODS OF CLINICAL MEASUREMENT. *The Lancet*, *327*(8476), 307–310. https://doi.org/10.1016/S0140-6736(86)90837-8

Massey, G. J. (2017). Muscle-tendon unit morphology, architecture and stiffness in relation to strength and responses to strength training. In *Loughborough University's Institutional Repository* (Issue March).

McGuigan, M. R., Newton, M. J., Winchester, J. B., & Nelson, A. G. (2010). Relationship between isometric and dynamic strength in recreationally trained men. *Journal of Strength and Conditioning Research*, *24*(9). https://doi.org/10.1519/JSC.0b013e3181ecd381

McGuigan, M. R., & Winchester, J. B. (2008). The relationship between isometric and dynamic strength in college football players. *Journal of Sports Science and Medicine*, *7*(1). https://doi.org/10.1249/01.mss.0000322664.81874.75

McGuigan, M. R., Winchester, J. B., & Erickson, T. (2006a). The importance of isometric maximum strength in college wrestlers. *Journal of Sports Science and Medicine*, *5*(CSSI-1).

McGuigan, M. R., Winchester, J. B., & Erickson, T. (2006b). The importance of isometric maximum strength in college wrestlers. *Journal of Sports Science and Medicine*, *5*(CSSI-1).

Menditto, A., Patriarca, M., & Magnusson, B. (2007). Understanding the meaning of accuracy, trueness and precision. In *Accreditation and Quality Assurance* (Vol. 12, Issue 1). https://doi.org/10.1007/s00769-006-0191-z

Merlo, A., Bò, M. C., & Campanini, I. (2021). Electrode size and placement for surface emg bipolar detection from the brachioradialis muscle: A scoping review. In *Sensors* (Vol. 21, Issue 21). https://doi.org/10.3390/s21217322

Mero, A., Luhtanen, P., Viitasalo, J. T., & Komi, P. V. (1981). Relationships between the maximal running velocity, muscle fiber characteristics, force production and force relaxation of sprinters. *Scandinavian Journal of Sports Sciences*, *3*(1).

Mitchell, B., & Whited, L. (2019). Anatomy, Shoulder and Upper Limb, Forearm Muscles. In *StatPearls*.

Moir, G. L., Garcia, A., & Dwyer, G. B. (2009). Intersession reliability of kinematic and kinetic variables during vertical jumps in men and women. *International Journal of Sports Physiology and Performance*, *4*(3). https://doi.org/10.1123/ijspp.4.3.317

Mukhopadhyay, S., & Ray, G. C. (1998). A new interpretation of nonlinear energy operator and its efficacy in spike detection. In *IEEE Transactions on Biomedical Engineering* (Vol. 45, Issue 2). https://doi.org/10.1109/10.661266

Murphy, A. J., Wilson, G. J., & Pryor, J. F. (1994). Use of the iso-inertial force mass relationship in the prediction of dynamic human performance. *European Journal of Applied Physiology and Occupational Physiology*, *69*(3). https://doi.org/10.1007/BF01094797

Murphy, A. J., Wilson, G. J., Pryor, J. F., & Newton, R. U. (1995). Isometric assessment of muscular function: The effect of joint angle. *Journal of Applied Biomechanics*, *11*(2). https://doi.org/10.1123/jab.11.2.205

Newton, R. U., & Dugan, E. (2002). Application of strength diagnosis. In *Strength and Conditioning Journal* (Vol. 24, Issue 5). https://doi.org/10.1519/00126548-200210000-00014

Nuzzo, J. L., Mcbride, J. M., Cormie, P., & Mccaulley, G. O. (2008). Relationship between countermovement jump performance and multijoint isometric and dynamic tests of strength. *Journal of Strength and Conditioning Research*, *22*(3). https://doi.org/10.1519/JSC.0b013e31816d5eda

Oliveira, A. S., Corvino, R. B., Caputo, F., Aagaard, P., & Denadai, B. S. (2016). Effects of fast-velocity eccentric resistance training on early and late rate of force development. *European Journal of Sport Science*, *16*(2). https://doi.org/10.1080/17461391.2015.1010593

Oranchuk, D. J., Robinson, T. L., Switaj, Z. J., & Drinkwater, E. J. (2019). Comparison of the Hang High Pull and Loaded Jump Squat for the Development of Vertical Jump and Isometric Force-Time Characteristics. *Journal of Strength and Conditioning Research*, *33*(1). https://doi.org/10.1519/JSC.0000000000001941

Owen, N. J., Watkins, J., Kilduff, L. P., Bevan, H. R., & Bennett, M. A. (2014). Development of a criterion method to determine peak mechanical power output in a countermovement jump. *Journal of Strength and Conditioning Research*, *28*(6). https://doi.org/10.1519/JSC.0000000000000311

Paavolainen, L., Häkkinen, K., Hämäläinen, I., Nummela, A., & Rusko, H. (1999). Explosive-strength training improves 5-km running time by improving running economy and muscle power. *Journal of Applied Physiology*, *86*(5). https://doi.org/10.1152/jappl.1999.86.5.1527

Peñailillo, L., Blazevich, A., Numazawa, H., & Nosaka, K. (2015). Rate of force development as a measure of muscle damage. *Scandinavian Journal of Medicine and Science in Sports*, *25*(3). https://doi.org/10.1111/sms.12241

Pohlmann, K. (2011). Digital Signal Processing. In *Principles of Digital Audio* (6th ed., pp. 645–691). McGraw-Hill.

Pohlmann, K. C. (2011). Sounds and Numbers. In *Principles of Digital Audio* (6th ed., Issue 3, pp. 1–16). McGraw-Hill.

Pratt, J., Hoffman, A., Grainger, A., & Ditroilo, M. (2020). Forearm electromyographic activity during the deadlift exercise is affected by grip type and sex. *Journal of Electromyography and Kinesiology*, *53*. https://doi.org/10.1016/j.jelekin.2020.102428

Prenesti, E., & Gosmaro, F. (2015). Trueness, precision and accuracy: a critical overview of the concepts as well as proposals for revision. *Accreditation and Quality Assurance*, *20*(1). https://doi.org/10.1007/s00769-014-1093-0

Pryor, J. F., Wilson, G. J., & Murphy, A. J. (1994). The effectiveness of eccentric, concentric and isometric rate of force development tests. *Journal of Human Movement Studies*, *27*(4).

Richardson, C. (1994). EMG study of erector spinae and multifidus in two isometric back extension exercises. *Australian Journal of Physiotherapy*, *40*(2). https://doi.org/10.1016/S0004-9514(14)60458-X

Rodgers, C. D., & Raja, A. (2020). Anatomy, Bony Pelvis and Lower Limb, Hamstring Muscle. In *StatPearls*.

Rodrigues, J., Santos-Faria, D., Silva, J., Azevedo, S., Tavares-Costa, J., & Teixeira, F. (2019). Sonoanatomy of anterior forearm muscles. *Journal of Ultrasound*, *22*(3). https://doi.org/10.1007/s40477-019-00388-z

Rodríguez-Rosell, D., Pareja-Blanco, F., Aagaard, P., & González-Badillo, J. J. (2018). Physiological and methodological aspects of rate of force development assessment in human skeletal muscle. In *Clinical Physiology and Functional Imaging* (Vol. 38, Issue 5). https://doi.org/10.1111/cpf.12495

Roetenberg, D., Buurke, J. H., Veltink, P. H., Cordero, A. F., & Hermens, H. J. (2003). Surface electromyography analysis for variable gait. *Gait and Posture*, *18*(2). https://doi.org/10.1016/S0966-6362(03)00005-5

Ryschon, T. W., Fowler, M. D., Wysong, R. E., Anthony, A. R., & Balaban, R. S. (1997). Efficiency of human skeletal muscle in vivo: Comparison of isometric, concentric, and eccentric muscle action. *Journal of Applied Physiology*, *83*(3). https://doi.org/10.1152/jappl.1997.83.3.867

Santos, P. D. G., Vaz, J. R., Correia, P. F., Valamatos, M. J., Veloso, A. P., & Pezarat-Correia, P. (2020). Muscle Synergies Reliability in the Power Clean Exercise. *Journal of Functional Morphology and Kinesiology*, *5*(4). https://doi.org/10.3390/jfmk5040075

Secher, N. H. (1975). Isometric rowing strength of experienced and inexperienced oarsmen. *Medicine and Science in Sports*, *7*(4). https://doi.org/10.1249/00005768-197500740-00006

Secomb, J. L., Farley, O. R. L., Lundgren, L., Tran, T. T., King, A., Nimphius, S., & Sheppard, J. M. (2015). Associations between the performance of scoring manoeuvres and lower-body strength and power in elite surfers. *International Journal of Sports Science and Coaching*, *10*(5). https://doi.org/10.1260/1747-9541.10.5.911

Secomb, J. L., Lundgren, L. E., Farley, O. R. L., Tran, T. T., Nimphius, S., & Sheppard, J. M. (2015). Relationships between Lower-Body Muscle Structure and Lower-Body Strength, Power, and Muscle-Tendon Complex Stiffness. *Journal of Strength and Conditioning Research*, *29*(8). https://doi.org/10.1519/JSC.0000000000000858

Secomb, J. L., Nimphius, S., Farley, O. R. L., Lundgren, L. E., Tran, T. T., & Sheppard, J. M. (2015). Relationships between lower-body muscle structure and, lower-body strength, explosiveness and eccentric leg stiffness in adolescent athletes. *Journal of Sports Science and Medicine*, *14*(4).

Shechtman, O. (2013). *The Coefficient of Variation as an Index of Measurement Reliability*. https://doi.org/10.1007/978-3-642-37131-8_4

Sheppard, J. M., Cormack, S., Taylor, K. L., Mcguigan, M. R., & Newton, R. U. (2008). Assessing the force-velocity characteristics of the leg extensors in well-trained athletes: The incremental load power profile. *Journal of Strength and Conditioning Research*, *22*(4). https://doi.org/10.1519/JSC.0b013e31816d671b

Sjökvist, J., Sandbakk, Willis, S. J., Andersson, E., & Holmberg, H. C. (2015). The effect of incline on sprint and bounding performance in cross-country skiers. *Journal of Sports Medicine and Physical Fitness*, *55*(5).

Solnik, S., DeVita, P., Rider, P., Long, B., & Hortobágyi, T. (2008). Teager-Kaiser operator improves the accuracy of EMG onset detection independent of signal-to-noise ratio. *Acta of Bioengineering and Biomechanics*, *10*(2).

Solnik, S., Rider, P., Steinweg, K., Devita, P., & Hortobágyi, T. (2010). Teager-Kaiser energy operator signal conditioning improves EMG onset detection. *European Journal of Applied Physiology*, *110*(3). https://doi.org/10.1007/s00421-010-1521-8

Souza, A. L., Shimada, S. D., & Koontz, A. (2002). Ground reaction forces during the power clean. *Journal of Strength and Conditioning Research*, *16*(3). https://doi.org/10.1519/1533-4287(2002)016<0423:GRFDTP>2.0.CO;2

Spiteri, T., Newton, R. U., & Nimphius, S. (2015). Neuromuscular strategies contributing to faster multidirectional agility performance. *Journal of Electromyography and Kinesiology*, *25*(4). https://doi.org/10.1016/j.jelekin.2015.04.009

Staude, G. H. (2001). Precise onset detection of human motor responses using a whitening filter and the log-likelihood-ratio test. *IEEE Transactions on Biomedical Engineering*, *48*(11). https://doi.org/10.1109/10.959325

Staude, G., Kafka, V., & Wolf, W. (2000). Determination of Premotor Silent periods from Surface Myoelectric signals. In *Biomedizinische Technik* (Vol. 45, Issue 2).

Staude, G., & Wolf, W. (1999). Objective motor response onset detection in surface myoelectric signals. *Medical Engineering and Physics*, *21*(6–7). https://doi.org/10.1016/S1350-4533(99)00067-3

Stokes, M. (1985). Reliability and repeatability of methods for measuring muscle in physiotherapy. In *Physiotherapy Theory and Practice* (Vol. 1, Issue 2). https://doi.org/10.3109/09593988509163853

Stone, M. H. ;, O'Bryant, H., Hornsby, G., Cunanan, A., Mizuguchi, S., Suarez, D., South, M., Marsh, D., Haff, G., Ramsey, M., Beckham, G., Santana, H., Wagle, J., Stone, M., & Pierce, Kyle. (2019). Using the Isometric Mid-thigh Pull in the Monitoring of Weightlifters: 25+ Years of Experience. *Professional Strength & Conditioning (2019) (54) 19-26*, *54*.

Stone, M. H., Sanborn, K., O'Bryant, H. S., Hartman, M., Stone, M. E., Proulx, C., Ward, B., & Hruby, J. (2003). Maximum Strength-Power-Performance Relationships in Collegiate Throwers. *Journal of Strength and Conditioning Research*, *17*(4). https://doi.org/10.1519/1533-4287(2003)017<0739:MSRICT>2.0.CO;2

Stone, M. H., Sands, W. A., Carlock, J., Callan, S., Dickie, D., Daigle, K., Cotton, J., Smith, S. L., & Hartman, M. (2004). The importance of isometric maximum strength and peak rate-of-force development in sprint cycling. *Journal of Strength and Conditioning Research*, *18*(4). https://doi.org/10.1519/14874.1

Stone, M. H., Sands, W. A., Pierce, K. C., Carlock, J., Cardinale, M., & Newton, R. U. (2005). Relationship of maximum strength to weightlifting performance. *Medicine and Science in Sports and Exercise*, *37*(6). https://doi.org/10.1249/01.mss.0000171621.45134.10

Strass, D. E. T. E. R. (1991). Force–time and electromyographic characteristics of arm shoulder muscles in explosive type force production in sprint swimmers. *The Journal of Swimming Research*, *7*(1), 19–27.

Strauss, G., Hofer, M., Korb, W., Trantakis, C., Winkler, D., Burgert, O., Schulz, T., Dietz, a, Meixensberger, J., & Koulechov, K. (2006). Accuracy and precision in the evaluation of computer assisted surgical systems. A definition. *Hno*, *54*(2).

Suchomel, T. J., Deweese, B. H., & Serrano, A. J. (2016). The Power Clean and Power Snatch from the Knee. *Strength and Conditioning Journal*, *38*(4). https://doi.org/10.1519/SSC.0000000000000216

Suchomel, T. J., Nimphius, S., & Stone, M. H. (2016). The Importance of Muscular Strength in Athletic Performance. In *Sports Medicine* (Vol. 46, Issue 10). https://doi.org/10.1007/s40279-016-0486-0

Takala, E. P., & Toivonen, R. (2013). Placement of forearm surface EMG electrodes in the assessment of hand loading in manual tasks. *Ergonomics*, *56*(7). https://doi.org/10.1080/00140139.2013.799235

Tenan, M. S., Tweedell, A. J., & Haynes, C. A. (2017). Analysis of statistical and standard algorithms for detecting muscle onset with surface electromyography. *PLoS ONE*, *12*(5). https://doi.org/10.1371/journal.pone.0177312

Thomas, C., Comfort, P., Chiang, C.-Y., & A. Jones, P. (2015). Relationship between isometric mid-thigh pull variables and sprint and change of direction performance in collegiate athletes. *Journal of Trainology*, *4*(1). https://doi.org/10.17338/trainology.4.1_6

Thomas, C., Dos'santos, T., Comfort, P., & Jones, P. A. (2017). Between-session reliability of common strength-and power-related measures in adolescent athletes. *Sports*, *5*(1). https://doi.org/10.3390/sports5010015

Thomas, C., Jones, P. A., & Comfort, P. (2015). Reliability of the dynamic strength index in college athletes. *International Journal of Sports Physiology and Performance*, *10*(5). https://doi.org/10.1123/ijspp.2014-0255

Thomas, C., Jones, P. A., Comfort, P., & Dos 'Santos Thomas. (2021). Positional comparison of isometric mid-thigh pull characteristics in youth female netball players. *The Journal of Sport and Exercise Science*, *5*(3). https://doi.org/10.36905/jses.2021.03.01

Thomas, C., Jones, P. A., Rothwell, J., Chiang, C. Y., & Comfort, P. (2015). An Investigation into the Relationship between Maximum Isometric Strength and Vertical Jump Performance. *Journal of Strength and Conditioning Research*, *29*(8). https://doi.org/10.1519/JSC.0000000000000866

Thomas R, J., Martin, P., Etnier, J., & Silverman J, S. (2022). Measuring Research Variables. In *Research Methods in Physical Activity* (8th ed., pp. 205–226). Human Kinetics.

Thompson, S. W., Rogerson, D., Ruddock, A., & Barnes, A. (2020). The Effectiveness of Two Methods of Prescribing Load on Maximal Strength Development: A Systematic Review. In *Sports Medicine* (Vol. 50, Issue 5). https://doi.org/10.1007/s40279-019-01241-3

Thorlund, J. B., Michalsik, L. B., Madsen, K., & Aagaard, P. (2008). Acute fatigue-induced changes in muscle mechanical properties and neuromuscular activity in elite handball players following a handball match. *Scandinavian Journal of Medicine and Science in Sports*, *18*(4). https://doi.org/10.1111/j.1600-0838.2007.00710.x

Till, K., Morris, R., Stokes, K., Trewartha, G., Twist, C., Dobbin, N., Hunwicks, R., & Jones, B. (2018). Validity of an isometric midthigh pull dynamometer in male youth athletes. *Journal of Strength and Conditioning Research*, *32*(2). https://doi.org/10.1519/jsc.0000000000002324

Tillin, N. A., Jimenez-Reyes, P., Pain, M. T. G., & Folland, J. P. (2010). Neuromuscular performance of explosive power athletes versus untrained individuals. *Medicine and Science in Sports and Exercise*, *42*(4). https://doi.org/10.1249/MSS.0b013e3181be9c7e

Tillin, N. A., Pain, M. T. G., & Folland, J. P. (2012). Contraction type influences the human ability to use the available torque capacity of skeletal muscle during explosive efforts. *Proceedings of the Royal Society B: Biological Sciences*, *279*(1736). https://doi.org/10.1098/rspb.2011.2109

Townsend, J. R., Bender, D., Vantrease, W. C., Hudy, J., Huet, K., Williamson, C., Bechke, E., Serafini, P. R., & Mangine, G. T. (2019). Isometric Midthigh Pull Performance Is Associated With Athletic Performance and Sprinting Kinetics in Division I Men and Women's Basketball Players. *Journal of Strength and Conditioning Research*, *33*(10). https://doi.org/10.1519/JSC.0000000000002165

Tran, T. T., Lundgren, L., Secomb, J., Farley, O. R. L., Haff, G. G., Seitz, L. B., Newton, R. U., Nimphius, S., & Sheppard, J. M. (2015). Comparison of physical capacities between

nonselected and selected elite male competitive surfers for the national junior team. *International Journal of Sports Physiology and Performance*, *10*(2). https://doi.org/10.1123/ijspp.2014-0222

VAN BOXTEL, G. J. M., GERAATS, L. H. D., VAN DEN BERG-LENSSEN, M. M. C., & BRUNIA, C. H. M. (1993). Detection of EMG onset in ERP research. *Psychophysiology*, *30*(4). https://doi.org/10.1111/j.1469-8986.1993.tb02062.x

Van Drongelen, W. (2018). Introduction. In *Signal Processing for Neuroscientists* (2nd ed., pp. 1–13). Academic Press. https://doi.org/10.1016/c2010-0-65662-8

Vecchio, L. Del. (2018). The health and performance benefits of the squat, deadlift, and bench press. *MOJ Yoga & Physical Therapy*, *3*(2). https://doi.org/10.15406/mojypt.2018.03.00042

Vigotsky, A. D., Halperin, I., Lehman, G. J., Trajano, G. S., & Vieira, T. M. (2018). Interpreting signal amplitudes in surface electromyography studies in sport and rehabilitation sciences. In *Frontiers in Physiology* (Vol. 8, Issue JAN). https://doi.org/10.3389/fphys.2017.00985

Viitasalo, J. T., & Aura, O. (1984). Seasonal fluctuations of force production in high jumpers. *Canadian Journal of Applied Sport Sciences. Journal Canadien Des Sciences Appliquees Au Sport*, *9*(4).

Viitasalo, J. T., Hakkinen, K., & Komi, P. V. (1981). Isometric and dynamic force production and muscle fibre composition in man. *Journal of Human Movement Studies*, *7*(3).

Wang, R., Hoffman, J. R., Tanigawa, S., Miramonti, A. A., La Monica, M. B., Beyer, K. S., Church, D. D., Fukuda, D. H., & Stout, J. R. (2016). Isometric Mid-Thigh Pull Correlates with Strength, Sprint, and Agility Performance in Collegiate Rugby Union Players. *Journal of Strength and Conditioning Research*, *30*(11). https://doi.org/10.1519/JSC.0000000000001416

Watkins, J. (2014). Fundamental biomechanics of sport and exercise. In *Fundamental Biomechanics of Sport and Exercise*. https://doi.org/10.4324/9780203066461

Welch, N., Moran, K., Antony, J., Richter, C., Marshall, B., Coyle, J., Falvey, E., & Franklyn-Miller, A. (2015). The effects of a free-weight-based resistance training intervention on pain, squat biomechanics and MRI-defined lumbar fat infiltration and functional cross-sectional area in those with chronic low back. *BMJ Open Sport and Exercise Medicine*, *1*(1). https://doi.org/10.1136/bmjsem-2015-000050

West, D. J., Owen, N. J., Jones, M. R., Bracken, R. M., Cook, C. J., Cunningham, D. J., Shearer, D. A., Finn, C. V., Newton, R. U., Crewther, B. T., & Kilduf, L. P. (2011). Relationships between force-time characteristics of the isometric midthigh pull anddynamic performance in professional rugby league players. *Journal of Strength and Conditioning Research*, *25*(11). https://doi.org/10.1519/JSC.0b013e318212dcd5

Whittington, J., Schoen, E., Labounty, L. L., Hamdy, R., Ramsey, M. W., Stone, M. E., Sands, W. A., Haff, G. G., & Stone, M. H. (2009). Bone mineral density and content of collegiate throwers: Influence of maximum strength. *Journal of Sports Medicine and Physical Fitness*, *49*(4).

Wilson, G. J., Lyttle, A. D., Ostrowski, K. J., & Murphy, A. J. (1995). Assessing dynamic performance: A comparison of rate of force development tests. *Journal of Strength and Conditioning Research*, *9*(3). https://doi.org/10.1519/00124278-199508000-00010

Wilson, G. J., & Murphy, A. J. (1996). The use of isometric tests of muscular function in athletic assessment. In *Sports Medicine* (Vol. 22, Issue 1). https://doi.org/10.2165/00007256-199622010-00003

Winchester, J. B., McBride, J. M., Maher, M. A., Mikat, R. P., Allen, B. K., Kline, D. E., & Mcguigan, M. R. (2008). Eight weeks of ballistic exercise improves power independently of changes in strength and muscle fiber type expression. *Journal of Strength and Conditioning Research*, *22*(6). https://doi.org/10.1519/JSC.0b013e3181821abb

Winter, D. A. (2009). Signal Processing. In *Biomechanics and Motor Control of Human Movement* (4th ed., pp. 14–43). JOHN WILEY & SONS, INC. https://doi.org/10.1002/9780470549148

Yang, D., Zhang, H., Gu, Y., & Liu, H. (2017). Accurate EMG onset detection in pathological, weak and noisy myoelectric signals. *Biomedical Signal Processing and Control*, *33*. https://doi.org/10.1016/j.bspc.2016.12.014

Young, W. B., & Bilby, G. E. (1993). The effect of voluntary effort to influence speed of contraction on strength, muscular power, and hypertrophy development. *Journal of Strength and Conditioning Research*, *7*(3). https://doi.org/10.1519/00124278-199308000-00009

Zipp, P. (1982). Recommendations for the standardization of lead positions in surface electromyography. *European Journal of Applied Physiology and Occupational Physiology*, *50*(1). https://doi.org/10.1007/BF00952243

Appendices

Appendix A: Ethical Approval Form

LEAD APPLICANT NAME: Sayyam Kathuria
DISCIPLINE/DEPARTMENT: SPEX
PROJECT TITLE: Investigations into neuromuscular variables derived from isometric force assessment and their association with dynamic performance.
APPLICATION REFFERENCE NUMBER: Sayyam_Kathuria_23-12-21

Swansea University
Prifysgol Abertawe

Date of review board: February
Committee members in attendance: Chairs

Date: Tuesday 8th February 2022

Dear Sayyam,

Thank you for your recent ethics application.

This decision letter is to inform you that the ethics application for the above titled project has been reviewed and approved. The ethical approval number for this application is SK_23-12-21 approved from 08/02/22 – end of approval 25/09/22.

This letter is for Swansea University, College of Engineering Research Ethics and Governance approval only. Local Health and Safety, in addition to appropriate risk assessment guidelines are required separate to this approval, unless otherwise stated herein, and must be adhered to.

Associated researchers must not deviate from the approved protocol or extend beyond the approval end date. Any desired deviations or approval date extensions are subject to the ethical approval amendment process. Upon completion of the approved project researchers responsible for this application must submit a final (short) statement to the ethical committee stating the completion of the project, unless a time extension is being requested through the amendment process.

Any significant un-anticipated adverse effects/events (i.e. not those predicted and stated in section 8 of the ethics application form) must be reported to the Ethics committee upon researcher realisation (email: coe-researchethics@swansea.ac.uk; with the subject title including the study approval number followed by "Adverse Effects/Events").

If you have any further questions relating to your application, please contact: coe-researchethics@swansea.ac.uk.

Please keep note of your approval number for future reference and correspondence relating to this application.

Best of luck with your research.

Warm regards,

Aynsley Fagan

(on behalf of the College of Engineering Research Ethics and Governance Chair)

College of Engineering Ethics and Governance Committee Administrator
College of Engineering | Y Coleg Peirianneg
Swansea University | Prifysgol Abertawe
Fabian Way | Ffordd Fabian Crymlyn Burrows
Swansea | Abertawe
Wales | Cymru
SA1 8EN

Email: coe-researchethics@swansea.ac.uk.

Appendix B: Participant information sheet

PARTICIPANT INFORMATION SHEET

(Version 1.1, Date: 15 /11/21)

Project Title:

1. Investigations into neuromuscular variables derived from isometric force assessment and their association with dynamic performance.
2. Identification of the onset of pull during the isometric mid0thigh pull using Surface Electromyography (sEMG).

Contact Details:

RESEARCHER	SUPERVISOR
Sayyam Kathuria MSc, Sports and Exercise Science. College of Engineering Swansea University, Bay Campus Fabian Way, Swansea SA1 8EN Phone: [redacted] Email: [redacted]	Dr. Nick Owen Associate Professor, Sports & Exercise Sciences. College of Engineering Swansea University, Bay Campus Fabian Way, Swansea SA1 8EN Phone: [redacted] Email: [redacted].

1. Invitation Paragraph

My name is Sayyam Kathuria and I am a MSc student at Swansea University. I am conducting a study which involves the use of a strength testing equipment, often used with athletes to assess their strength generating ability

2. What is the purpose of the study?

Muscular strength is an important characteristic in all sports, however, there are many different ways of measuring strength. The data obtained in this study will allow us to better understand how a newly developed device for measuring strength both at hands and at feet can help train athletes. The results from the study will contribute towards player profiling, monitoring and prescription of appropriate conditioning programs to elevate overall sporting performance of the participant involved. The study will attempt to address the limitations of equipment cost, access, availability and restrictions on field-based testing. Validation of the portable isometric mid-thigh pull and exploring its relationship to dynamic performance will ultimately contribute to safer testing practices associated with isometric testing in comparison to repetition maximum tests.

3. Why have I been chosen?

You have been chosen to participate in this study as you are currently playing elite or sub-elite sport. Your participation in this research is completely voluntary. You are free to withdraw consent and discontinue participation at any time without influencing any present and/or future involvement with Swansea University. Your consent to participate in this research will be indicated by your signing and dating the consent form. Signing the consent form indicates that you have given your consent to participate, and that there has been no coercion or inducement to participate by the researchers from Swansea University

4. What will happen to me if I take part?

You will be asked to perform a series of jump, agility, speed and strength tests, all lasting less than 20-seconds.

5. What are the possible disadvantages of taking part?

Testing procedure may contribute to fatigue and tiredness with possibility of muscle soreness. Appropriate recovery protocols will be discussed with the strength & conditioning coaches beforehand.

6. What are the possible benefits of taking part?

The information gained from this research will help support and build on the few existing literature on isometric testing. Given the benefits of isometric testing, the information gained from this study will further help strengthen its relationship with dynamic performance. The portable rig validation could pave the path for a new product to measure strength in a safe and time efficient manner. It would also extend the products accessibility available at a relatively cheaper cost.

7. Will my taking part in the study be kept confidential?

Your taking part in the study will be kept confidential by making sure only the research supervisor and I can access the data outside of the academy. Non-anonymized data will only be accessible by the supervisor and the researcher. Specific identification features and participant names not relevant to the study will be removed to protect the identity of the participant. Unique ID codes will be assigned to participants and a separate file linking ID codes to participant's names will confidential to all apart from the lead investigator, project supervisor and area supervisors where appropriate. Nothing that will breach the participant's confidentiality and anonymity agreement will be published

Data Protection and Confidentiality

Your data will be processed in accordance with the Data Protection Act 2018 and the General Data Protection Regulation 2016 (GDPR). All information collected about you will be kept strictly confidential. Your data will only be viewed by the researcher/research team.

All electronic data will be stored on a password-protected computer file stored in Dr Owen's office All paper records will be stored in a locked filing cabinet in Dr Owen's office. Your consent information will be kept separately from your responses to minimise risk in the event of a data breach.

Please note that the data we will collect for our study will be made anonymous, after its initial collection but before the end of the study, thus it will not be possible to identify and remove your data at a later date, should you decide to withdraw from the study. Therefore, if at the end of this research you decide to have your data withdrawn, please let us know before you leave.

Data Protection Privacy Notice

The data controller for this project will be Swansea University. The University Data Protection Officer provides oversight of university activities involving the processing of personal data, and can be contacted at the Vice Chancellors Office.

Your personal data will be processed for the purposes outlined in this information sheet.
Standard ethical procedures will involve you providing your consent to participate in this study by completing the consent form that has been provided to you.

The legal basis that we will rely on to process your personal data will be processing is necessary for the performance of a task carried out in the public interest. This public interest justification is approved by the College of Engineering Research Ethics Committee, Swansea University.

The legal basis that we will rely on to process special categories of data will be processing is necessary for archiving purposes in the public interest, scientific or historical research purposes or statistical purposes.

How long will your information be held?
We will hold any personal data and special categories of data for the duration of the study or a maximum of 5 years, whichever is the sooner.

What are your rights?
You have a right to access your personal information, to object to the processing of your personal information, to rectify, to erase, to restrict and to port your personal information. Please visit the University Data Protection webpages for further information in relation to your rights.

Any requests or objections should be made in writing to the University Data Protection Officer:-

University Compliance Officer (FOI/DP)
Vice-Chancellor's Office
Swansea University
Singleton Park
Swansea
SA2 8PP
Email: dataprotection@swansea.ac.uk

How to make a complaint
If you are unhappy with the way in which your personal data has been processed you may in the first instance contact the University Data Protection Officer using the contact details above.

If you remain dissatisfied then you have the right to apply directly to the Information Commissioner for a decision. The Information Commissioner can be contacted at: -

Information Commissioner's Office,
Wycliffe House,
Water Lane,
Wilmslow,
Cheshire,
SK9 5AF
www.ico.org.uk

8. **What if I have any questions?**
Re-iterate that further information can be obtained from the researcher contact stated above. Also state

that “the project has been approved by the College of Engineering Research Ethics Committee at Swansea University. If you have any questions regarding this, any complaint, or concerns about the ethics and governance of this research please contact the Chair of the College of Engineering Research Ethics Committee, Swansea University: coe-researchethics@swansea.ac.uk. The institutional contact for reporting cases of research conduct is Registrar & Chief Operating Officer Mr Andrew Rhodes. Email: researchmisconduct@swansea.ac.uk. Further details are available at the Swansea University webpages for Research Integrity. http://www.swansea.ac.uk/research/researchintegrity/.”

Appendix C: Participant consent form

PARTICIPANT CONSENT FORM
(Version 1.1, Date: 15/11/2021)

Project Title:

1. Investigations into neuromuscular variables derived from isometric force assessment and their association with dynamic performance.
2. Identification of the onset of pull during the isometric mid0thigh pull using Surface Electromyography (sEMG).

Contact Details:

RESEARCHER Sayyam Kathuria MSc, Sports and Exercise Science. College of Engineering Swansea University, Bay Campus Fabian Way, Swansea SA1 8EN Phone: [redacted] Email: [redacted]	SUPERVISOR Dr. Nick Owen Associate Professor, Sports & Exercise Sciences. College of Engineering Swansea University, Bay Campus Fabian Way, Swansea SA1 8EN Phone: [redacted] Email: [redacted]

Please initial box

1. I confirm that I have read and understood the information sheet dated//20 (version number .....) for the above study and have had the opportunity to ask questions. ☐
2. I understand that my participation is voluntary and that I am free to withdraw at any time, without giving any reason, without my medical care or legal rights being affected. ☐
3. I understand that sections of any of data obtained may be looked at by responsible individuals from the Swansea University or from regulatory authorities where it is relevant to my taking part in research. I give permission for these individuals to have access these records. ☐
4. I understand that data I provide may be used in reports and academic publications in anonymous fashion ☐
5. I agree to take part in the above study. ☐

Name of Participant	Date	Signature
Name of Person taking consent	Date	Signature
Researcher	Date	Signature

Appendix D: Handbook/ Guide for using the 2-step visual detection method to determine the time of muscle onset.

Guide to use the 2-step visual detection method in:

Methodological considerations and reliability of visually detecting muscle activity onset during an isometric midthigh pull.

1.0 Background

In accordance with the purpose of this study you will be required to visually detect muscle onset times of the same data set on two different occasions separated by a minimum of three days. Your output will be compared to the one produced by Rater 1 to check for inter-rater reliability.

1.1 MATLAB Installation

Before we start, please ensure you have downloaded MATLAB on your PC/laptop. Downloads for MATLAB can be done via the University License for the software, found easily on your Student/Staff Account.

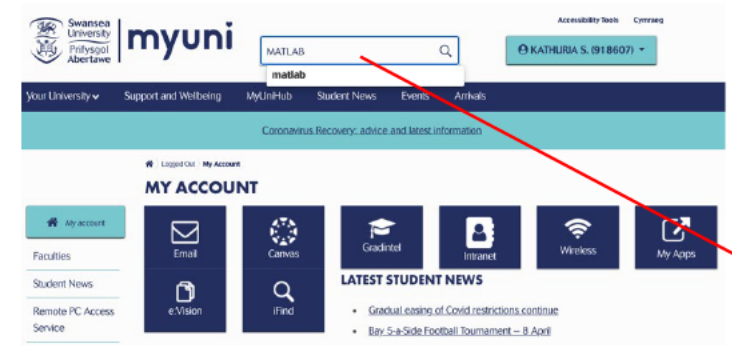

1. Open your staff/student account and search for

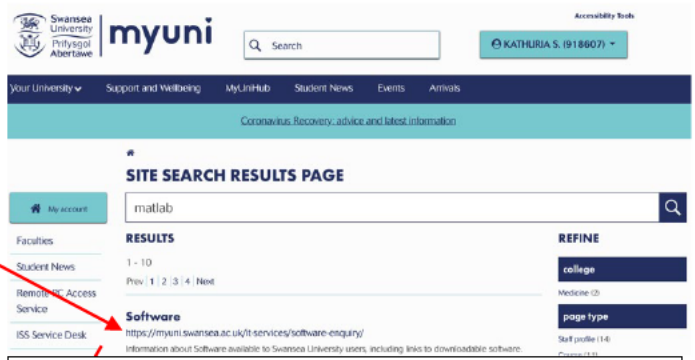

2. Click on software to view licenses for MATLAB.

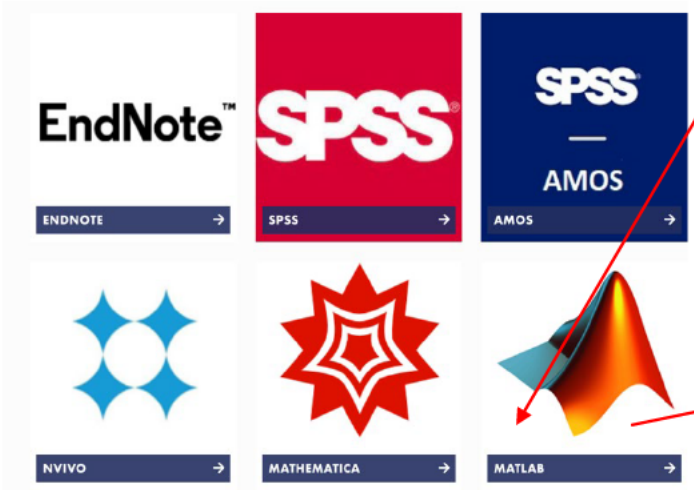

3. Scroll down to find & click on MATLAB to view the university's instructions on how to download the software.

4. Follow the instructions to successfully install the software on your laptop/PC.

Figure 1.1 *Steps to guide MATLAB installation*

2.1 Loading and running data using the bespoke MATLAB script.

The data will be transferred using a hard drive to ensure the script and the raw data have the same pathway. MATLAB requires the data to be imported and the respective script to be in the same folder to be able to detect the file and run it through the code.

2.1.1 Step 1

After successfully installing the software, open MATLAB on your PC/LAPTOP.

2.1.2 Step 2

Select your pathway based on where you have saved the data on your device. ***For example, refer to the image below***. The red box shows where you can select the pathway. In the folder select the condition you wish to analyse first: "AS EMG ONOFF" / "AS EMG ONON" / "Weightlifters"

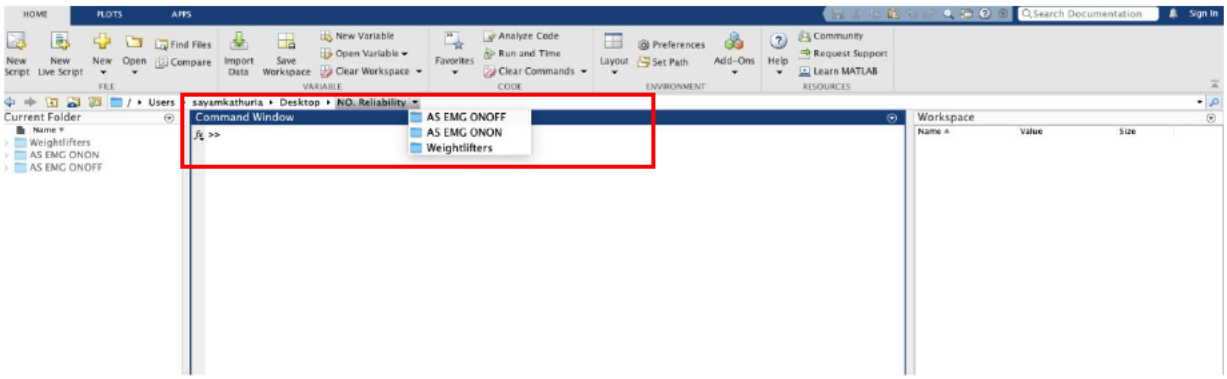

Figure 2.1 *Pathway and condition selection*

2.1.3 Step 3

On selecting the desired condition, the raw data and the respective script should be displayed on the left-hand side of the window under 'Current Folder'. Double click on the file with the extension **'.m'** to open the script. ***Refer to the image below***.

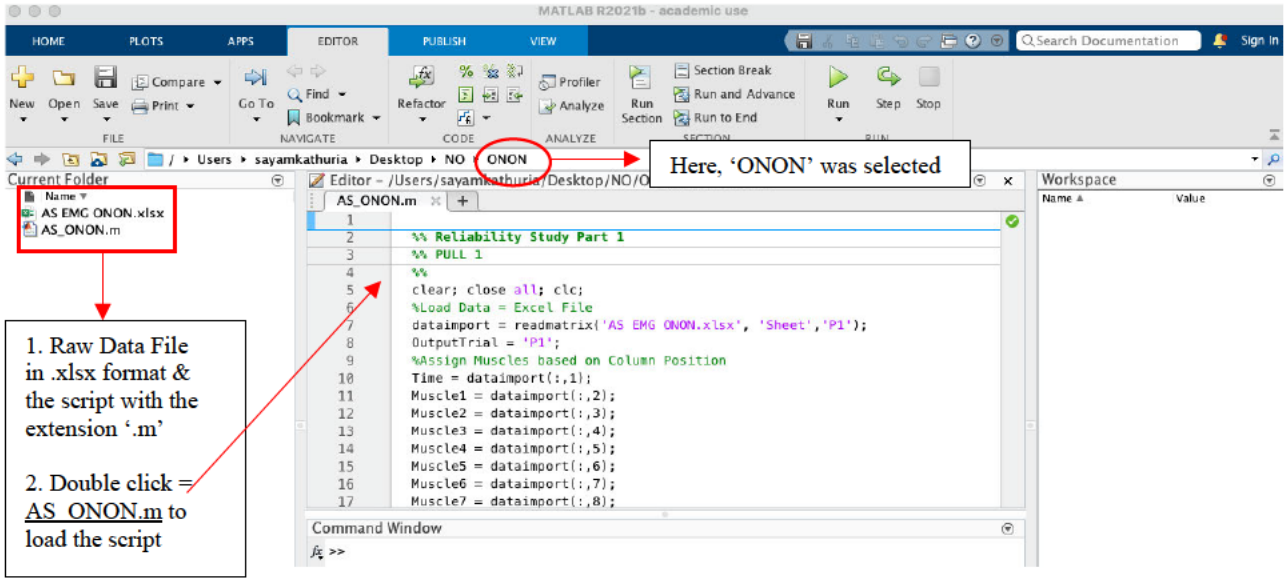

Figure 2.2 *Confirmation of script selection*

2.1.4 Step 4.

You're all set to now RUN the script. ***Please refer to the complete document to see what to expect when you run the script***.

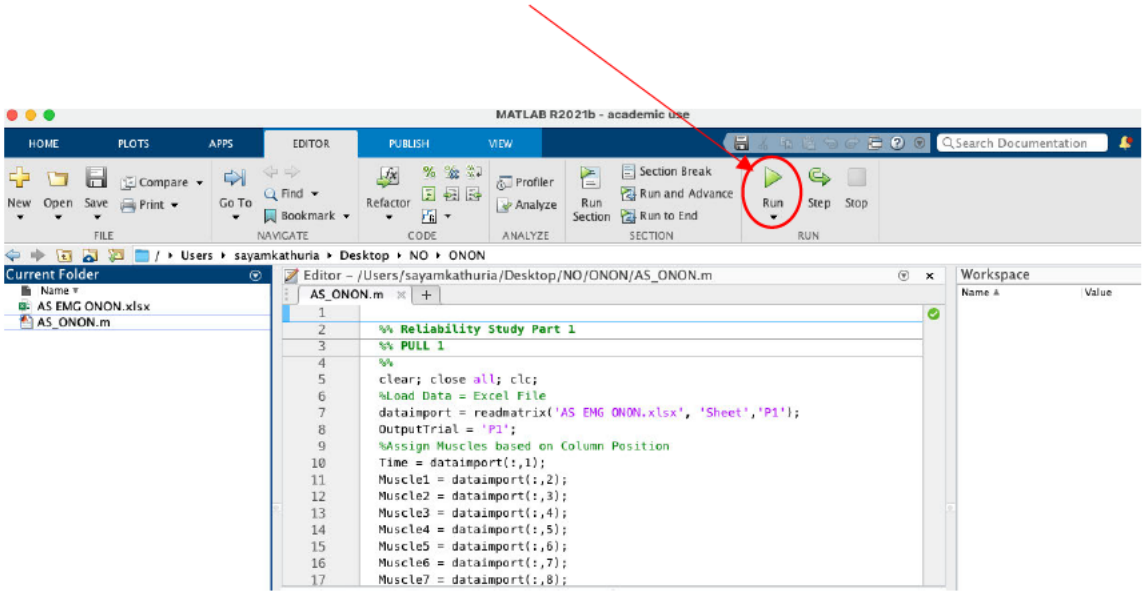

Figure 2.3 *Script ready and set up for analysis. Clicking on 'Run' to initiate analysis.*

3.0 The 2-step visual detection method

3.1 Signal Onset – Time of muscle onset

The time of muscle onset (T_{mo}) to be determined as the last trough (base of the first peak) before the signal deflects away from baseline noise.

It is worth noting that the baseline noise pattern may differ for different muscles, therefore it requires the Rater to identify the noisy pattern seen in a set zoom window and a mark a point (base of first spike) that deflects away drastically from this pattern.

Raters must remember that all detection points must lie between the 5th and 6th second, any number seen out of this range will be marked as '0'. This is due to the IMTP methodological set-up.

On clicking RUN (Section 2.4.1), you will see a series of graphs being displayed on your screen one at a time.

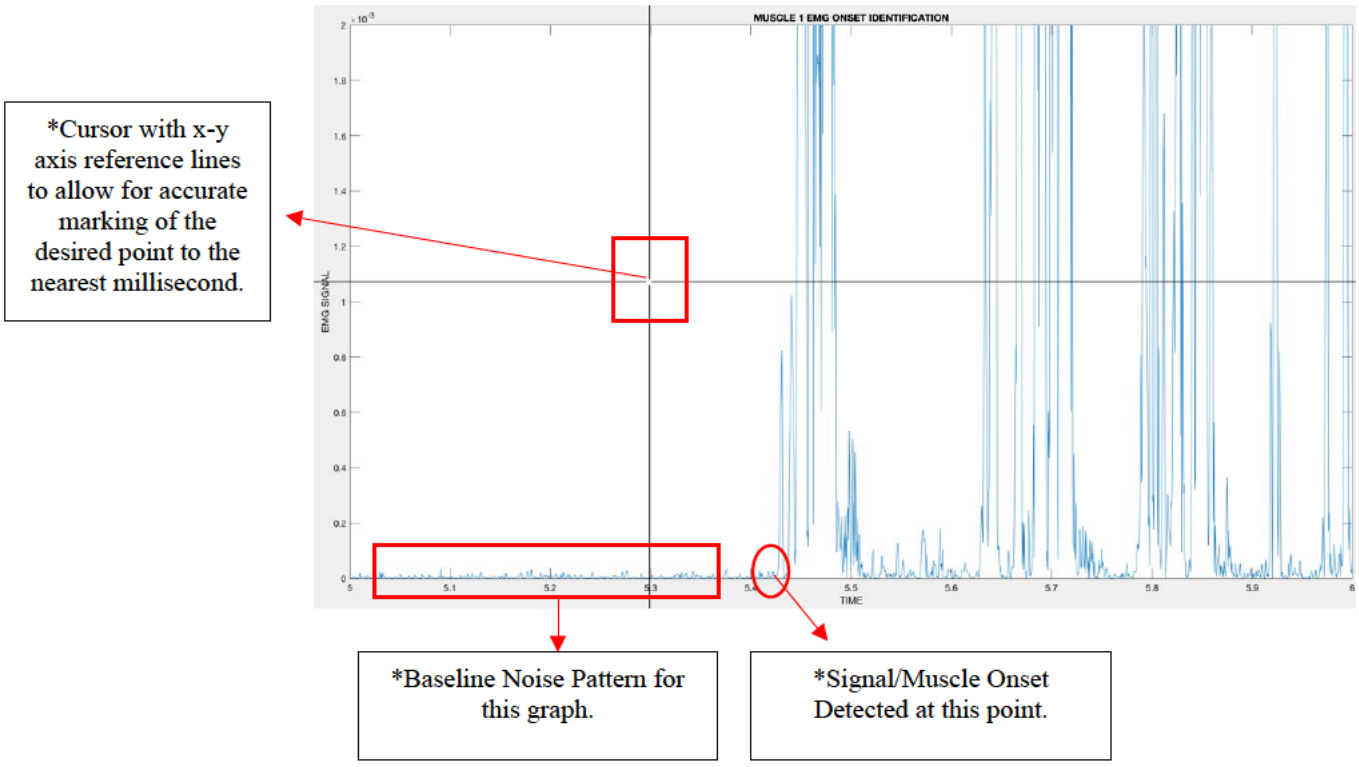

Figure 3.1 *Initial window viewed with a y-axis scale of 2mV and an x-axis scale of 1000 m*

3.2 Selecting the point of signal onset

The 2-step visual detection method was developed to analyse sEMG traces at two different resolutions with the help of three distinctive categories. In the first step, the initial window (y-axis: 2 mV and x-axis: 1000 ms) enabled clear visualisation of baseline noise patterns and selection of the region of interest. In the second step, the final window of higher resolution along the x-axis (x-axis: 50 ms, 100 points; resolution of 0.0005 s) allowed for the accurate location of a single time point representative of muscular onset.

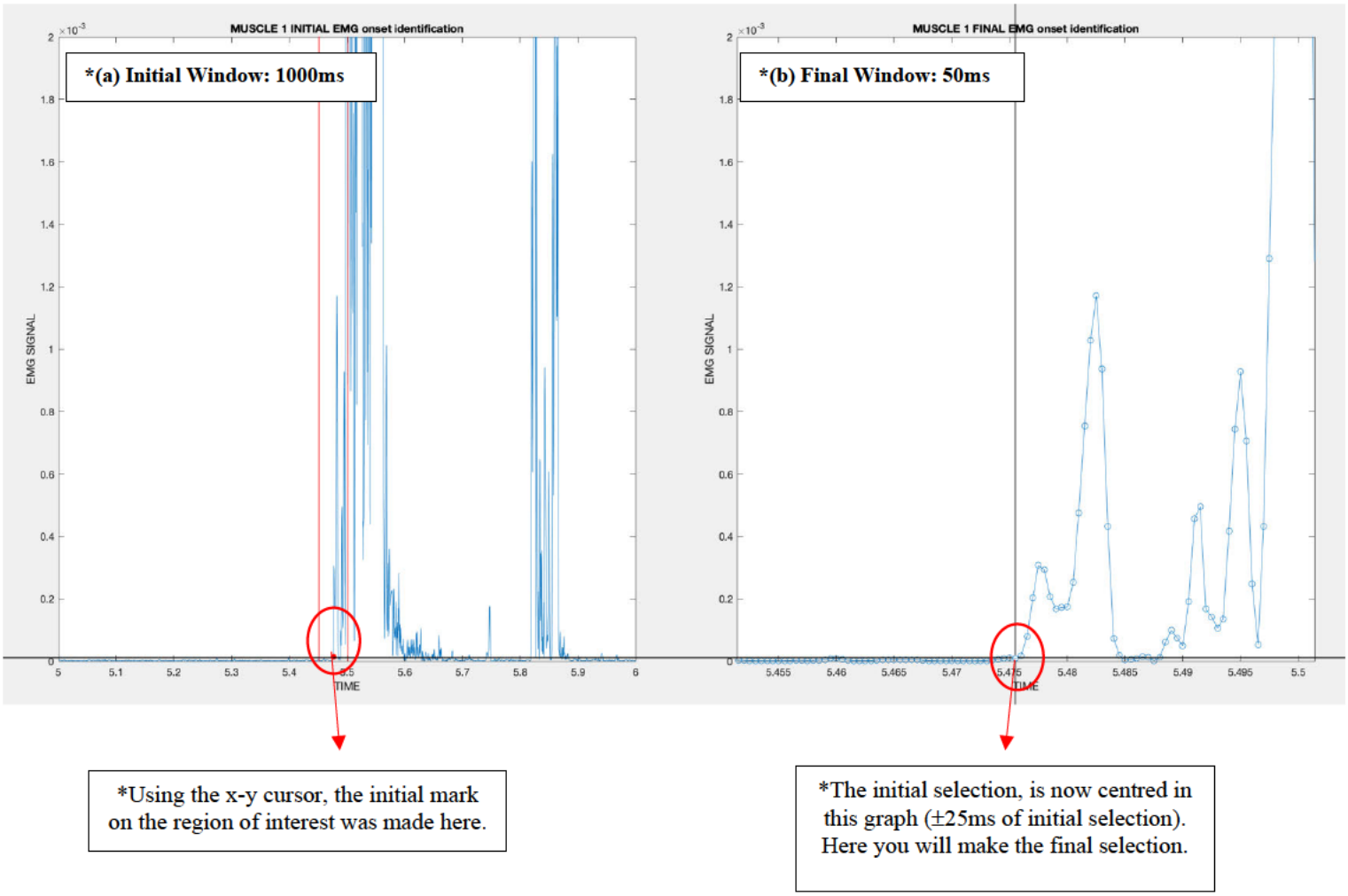

Figure 3.2 (A) *Initial window viewed with a y-axis scale of 2mV and an x-axis scale of 1000 ms. (B) Final window viewed with a y-axis of 2 mV and an x-axis of 50 ms.*

3.2.1 Confirmation of selection

On selecting the desired point in the higher resolution window, a dialog box will pop up to confirm your selection. This dialog box will appear after a selection is made on each of the sEMG traces obtained from the respective trial.

- Yes = Moves you onto the next graph.
- No = Will take you back to the initial resolution window of 1000 ms (Fig.4.) to allow you to repick the region of interest.
- Cancel = Random, saves an output value based on where the cursor was last positioned.

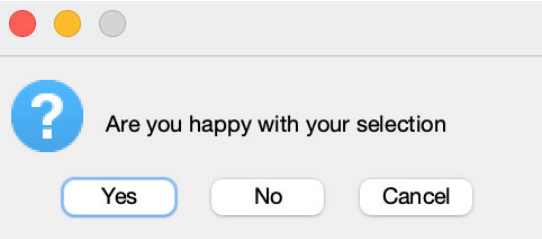

Fig. 3.3 *Confirmation of Selection*

Your selection will be saved automatically. Following the completion of a trail, you will see another pop-up dialog box like the one below. This is an indication point, notifying you about the completion of the trial. Click 'OK' to move onto the next trial.

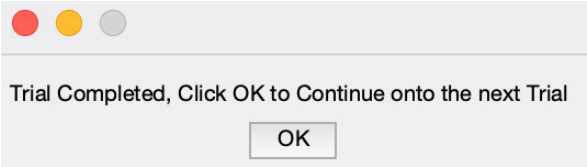

Figure 3.4 *Notification of trial Completion*

On completion of analysis for the current condition, you will see that all your marked points have been saved automatically as an EXCEL file. This can be seen on the left hand side of the window under 'Current Folder'

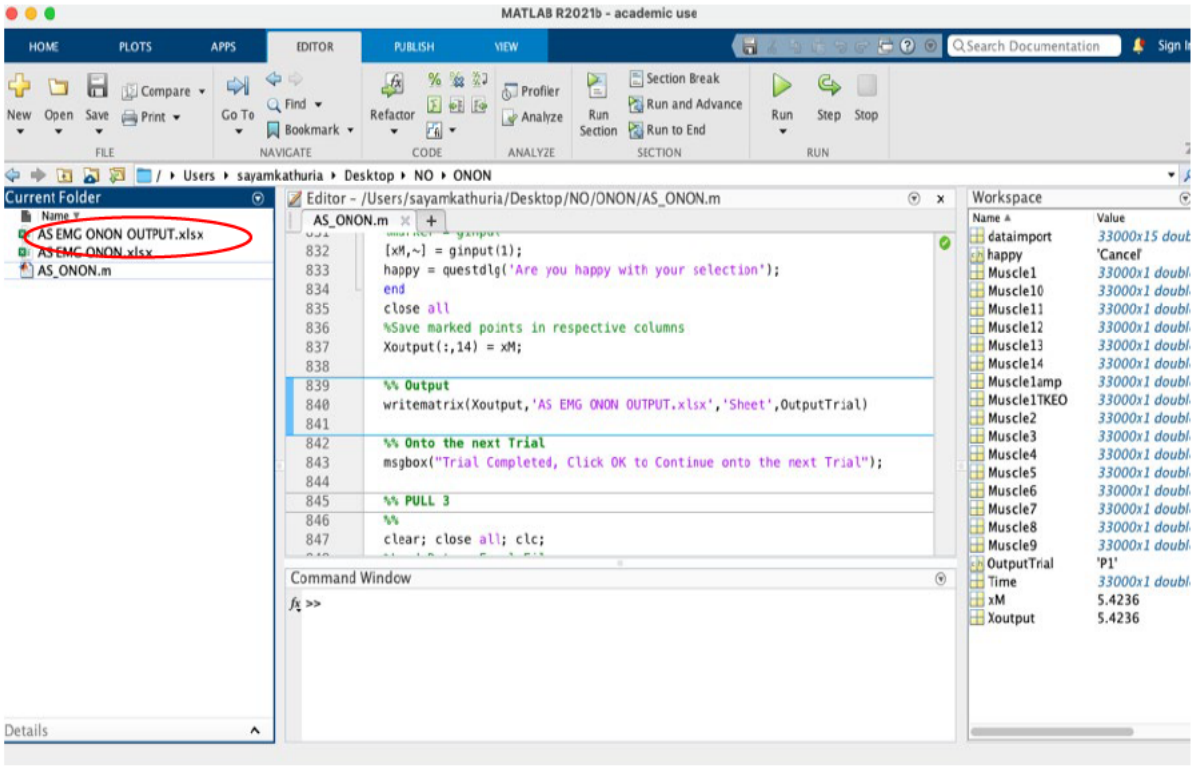

Fig 3.5 *Output excel file seen in the 'current folder window'.*

4.0 Categorisation of sEMG traces

Pilot analysis revealed that different muscles present varying baseline noise patterns. This may differ from muscle to muscle and/or between participants. Therefore, in accordance to this, we established 3 categories to help with the visual detection procedure.

4.1 Category 1

This category consists of sEMG traces, with minimal baseline noise and an apparent deflection of the signal. The region of interest is displayed in A, with two vertical red lines, 25 ms on either side (± 25 ms) of the estimated T_{mo} (red dot). This region was displayed as a full scale of 50 ms along the x-axis in Figure 3.3 B, for the final selection of a point representative of T_{mo}.

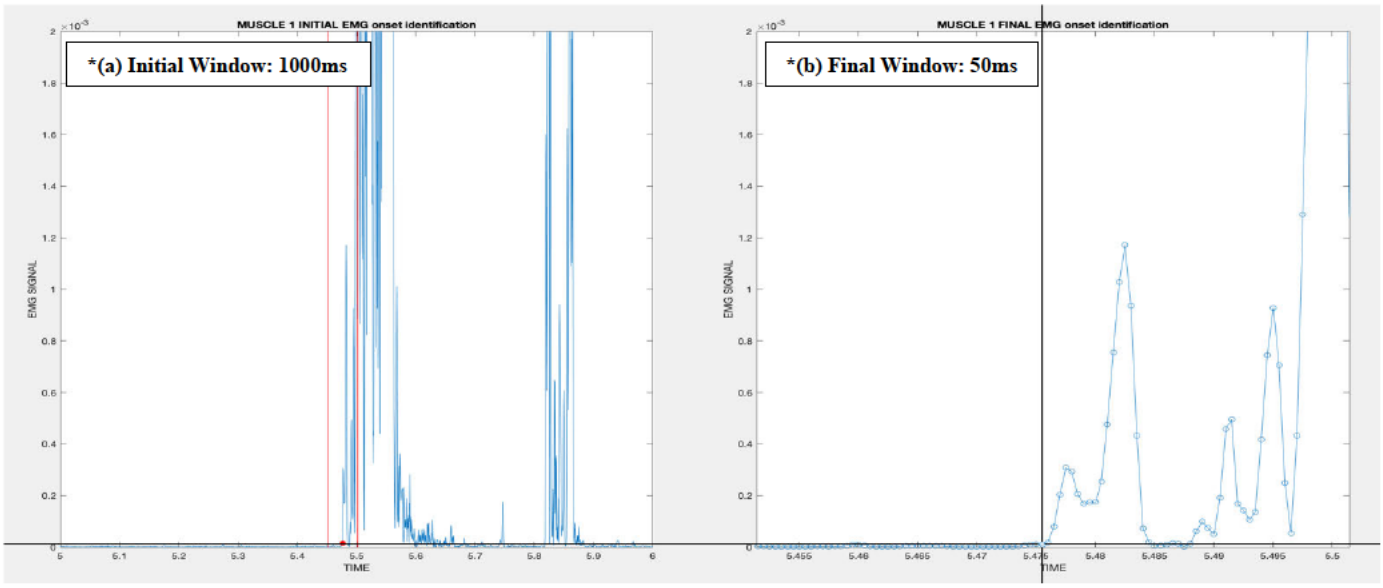

Figure 4.1 *Category 1, example 1.*

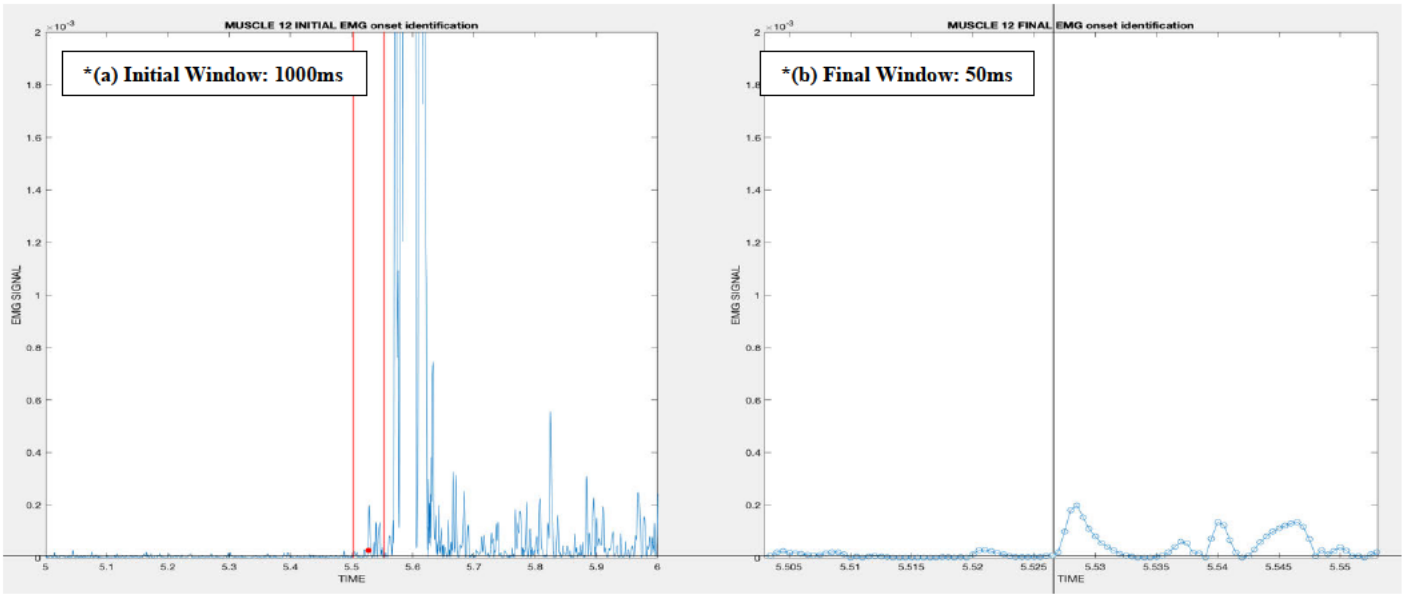

Figure 4.2 *Category 1, example 2.*

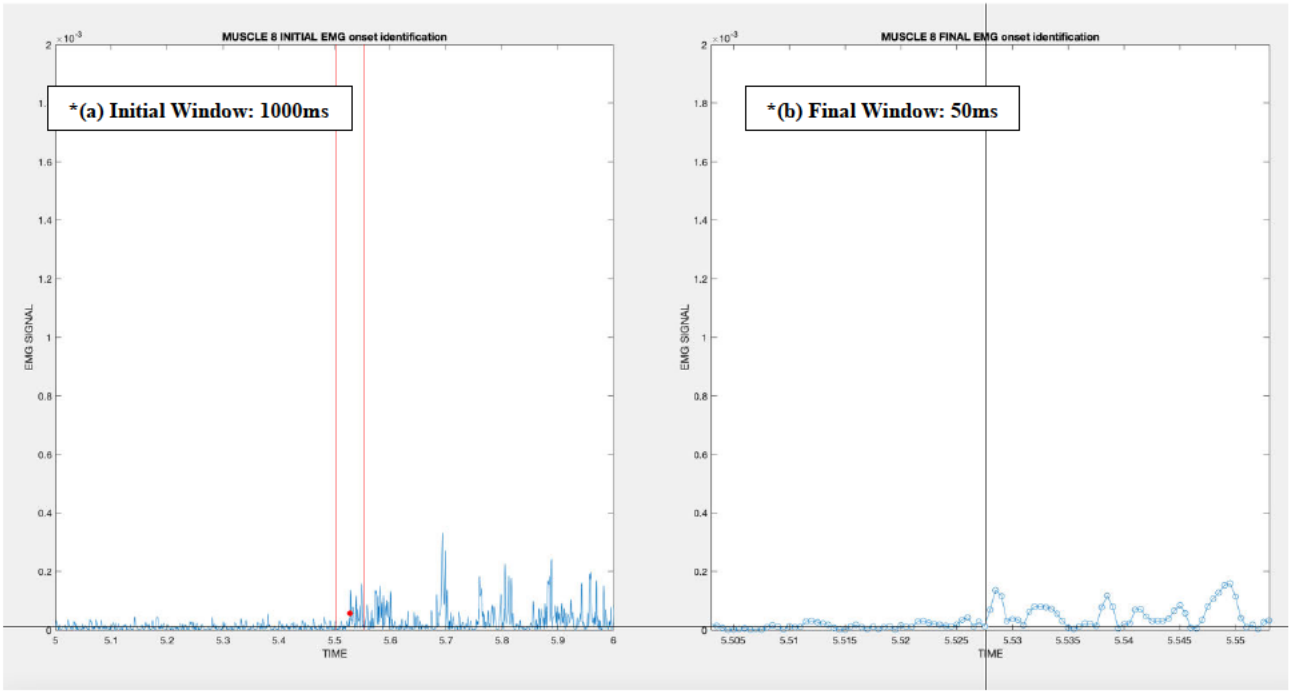

Figure 4.3 *Category 1, example 3.*

4.2 Category 2

This category is composed of signals with distinctively high baseline noise as compared to those in Category 1, yet a visible deflection of the onset signal can be observed. The region of interest is displayed in A, with two vertical red lines, 25 ms on either side (± 25 ms) of the estimated T_{mo} (red dot). This region was displayed as a full scale of 50 ms along the x-axis in B, for the final selection of a point representative of T_{mo}

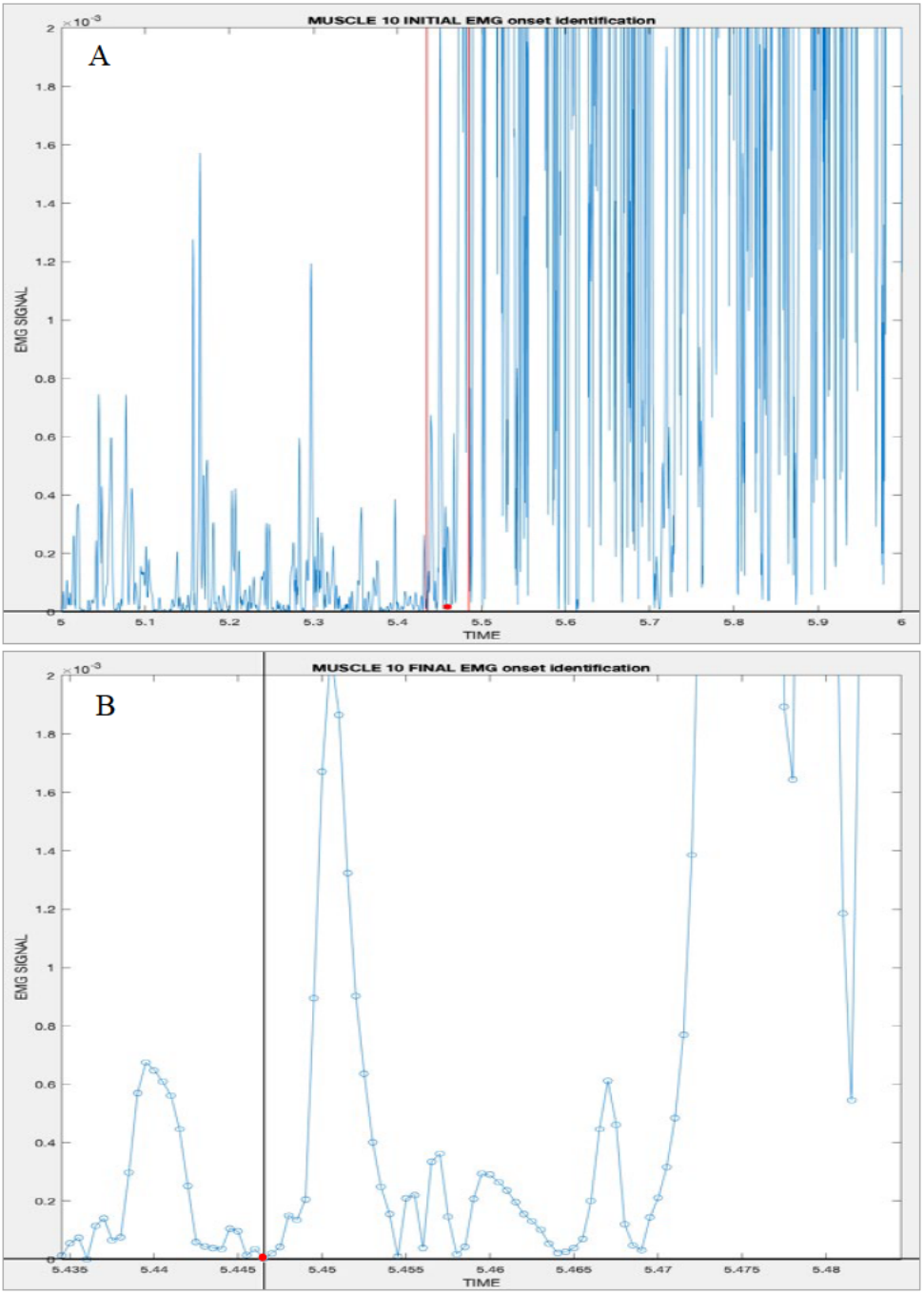

Figure 4.4 *Category 2, example 1.*

4.3 Category 3

This category comprises of sEMG traces that displayed high amplitude baseline activity. For such traces, the definition of signal onset required amendments, accounting for the frequency characteristics of the signal. Consequently, signal onset was defined as the point at the trough (base) of the first spike of the sustained deflected signal, displaying a distinctively frequency-dense area as opposed to the baseline muscle activity.

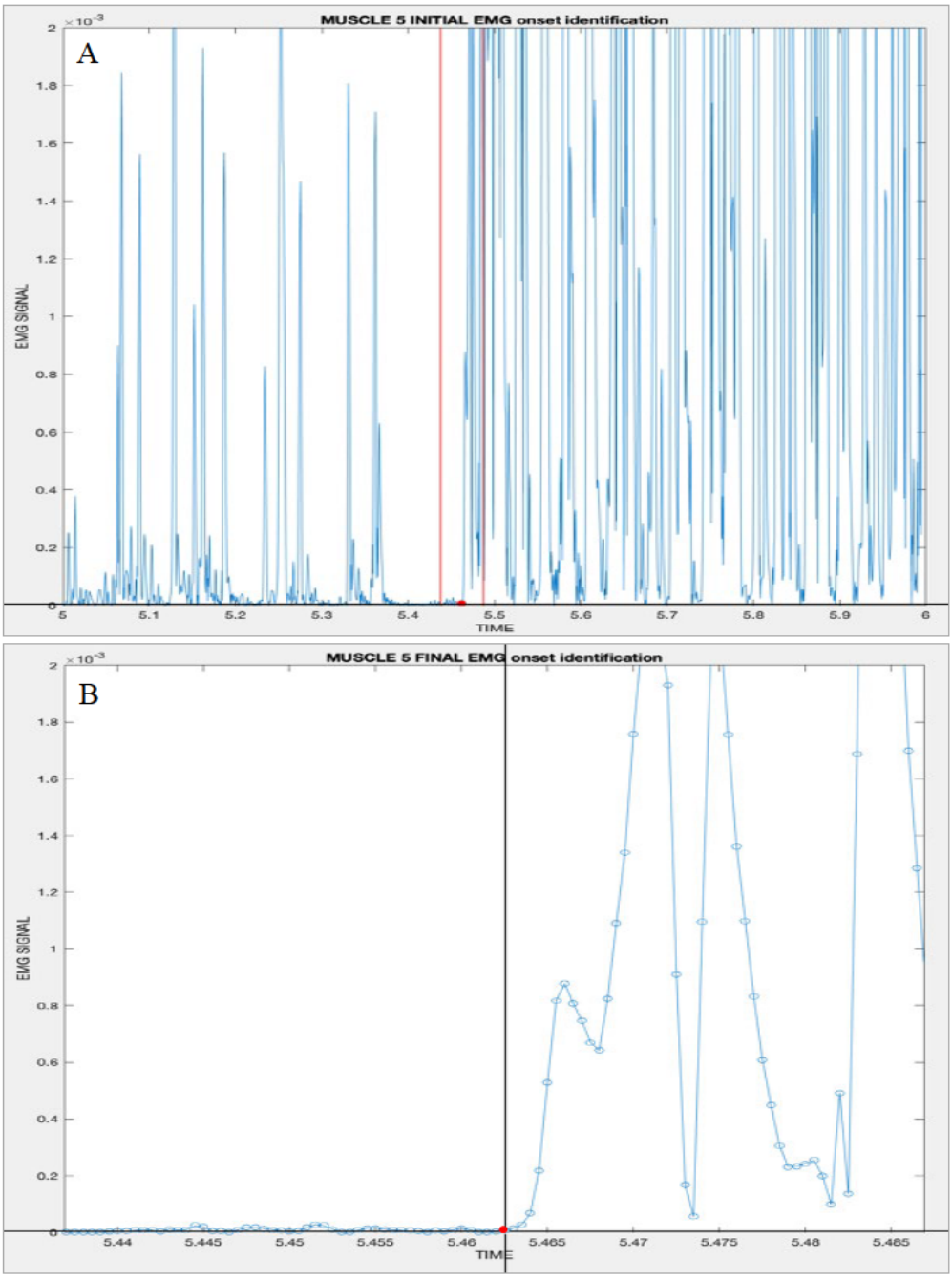

Figure 4.4 *Category 3, example 1.*

4.4 Discarded signals

Noisy signal or no signal detected. sEMG traces labelled as outliers, wherein no signal was detected, or the display window was cluttered with high noise and no visible baseline pattern.

In case of a graph with very noisy signal or unclear detection point (no peak, just baseline noise), drag your cursor off the graph to the extreme left of the screen and press 'esc' on your keyboard 3 times. This will give an output data point before the onset window, which can be detected by the examiner when the results are returned. ***Refer to image below***.

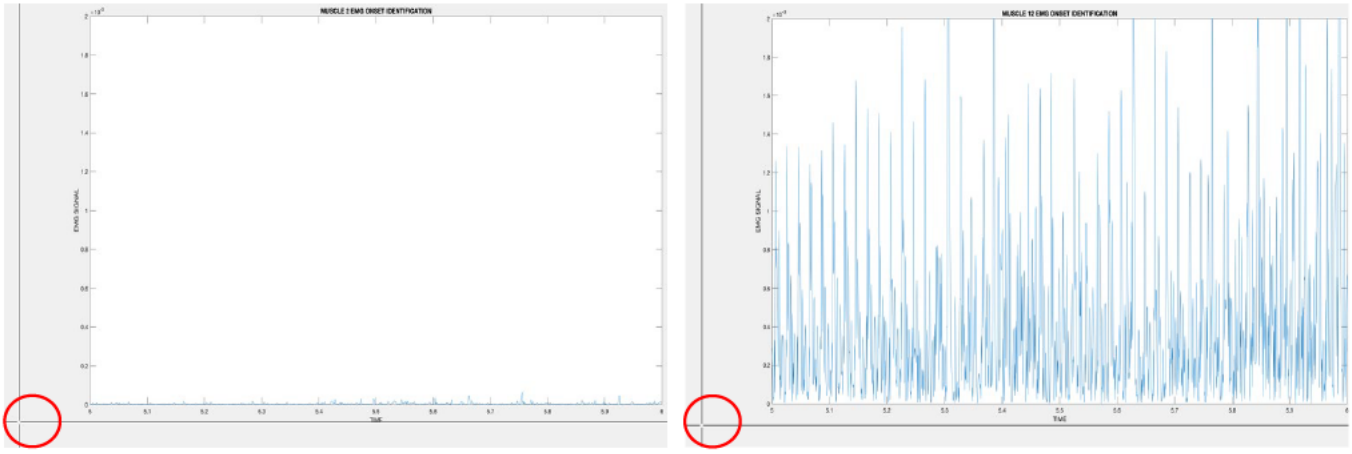

Figure 4.5 *Discarded signals.*

5.0 Selection of the next condition and concluding statement

On completion of the current condition, leave MATLAB running and close the current script. ***Refer to image below***. Then select the next condition from the same pathway as shown in the reference image for step 2. Follow the same steps as above for the next condition.

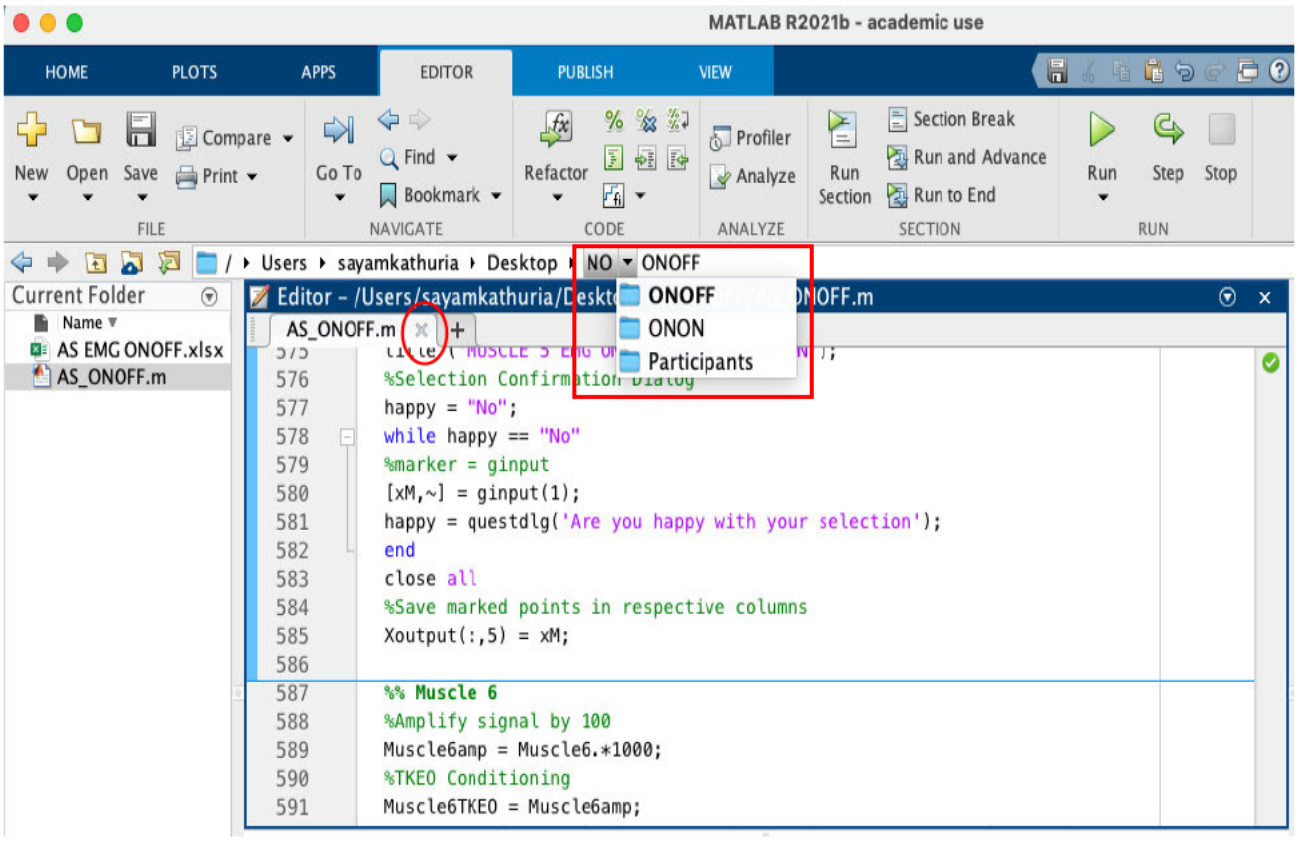

Figure 5.1 *Selection of next condition*

5.1 Conclusion

On completion of analysing all 3 conditions, return the ('File Name OUTPUT 1.xlsx/ 'File Name OUTPUT 2.xlsx') output excel sheet from respective folders back to the primary examiner for further analysis.

6.0 Contact information for questions regarding the study

RESEARCHER (Primary Investigator/ Rater 1)	SUPERVISOR (Secondary Investigator/Rater 2)
Sayyam Kathuria MSc, Sports and Exercise Science. College of Engineering Swansea University, Bay Campus Fabian Way, Swansea SA1 8EN Phone: [redacted] Email: [redacted]	Dr. Nick Owen Associate Professor, Sports & Exercise Sciences. College of Engineering Swansea University, Bay Campus Fabian Way, Swansea SA1 8EN Phone: [redacted] Email: [redacted]

Appendix E 1: Sample MATLAB script to load the muscle activity data from excel

```
clear; close all; clc;
%Load Data = Excel File
dataimport = readmatrix('AS EMG ONON.xlsx', 'Sheet','P1');
OutputTrial = 'P1';
%Assign Muscles based on Column Position
Time = dataimport(:,1);
Muscle1 = dataimport(:,2);
Muscle2 = dataimport(:,3);
Muscle3 = dataimport(:,4);
Muscle4 = dataimport(:,5);
Muscle5 = dataimport(:,6);
Muscle6 = dataimport(:,7);
Muscle7 = dataimport(:,8);
Muscle8 = dataimport(:,9);
Muscle9 = dataimport(:,10);
Muscle10 = dataimport(:,11);
Muscle11 = dataimport (:,12);
Muscle12 = dataimport(:,13);
Muscle13 = dataimport(:,14);
Muscle14 = dataimport(:,15);
```

Appendix E 2: Sample script from the first iteration of the MATLAB programme used to view and analyse the sEMG traces of respective muscles

```
%Amplify signal by 1000
Muscle1amp = Muscle1.*1000;
%TKEO Conditioning
Muscle1TKEO = Muscle1amp;
Muscle1TKEO(2:end-1) = Muscle1amp(2:end-1).^2 - Muscle1amp(1:end-2).*Muscle1amp(3:end);
%Rectification (post TKEO conditioning)
Muscle1TKEO = abs(Muscle1TKEO);
%Selection Confirmation Dialog
happy = "No";
while happy == "No"
    close all
%Setting Figure to maximum
figure('Units','normalized','OuterPosition',[0 0 1 1]);
tiledlayout('flow')
%Visual Detection
nexttile
plot(Time,Muscle1TKEO);
xlim([5 6]);
ylim([0 0.002]);
xlabel ('TIME');
ylabel ('EMG SIGNAL');
title ('MUSCLE 1 INITIAL EMG onset identification');
%marker = ginput
[xM,yM] = ginput(1);
% Create new axis limits for zoom plot. Will need to change numbers
% for Sayyam's data
Xlow = xM-0.025;
Xhi = xM+0.025;
hold on
x1 = xline(Xlow,'r'); x1.LineWidth=1;
x2 = xline(Xhi,'r'); x2.LineWidth=1;
scatter(xM,yM,'filled','r') % scatter point to highlight specifc data point selected
% Creating a plot of zoomed in selection area
nexttile
plot(Time,Muscle1TKEO,'-o')
xlabel ('TIME');
ylabel ('EMG SIGNAL');
title ('MUSCLE 1 FINAL EMG onset identification');
ax = gca; %grab current axis gca
ax.Interactions = (dataTipInteraction);
% Create x-axis limits based on initial selection
xlim([Xlow Xhi])
ylim([0 0.002])
% Select final point
[xM,~] = ginput(1);
happy = questdlg('Are you happy with your selection');
end
close all
%Save marked points in respective columns
Xoutput(:,1) = xM;
```

Appendix E 3: Sample script from the second iteration of the MATLAB programme used to view and analyse the sEMG traces of respective muscles

```
%Amplify signal by 1000
Muscle1amp = Muscle1.*1000;
%TKEO Conditioning
Muscle1TKEO = Muscle1amp;
Muscle1TKEO(2:end-1) = Muscle1amp(2:end-1).^2 - Muscle1amp(1:end-2).*Muscle1amp(3:end);
%Rectification (post TKEO conditioning)
Muscle1TKEO = abs(Muscle1TKEO);
%Selection Confirmation Dialog
happy = "No";
while happy == "No"
    close all
%Setting Figure to maximum
figure('Units','normalized','OuterPosition',[0 0 1 1]);
tiledlayout('flow')
%Visual Detection
nexttile
plot(Time,Muscle1TKEO);
xlim([4 6]);
ylim([0 0.002]);
xlabel ('TIME');
ylabel ('EMG SIGNAL');
title ('MUSCLE 1 INITIAL EMG onset identification');
%marker = ginput
[xM,yM] = ginput(1);
% Create new axis limits for zoom plot. Will need to change numbers
% for Sayyam's data
Xlow = xM-0.025;
Xhi = xM+0.025;
hold on
x1 = xline(Xlow,'r'); x1.LineWidth=1;
x2 = xline(Xhi,'r'); x2.LineWidth=1;
scatter(xM,yM,'filled','r') % scatter point to highlight specifc data point selected
% Creating a plot of zoomed in selection area
nexttile
plot(Time,Muscle1TKEO,'-o')
xlabel ('TIME');
ylabel ('EMG SIGNAL');
title ('MUSCLE 1 FINAL EMG onset identification');
ax = gca; %grab current axis gca
ax.Interactions = (dataTipInteraction);
% Create x-axis limits based on initial selection
xlim([Xlow Xhi])
ylim([0 0.002])
% Select final point
[xM,~] = ginput(1);
happy = questdlg('Are you happy with your selection');
end
close all
%Save marked points in respective columns
Xoutput(:,1) = xM;
```

Appendix E 3: Sample MATLAB code used to save the Rater output.

Output

```
writematrix(Xoutput,'AS EMG ONON OUTPUT.xlsx', 'Sheet',OutputTrial)
```

Onto the next Trial

```
msgbox("Trial Completed, Click OK to Continue onto the next Trial");
```